Bogoliubov Theory of Anyons in One Dimensional Lattice

Bogoliubov-Theorie der Anyonen im eindimensionalen Gitter

A thesis presented for the degree of
Master of Science submitted by

Bin-Han Tang

under supervision of
Priv.-Doz. Dr. Axel Pelster

Department of Physics
Rheinland-Pfälzischen Technischen Universität
Kaiserslautern-Landau
Germany

October 2024

Abstract

In this thesis, we study the behaviours of anyons in a one-dimensional lattice with periodic boundary conditions. To this end, we investigate the Anyon-Hubbard model (AHM), which can be mapped to an extended Bose-Hubbard model via a Jordan-Wigner transformation that induces a density-dependent Peierls phase. This bosonic Hamiltonian then violates the spatial inversion and time reversal symmetries and thus indicates unusual properties like an asymmetric quasi-momentum condensation and imbalanced transport. To address those features, we propose a modified Bogoliubov *ansatz* with variable momentum of the condensate. In general, We find that the anyonic statistical interaction plays a crucial role. On the mean-field level, the statistic interaction achieves an interpolation between Bose-Einstein and Fermi-Dirac statistics by imposing a restriction on the particle density. On the Bogoliubov level, there are also statistic-induced quantum depletion and asymmetric sound velocities in the absence of real Hubbard interaction. Furthermore, several experimentally relevant correlation functions are calculated and discussed.

Zusammenfassung

In dieser Masterarbeit untersuchen wir das Verhalten von Anyonen in einem eindimensionalen Gitter mit periodischen Randbedingungen. Zu diesem Zweck untersuchen wir das Anyon-Hubbard-Modell (AHM), das über eine Jordan-Wigner-Transformation, die eine dichteabhängige Peierls-Phase induziert, auf ein erweitertes Bose-Hubbard-Modell abgebildet werden kann. Dieser bosonische Hamiltonian verletzt dann die räumliche Inversion und die Zeitumkehrsymmetrie und zeigt daher ungewöhnliche Eigenschaften wie eine asymmetrische Quasiimpluskondensation und einen unausgewogenen Transport. Um diese Eigenschaften zu berücksichtigen, schlagen wir einen modifizierten Bogoliubov-*ansatz* mit variablem Impuls des Kondensats vor. Im Allgemeinen stellen wir fest, dass die statistische Wechselwirkung von Anyon eine entscheidende Rolle spielt. Auf der Ebene der Molekularfeldtheorie erreicht die statistische Wechselwirkung eine Interpolation zwischen der Bose-Einstein- und der Fermi-Dirac-Statistik, indem sie eine Beschränkung der Teilchendichte auferlegt. Auf der Bogoliubov-Ebene gibt es auch statistisch induzierte Quantenverarmung und asymmetrische Schallgeschwindigkeiten in Abwesenheit einer echten Hubbard-Wechselwirkung. Darüber hinaus werden mehrere experimentell relevante Korrelationsfunktionen berechnet und diskutiert.

To my grandmother, a good farewell, and I know the love shall remain.

To Zhe Yuan, for our friendship. The long-coveted Daddomain mountain has embraced you for the eternal. But you were not, nor will you ever be, a lone climber.

Contents

1 Introduction **1**
1.1 Anyons in two spatial dimensions . . . 3
1.1.1 Topological interpretation . . . 3
1.1.2 Fractional quantum Hall effect . . . 6
1.2 Anyons in one spatial dimension . . . 6
1.3 Outline of the thesis . . . 9

2 Anyon-Hubbard Model **11**
2.1 Anyon-Hubbard Hamiltonian . . . 11
2.2 Braiding in A Discrete 1D and Anyonic Algebra . . . 12
2.3 Fractional Jordan-Wigner Transformation . . . 14
2.4 Symmetry Breaking of the Bosonic Hamiltonian . . . 17
2.4.1 Parity . . . 17
2.4.2 Time reversal . . . 17
2.4.3 Combined symmetry: anyonic parity . . . 18
2.5 Experimental realization . . . 18

3 Modified Bogoliubov Theory for Anyons **21**
3.1 Generalized Bogoliubov *Ansatz* . . . 21
3.2 Ground state properties . . . 24
3.3 Higher excitations and Bogoliubov transformation . . . 29
3.4 Anyonic Bogoliubov Dispersion . . . 33
3.5 Anyonic Quantum Depletion . . . 34
3.6 Asymmetric Two-Mode Sound Velocities . . . 37
3.6.1 Weak coupling-Bogoliubov velocities . . . 37
3.6.2 Estimation between Bogoliubov and Luttinger theory . . . 39

4 Correlation Functions **44**
4.1 Spatial Coherence for Bosons . . . 44
4.2 Quasi-momentum Distribution for Bosons . . . 45
4.3 Pair Correlation for Bosons . . . 47
4.4 Structure Factor . . . 49

5 Conclusion and Outlook **51**

6 Acknowledgement **55**

7 Bibliography **56**

A Combinatorics and Normal Ordering **63**

B Periodic Boundary Condition **65**
B.1 Discretization of momentum space 65
B.2 1D discrete Fourier transformation 66

C Extended Tomonaga-Luttinger Liquid Theory **67**
C.1 Harmonic fluid approach 68
C.2 Mode expansion 69

Chapter 1

Introduction

One of the most exotic features in quantum mechanics is the indistinguishability of identical particles, which inherently indicates how they interact with each other or conversely to different types of statistics [1–3]. These statistics are so fundamental that they play a crucial role in both few-body and many-body physics. From the spin-statistics theorem first introduced by Wolfgang Pauli in 1940 [4], there are two fundamental classes of particles in three spatial dimension space, which are distinguished via their quantized spin in units of Planck constant $\hbar$.

For the integer spins case, there are bosons whose wavefunction remains symmetric under permutation and they obey Bose-Einstein statistics. Such symmetry would lead to an effective attraction, allowing bosons to occupy the same quantum state. This is also the reason for the formulation of Bose-Einstein condensation (BEC) [5], a phenomenon predicted by Bose and Einstein in 1924. When the de Broglie wavelength exceeds the average interparticle distance, the system undergoes a phase transition, and all ground-state bosons exhibit long-range correlations and behave collectively. Thus BEC can be described by a single macroscopic wavefunction. This is the case of effective attraction. As Bose assumed here non-interacting bosons, the emergence of BEC arises intrinsically from the principles of Bose-Einstein statistics. The first experimental realization of BEC was not achieved until 1995, following significant technical advancements such as magnetic trapping, laser cooling, and evaporative cooling. This milestone was reached by C. Wieman and E. Cornell using ^{87}Rb atoms (as shown in **Fig.** 1.1.)[6, 7], and W. Ketterle with ^{23}Na atoms [8].

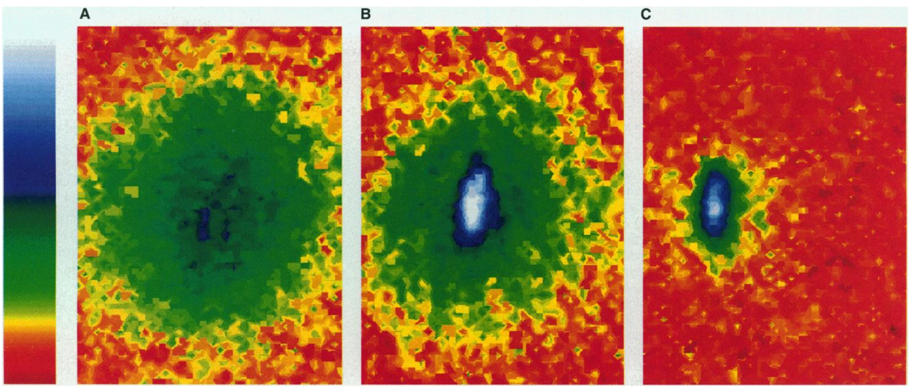

Figure 1.1: The first realized Bose-Einstein condensate by C. Wieman and E. Cornell [6]. The row of false-colour images shows the change of velocity distribution of the ^{87}Rb atom cloud. In **(A)**, there is yet only a thermal cloud, and in **(B)**, the condensate starts to appear (the white and blue area), dressed by non-condensed part (green and yellow area). Then, in **(C)**, via further cooling by evaporation, the thermal part is also condensed.

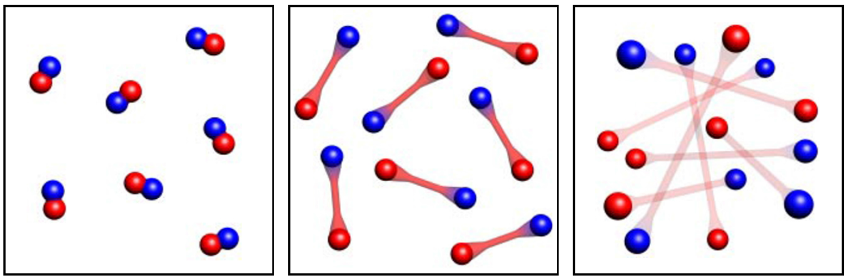

Figure 1.2: Illustration of the BEC-BCS crossover [9]. By tuning the interaction strength of opposite spin particles, a continuous crossover from tightly bound molecules to long-range correlated Cooper pairs exists, and in-between is the crossover regime where the pair size is comparable to the interparticle spacing.

On the other hand, fermions with half-integer spin, satisfying Fermi-Dirac statistics, would result in anti-symmetric wavefunction after permutation. The anti-symmetry then leads to an effective repulsion. The repulsive interaction is so strong that two fermions with identical external and internal properties cannot simultaneously occupy the same quantum state. This is the celebrated Pauli exclusion principle [10]. To provide a pertinent example of statistical interactions in the fermionic case, one must consider the BEC-BCS crossover, a prominent topic in the study of ultracold Fermi gases.

To explain the emergence of BEC with fermions, we have to introduce first the second part of the BEC-BCS crossover, the Bardeen–Cooper–Schrieffer (BCS) theory. Following the name of J. Bardeen, L. N. Cooper and J. R. Schrieffer, BCS theory was proposed in 1957 [11] in order to solve the problem of superconductivity, i.e. the vanishing electric resistance of cold metals [12], together with the subsequent Messner-Ochsenfeld effect [13], which describe the expulsion of a magnetic field from a superconductor. The idea is that due to the vanishing weak attractive interaction between electrons and the vibrating crystal lattice (the phonons), two electrons with opposite spins can form a Cooper pair with integer spin ($S = 0$ or unconventionally $S = 1$ [14]). Such pairs as composite particles behave as bosons, and therefore can undergo the phase transition to superfluid that has no frictions [15]. Also, Cooper recognized that the two fermions forming a Cooper pair in BCS theory exhibit a significantly large correlation distance, attributed to the arbitrarily weak interaction [16], as illustrated in the rightmost plot of **Fig.** 1.2. This implies that the Pauli exclusion principle still leads to the interactions between unbound fermions with identical spin, suggesting that one can not have a point-like description for Cooper pairs in such circumstances. To apply the general BEC theory for point-like particles, one needs to sufficiently increase the attraction such that the correlation distance of Cooper pairs decreases (the middle of **Fig.** 1.2) and finally the pairs become tightly bound molecules in real space (the leftmost of **Fig.** 1.2). This is then the framework of the BEC-BCS crossover [17, 18]. Experimentally, the crossover is realized by tuning the Feshbach resonance such that the s-wave scattering length $a_s(B)$ is controlled by the external magnetic field strength B [19]. Consequently, the change of a_s modifies the interaction strength between identical particles [20]. The effective repulsion for fermions is depicted in **Fig.** 1.3, when one goes from the BEC-limit from the left to the BCS-limit on the right, the diameter of ^{5}Li cloud increases due to the Pauli exclusion of the identical fermions in different Cooper pairs, such that they are pushed away from each other.

The two examples discussed above illustrate that from both bosonic and fermionic perspectives, the effective interactions resulting from the statistics of indistinguishable particles can lead

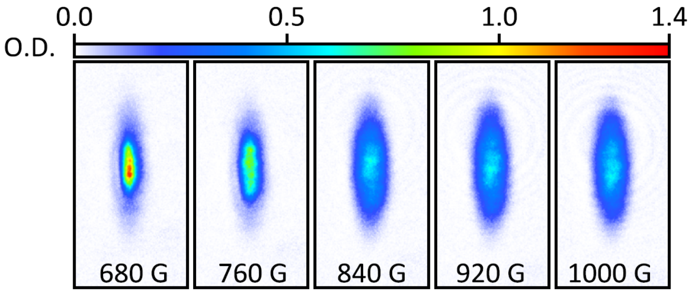

Figure 1.3: The optical density (O.D.) distribution of ^{5}Li atom cloud across the BEC-BCS crossover via time of flight experiment [19]. The size of the atomic cloud is enlarged from the BEC limit to the BCS limit due to the fermionic statistical repulsion between the identical fermions in different Cooper pairs.

to intriguing physical phenomena. The two classes of particles describe our familiar $(3+1)$-dimensional world and have been fundamental to quantum mechanics for over half a century since it's foundation. However, the scenario becomes remarkably complex when examining lower spatial dimensions.

1.1 Anyons in two spatial dimensions

In 1977, Leinaas and Myrheim [21] investigated explicitly the relation between particle exchange statistics and topology, where they found only in the three or higher dimensional space the *symmetry group* S_N is the fundamental group for the configuration space for the exchange of identical particles. In contrast, in two dimensions, the underlying fundamental group is the *braid group* B_N which enables so-called fractional statistics [22]. Such statistics interpolates between Bose-Einstein statistics and Fermi-Dirac statistics. Besides topology, Frank Wilczek also approached such fractional statistics by looking at the relation between spin and particle statistics [23, 24]. It was also Wilczek who first proposed in 1982 [25] the name *anyon* [26] for the sake of describing the behaviours of charged particles encircling magnetic flux tubes. Due to the Aharonov-Bohm effect [27], such winding would acquire a geometric phase shift for the particles. This then leads to unusual fractional statistics for the particle-flux tube composite that interpolates continuously between bosons and fermions.

> *"Since the interchange of two of these particles can give any phase, I will call them generically anyons."[25]*

The existence of anyons could be simply explained by the basic quantum mechanics: in two-dimensional space, i.e. the flatland [28], there exists only one rotation axis, i.e. the one perpendicular to the 2D plane, we have only one generator of spin angular momentum $\hat{S}_z$ [3], which would then lead to a fractional eigenvalue of the spin and thus new types of exchange statistics can emergent.

1.1.1 Topological interpretation

In the following, we investigate the topological properties of the configuration space of identical particles in the sense of Leinaas and Myrheim [3, 21, 29–31].

Consider a system with N identical particles, and the configuration space for a single particle is denoted by X. In the classic case, the configuration space of the N-particle system is simply a N-fold manifold omitted by its singularities, which is the coincidence set Δ, defined as

$$\Delta = \left\{ (\mathbf{x}_1, \ldots, \mathbf{x}_N) \,\middle|\, \mathbf{x}_i = \mathbf{x}_j \text{ for any } i \neq j \right\}, \tag{1.1}$$

where $\mathbf{x}_1, \ldots, \mathbf{x}_N$ are the coordinates of the N-particles. Therefore, in the classic case, the configuration space is $(X^N \setminus \Delta)$, as the permutation of any two of the distinguishable particles would lead to a different physical system. Things change drastically when the quantum mechanic steps in. The indistinguishability of identical particles would lead to no change to the physical observables after the permutation of the index set that labels the particles. The resulting configuration space would then be reduced to $(X^N \setminus \Delta)/S_N$. S_N is the symmetric group for the permutations of N identical particles and thus a discrete finite group when $N > 2$. Therefore, it is locally isomorphic to $(X^N \setminus \Delta)$ but not at the singularities Δ.

To unveil the topological structure of the N-particle system in detail, we first denote the one-particle coordinate space as the d-dimensional Euclidean space $\mathbb{R}^d$. Then we define the center-of-mass space

$$\mathbf{x}_{\text{com}} = \frac{1}{N} \sum_{i=1}^{N} \mathbf{x}_i \;\; \in \mathbb{R}^d \,, \tag{1.2}$$

which remains invariant under the action of S_N. Therefore the configuration can be written as a Cartesian product

$$\frac{X^N \setminus \Delta}{S_N} = \mathbb{R}^d \times r(d, N) \,, \tag{1.3}$$

with $r(d, N)$ the relative configuration space,

$$r(d, N) \in \mathbb{R}^{d(N-1)} \,. \tag{1.4}$$

To give an example, for two particles $N = 2$ we have a singular point at the origin $\Delta = \{0\}$, and the symmetric group is the relative two-particle exchange S_2, meaning $\mathbf{x}_\text{r} = -\mathbf{x}_\text{r}$. Therefore we have

$$\frac{X^2 \setminus \Delta}{S_2} = \mathbb{R}^d \times \frac{\mathbb{R}^d \setminus \{0\}}{S_2} = \mathbb{R}^d \times \left[\frac{S^{d-1}}{S_2} \times (0, +\infty) \right] \tag{1.5}$$

where S^{d-1} represents the $(d-1)$-dimensional sphere, and S^{d-1}/S_2 in this case can also be written as $\mathbb{R}P^{d-1}$, which represents the real projective space as the $(d-1)$-dimensional topological lines that cross the origin $\{0\}$ in the d-dimensional space $\mathbb{R}^d$. To study the topological properties of the configuration space, it is necessary to identify the corresponding fundamental group, i.e. the first homotopy group, π_1. It gives information about the continuous deformation of connecting paths between the fixed start- and end-points. With the product rule $\pi_1(X \times Y) = \pi_1(X) \otimes \pi_1(Y)$ and the fact that $\mathbb{R}^d$ and $(0, \infty)$ are simply connected topological objects, one would have

$$\pi_1 \left(\mathbb{R}^d \times \left[\frac{S^{d-1}}{S_2} \times (0, +\infty) \right] \right) = \pi_1 \left(\frac{S^{d-1}}{S_2} \right) = \pi_1 \left(\mathbb{R}P^{d-1} \right) \,. \tag{1.6}$$

One can then discuss the topological difference for $d \geq 3$, $d = 2$ and $d = 1$. As shown in **Fig.** 1.4, for $d \geq 3$, there are three kinds of closed paths on the $(d-1)$-dimensional sphere S^{d-1} with the diametrically opposite poles marked with $\times$: **(a)** No particle exchange corresponds a closed path A which can be continuously deformed into one point. **(b)** An exchange of two particles which go from one point to the diametrically opposite point that can not be deformed to a point continuously. However, in **(c)** two times of particle exchange can again form a simply connected closed path, corresponding to the case in **(a)**, i.e. no change. Therefore, the phase change is the same for no exchange and double exchange, which means the phase change for a single change can only have two possible values: $+1$ for bosons and -1 for fermions. And we have $\pi_1^{d\geq 3}\left(\mathbb{R}P^{d-1}\right) = \mathbb{Z}_2$, where $\mathbb{Z}_2$ is the cyclic group of order 2 [30].

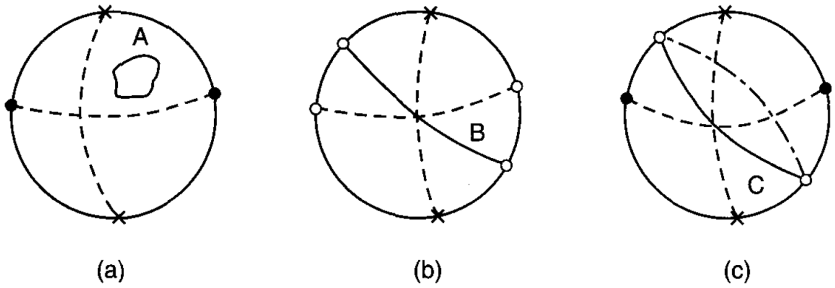

Figure 1.4: All possible closed paths in the configuration space in $d \geq 3$ [3].

In the case of $d = 2$, the relative configuration space can be continuously deformed into a ring, as shown in **Fig.** 1.5. The closed path for no exchange in **(a)** can again be continuously deformed into a point as in $d = 3$. The same applies to **(b)**, where the single exchange is non-contractible with fixed endpoints. The real surprise arises with the double exchange of two particles: the exchange is non-contractible, and the particles' impenetrability causes the trajectory distinguishable. For instance, one must also specify the winding direction in **(c)**. For a single exchange, depending on the clockwise or anti-clockwise exchange one would end up with a phase factor with either $e^{-i\theta}$ or $e^{i\theta}$. As $\mathbb{R}P^1$ is homeomorphic to S^1 and S^1 is universally covered by $\mathbb{R}^1$, the fundamental group now is $\pi_1^{d=2}\left(\mathbb{R}P^1\right) = \mathbb{Z}$, where $\mathbb{Z}$ represents the infinite cyclic group [30]. θ is thus a continuous variable and $e^{\pm\theta}$ would lead to a 2π periodicity for θ. Then $\theta = 0$ corresponds to the symmetric exchange for bosons and $\theta = \pi$ the anti-symmetric exchange for fermions, respectively.

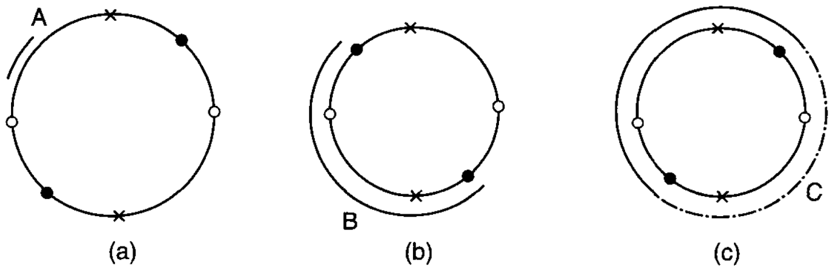

Figure 1.5: All possible closed paths in the configuration space in $d = 2$ [3].

The case of $d = 1$ is the trivial $\pi_1(\mathbb{R}P^0) = id$, as now the relative configuration space corresponds to just a single point. A generalization of the two particle cases to N-particle cases [32] leads to

$$\pi_1^{d\geq 3}\left(\frac{\mathbb{R}^{d\cdot N} \setminus \Delta}{S_N}\right) = S_N\,, \tag{1.7}$$

$$\pi_1^{d=2}\left(\frac{\mathbb{R}^{2\cdot N} \setminus \Delta}{S_N}\right) = B_N\,, \tag{1.8}$$

$$\pi_1^{d=1}\left(\frac{\mathbb{R}^{1\cdot N} \setminus \Delta}{S_N}\right) = id\,, \tag{1.9}$$

with B_N the *braid group of N-strands*. Unlike in the $d \geq 3$ cases, where the permutation group S_N admits only two corresponding one-dimensional representations to bosons and fermions, the braid group in $d = 2$ is infinite and allows for a continuous set of one-dimensional representations, which correspond to different Abelian anyons characterized by an arbitrary exchange phase θ [3, 21]. In the case of $d = 1$, as the braid group is not fundamental, the anyons do not appear naturally. But it is shown recently by Nathan Harshman *et al.* that one can construct artificially various types of fractional exchange statistics on discretized one-dimensional space [33]. This then justifies the existence of braid anyons in one dimension, which we shall briefly discuss in **Sec.** 2.2.

Up to now, this peculiar anyons seems merely a theoretical construct in low-dimensional space and is untouchable for us who live in three spatial dimensions. To make the connections between anyons and our daily world, in the following, we briefly highlight the fractional quantum Hall effect (FQHE), which is the first phenomenon discovered in the laboratory that is later explained as anyons.

1.1.2 Fractional quantum Hall effect

The integer quantum Hall effect (IQHE) was found in 1980 [34]. It describes that under the action of a strong applied magnetic field perpendicular to the surface of the film, the in-plane Hall resistance of the film will be quantized in units of h/e^2 and expressed through an integer fill factor ν. This is explained by the discretized Landau energy bands and the Pauli exclusion principle [35]. However, just two years later, in 1982, D. C. Tsui, H. L. Stormer and A. C. Gossard [36] found in laboratory that other than the IQHE, there is a step-like signal for a filling factor $\nu = 1/3$. Laughlin conjected in 1983 that the fractional quantized Hall conductance corresponds to a new state of matter that has elementary excitations with fractional charge [37]. Halperin then suggested that those elementary excitations, i.e. quasi-particles, are essentially anyons [38], therefore confirming the existence of anyons in our real world. The most recent theoretical explanation of FQHE is the composite fermion theory by J. K. Jain [39], which tries to handle the different fractions of the filling number. The basic idea is that the two-dimensional electrons that are confined in a strong magnetic field would bind with multiple numbers of magnetic flux quanta (see **Fig.** 1.7) and result in a composite. Such composite would then follow the fractional statistics and behave as anyons.

Since the discovery of FQHE, the field of research on anyons has sprang with many promising applications, including high-T_c superconductors [42], topological insulators [43]. Further, the FQHE with filling factor $\nu = 5/2$ is considered a promising candidate for the realization of fault-tolerant topological quantum computation, as this number corresponds to non-Abelian anyons and are robust to local defects [35, 44].

1.2 Anyons in one spatial dimension

Having given the significant role of anyons in two spatial dimensions, it's reasonable to ask how their counterparts are in the 'lineland', i.e. one spatial dimension. However, due to the topological difference of configuration space for two- and one-dimensional space as mentioned in **Sec.** 1.1.1, for $d = 1$, the particles can not exchange without interacting with each other, and there's no direct winding as in $d = 2$. Therefore particle statistics is inclusively related to the interactions [21] and therefore can be defined ambivalently [3, 45, 46].

However, based on the fundamental definition of anyons that particle exchange induces an arbitrary phase $e^{i\theta}$, one can nevertheless construct this phase in one spatial dimension, fully analogous to the two-dimensional case, thereby yielding valid one-dimensional anyons from various perspec-

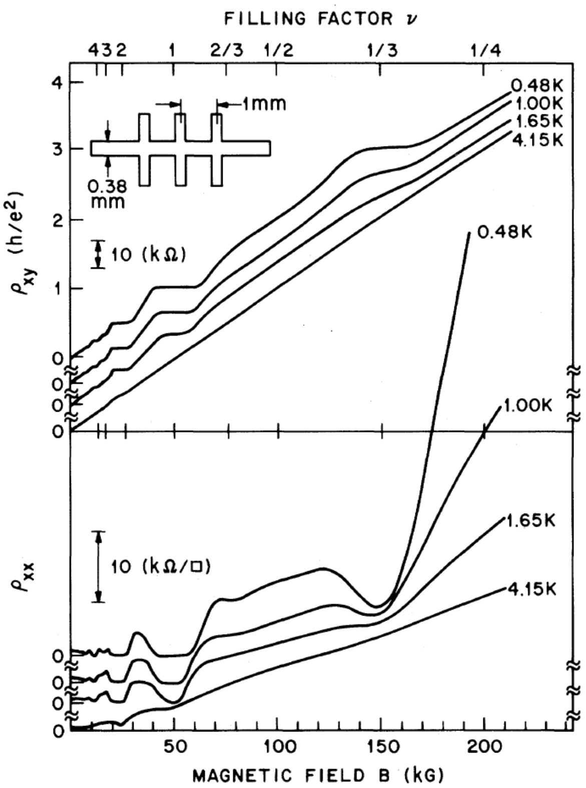

Figure 1.6: The first experimental plot of the FQHE [36]. The in-plane Hall resistance ρ_{xy} has a plateaus at fractional quantized filling number $\nu = 1/3$.

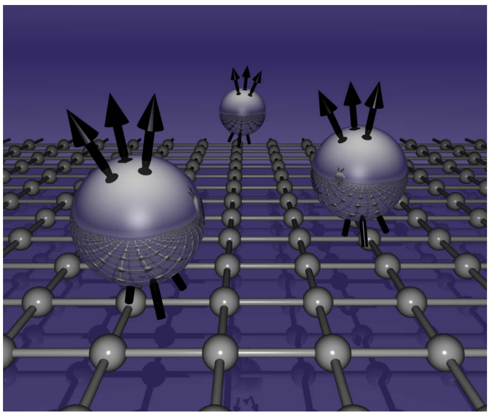

Figure 1.7: The composite fermion theory to the FQHE [40, 41]. There, each electron in the two spatial dimensions binds with three magnetic flux quanta.

tives. The pioneering example, that is the model by Leinaas and Myrheim [21], was proven to be equivalent to the Lieb-Liniger model [47], which describes a bose gas with δ-interaction in one-dimensional continuous space. Somehow, the Leinaas-Myrheim anyon doesn't break the spatial- and temporal-inversion symmetries in the corresponding bosonic representations, which is a fundamental feature for its two-dimensional counterpart [3, 48]. Anjan Kundu then achieved those symmetry breakings for anyons in one dimension by adding a current-density coupling (double δ interacting) term to the Lieb-Liniger model in 1999 [49, 50]. Also, Kundu introduced *a priori* the generalized commutation relation for one-dimensional anyons, which mimics the case in two dimensions. Somehow, the Kundu anyons do not hold the 2π periodicity of the phase factor θ when considering the mapping of anyons to either interacting bosons or fermions via the fractional Jordan-Wigner transformation. This means that after the transformation, the corresponding topological characters would be gone [49, 51]. Marin Bonkhoff et al. approached this issue by proposing the extended Tomonaga-Luttinger liquid theory (eTLL) in **Ref.** [51]. The Tomonaga-Luttinger liquid theory (TLL) [52] describes the low-energy excitations of strongly coupled dilute bosons in a one-dimensional continuous space. Using the so-called harmonic fluid approach and introducing a parity-breaking interaction Δ, TLL is extended to the corresponding anyonic version. eTLL also predicts the asymmetric sound velocities for left- and right-moving components, indicating the symmetry breaking even in the continuum limit [51, 53].

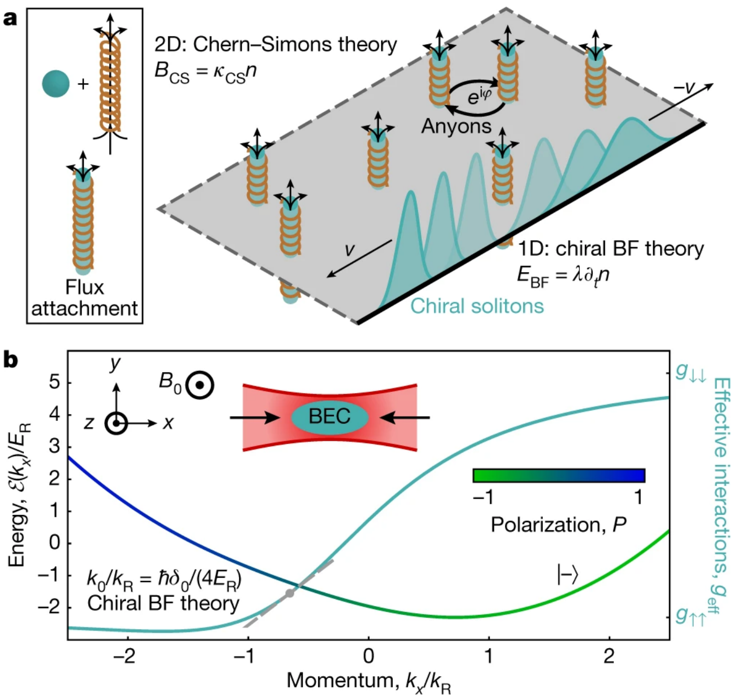

Figure 1.8: The realization of chiral BF anyons [54]. **a** demonstrate that the chiral BF theory is a 1D reduction of the 2D Chern–Simons theory of fractional quantum Hall states and describes chiral solitons. **b** shows the experimental realization with an optically dressed BEC.

In parallel, it is also worth mentioning the existence of other types of one-dimensional anyons. F. D. M. Haldane generalized the Pauli exclusion principle to the anyonic case in arbitrary dimensions [55] and discovered individually with B. S. Shastry the corresponding Haldane-Shastry model, which describes spinon excitations of an exactly solvable model of a spin chain, and the spinons exhibit the anyonic statistics [22, 56]. The Calogero-Sutherland model [57] is mathematically equivalent to the Haldane-Shastry model, but the particles are either bosons or fermions with long-range interaction, where the anyonic statistics is tuned by a parameter λ in its interaction term [57, 58]. In 2022, the Tarruell group from Barcelona has realized the chiral BF anyons in an optical dressed BEC [54, 59], based on the one-dimensional topological gauge field theory developed by S. J. Rabello [60] and L. Griguolo [61, 62] that is the one-dimensional reduction of Chern-Simon field theory [3, 35] and is also an equivalent theory to the Kundu model in the regime of vanishing contact interactions [59, 62].

Inspired by the generalized commutation relation by Kundu [49], and the result by C. Vitoriano and M. D. Coutinho-Filho [63] that the fractional statistics can be realized by a Hubbard model with correlated hopping, in 2011 Tassilo Keilmann et al. proposed the *Anyon-Hubbard model* (AHM) that is described by second quantized anyonic operators in an optical lattice [64], which is also the framework of the thesis and will be discussed elaborately in **Ch.** 2. The intriguing point about AHM is that although the braid group B_N doesn't show up naturally in $d = 1$, the discrete configuration enables the definition of the braid anyons in one dimension [33]. By performing the fractional Jordan-Wigner transformation [45, 46, 64, 65], an exact non-local mapping of anyonic operators to the bosonic operators, AHM would result in its bosonic representation which is essentially an extended Bose-Hubbard model [66]. The hopping terms in the bosonic representation are attached by a density-dependent Peierls phase, which tickles the issue of experimental realizations. Up to now, there are several experimental proposals in the optical lattice, such as optical waveguide [67], Raman-tunneling [64] and Floquet engineering [68, 69]. The Greiner group realized two Abelian anyons in one dimension in 2023 via the Floquet engineering of the optical lattice [70]. In their work, three-tone modulations are applied to the optical lattice which allows a maximum local occupation of $n = 2$. In **Fig.** 1.9 shows two anyons undergoing a quantum walk in the one-dimensional optical lattice, and the asymmetric transport behaviour shows the parity-breaking feature of anyons, which we will also show in **Sec.** 2.4 and **Sec.** 3.6.

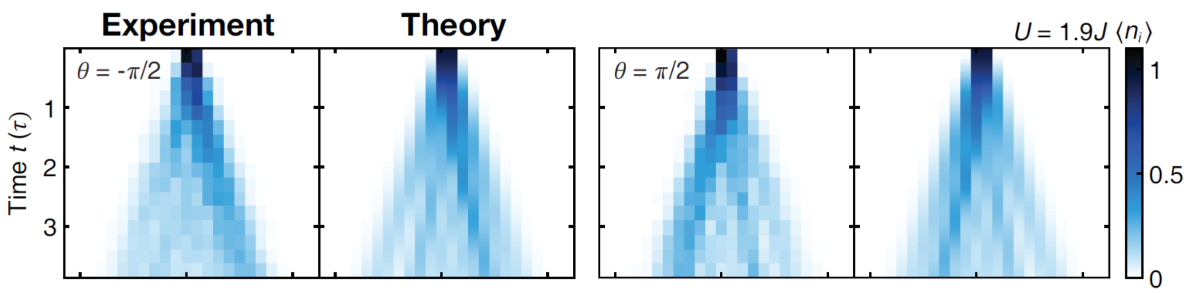

Figure 1.9: The density plot of the asymmetric transport [70]. Two anyons with either $\theta = \pi/2$ or $\theta = -\pi/2$ are prepared on the same lattice site with on-site interaction $U = 1.9J$, then they go through a quantum random walk. The evolution of average particle density shows an asymmetric feature: For $\theta = -\pi/2$, more density goes to the right, and reversely more density goes to the left for $\theta = \pi/2$. This indicates that the inversion of statistical parameter θ corresponds to either a spatial inversion or temporal inversion. Also, the experimental results align with the effective theory proposed in **Ref.** [70].

1.3 Outline of the thesis

Although the AHM has been proposed for more than a decade, it still remains a *terra incognita*. Especially the experimental implementations for many-body anyons in a discrete one dimension are also missing. This encourages us to look from the theoretical perspective and try to understand the many-body behaviours of one-dimensional anyons in a lattice, which we hope will also motivate the respective experimental progresses.

In the following, we first introduce the Anyon-Hubbard model in **Ch.** 2, where we discuss the braiding in one dimension, from which one can construct the generalized commutation relation for anyons in a discrete one dimension. The properties of the anyonic operator algebra would be then investigated, which will be largely distinct from the conventional canonical commutation relation for bosons and canonical anti-commutation relation for fermions. Then, we show how to map AHM to its bosonic representation via the fractional Jordan-Wigner transformation, and discuss subsequently that the symmetry breakings are encoded in the bosonic Hamiltonian, which is one of the deep-rooted features of anyons that would be mentioned from time to time among the thesis. Furthermore, we discuss how the Jordan-Wigner transformation induces a twist to the periodic boundary condition and how to cure this twist via a local gauge transformation.

The main part of the thesis is devoted to **Ch.** 3, where we propose the modified Bogoliubov *ansatz*, which encodes the non-vanishing momentum shift of the condensate. Inserting this *ansatz* in the bosonic Hamiltonian, we are allowed to discuss in two steps. In first step we focus on the mean-field part of the *ansatz*. With condensate density and condensate quasi-momentum as two parameters in the complex order parameter, we find under the minimalization requirement for the mean-field energy that the condensate density is restrained by the statistical parameter θ with non-negative on-site interaction. It also resembles the generalized Pauli principle [55] that transmutates from Bose-Einstein statistics to Fermi-Dirac statistics. Subsequently the anyonic effective mass is derived. Then from the discussion about isothermal compressibility, we find an explicit expression for the statistical interaction. Then in the second step, we go through the Bogoliubov transformation, which converts the interacting canonical bosons to non-interacting bosonic Landau quasi-particles. With the resulting asymmetric Bogoliubov dispersion, we investigate the quantum depletion solely caused by statistical interaction. Also, the asymmetric sound velocities, which are rooted in the breaking of spatio-temporal inversion, are discussed and compared with the result from the extended Tomonaga-Luttinger liquid theory, which is a strong coupling theory in the continuum.

Based on the Bogoliubov dispersion and the valid range of modified Bogoliubov theory, we further investigate the different types of correlation functions in **Ch.** 4, which characterize the low-energy and collective behaviours of the quantum system that are experimentally measurable: the spatial coherence, the quasi-momentum distribution for bosons, the pair correlation and the corresponding static structure factor. Finally, in **Ch.** 5 we conclude the present work and give some hints on further relevant research topics. Some supplementary discussions are distributed to the appendices.

Chapter 2

Anyon-Hubbard Model

In the following, we introduce the core model of this thesis: the Anyon-Hubbard model (AHM) in a one-dimensional lattice. As mentioned, Tassilo Keilmann *et al.* proposed this model in 2011 [64]. It should be remarked that AHM does not originate from the microscopic deduction but rather from the inspirations of the correlated hopping [63] and the generalized commutation relation for anyons [49]. Starting from this model, one can make an exact mapping between bosons and anyons via the so-called generalized Jordan-Wigner transformation, giving the possibility to experimentally realize anyons in one dimension via their bosonic parent particles [70, 71]. To this end, we first introduce the Anyon-Hubbard Hamiltonian, and show how the braiding in a discrete one dimension legitimates the anyons in the lattice and correspondingly anyonic algebra can nest therein. Then we derive the bosonic representation of AHM and investigate the effects of boundary conditions and the symmetries. We will close this chapter with the latest experimental realization about 1D anyons.

2.1 Anyon-Hubbard Hamiltonian

The form of the Anyon-Hubbard model (AHM) in a one-dimensional optical lattice reads in the second quantization language

$$\hat{H}_{\mathrm{AHM}} = -J \sum_{j=1}^{L} \left(\hat{a}_j^\dagger \hat{a}_{j+1} + \mathrm{h.c.} \right) - \mu \sum_{j=1}^{L} \hat{n}_j + \frac{U}{2} \sum_{j=1}^{L} \hat{n}_j (\hat{n}_j - 1) \,, \tag{2.1}$$

which describes the hopping process of the anyons between the nearest neighbour lattice sites with two-body contact interaction strength U, which is related to the depth of the lattice site. The lattice size is $l = L \cdot a$, where L is the number of lattice sites and a is the lattice spacing. The appearance of chemical potential μ in (2.1) indicates that we are working with the grand canonical ensemble. The boundary condition to consider here is either periodic boundary condition (PBC) which demands $\hat{a}_j = \hat{a}_{L+j}$, or open boundary condition (OBC) $\hat{a}_0 = \hat{a}_{L+1} = 0$. Depending on the chosen boundary condition, there will be special restrictions on the anyon-Hubbard Hamiltonian. Throughout this thesis, we use only the PBC and will discuss it in a later section.

AHM (2.1) shares the same mathematical form as the usual Bose-Hubbard model [72]. The distinction comes from the fact that 1D anyons obey fractional statistics [21, 25] and therefore the generalized commutation relation for anyons changes the whole game and one must take it into account. In one-dimensional lattice, we have discrete local anyonic operators $\hat{a}_j$ and $\hat{a}_j^\dagger$, and the particle number operator is then conventionally defined as $\hat{n}_j = \hat{a}_j^\dagger \hat{a}_j$. As already discussed in **Sec.** 1.1.1, in one spatial dimension the braid group is not fundamental but can nevertheless be constructed artificially. Here below, we show that the generalized commutation relation for anyons in a one-dimensional lattice can be implemented as described in **Ref.** [33].

2.2 Braiding in A Discrete 1D and Anyonic Algebra

To extend the discussion in **Sec.** 1.1.1, we first introduce the pairwise exchange operation that interchanges the particle labelled i with the one labelled $(i+1)$. In the symmetry group S_N it is simply the elementary transposition $\hat{S}_i$. It obeys the following exchange relations [31]

$$\text{Self-inverse: } \hat{S}_i^2 = 1\,, \tag{2.2a}$$
$$\text{Yang-Baxter: } \hat{S}_i\hat{S}_{i+1}\hat{S}_i = \hat{S}_{i+1}\hat{S}_i\hat{S}_{i+1}\,, \tag{2.2b}$$
$$\text{Locality: } \hat{S}_i\hat{S}_j = \hat{S}_j\hat{S}_i\,,\ \text{for } |i-j| > 1\,. \tag{2.2c}$$

The first relation corresponds to the property that the double exchange of the label is the same as no exchange, as mentioned in **Sec.** 1.1.1. Therefore there are only two possible exchange phases for $\hat{S}_i$,

$$\hat{S}_i^2\,|\Psi\rangle = S_i^2\,|\Psi\rangle = 1\cdot|\Psi\rangle \quad \Rightarrow \quad S_i = \pm 1\,. \tag{2.3}$$

Then the Yang-Baxter relation (2.2b) describes the homogeneity for the action of $\hat{S}_i$ in the discrete one dimension, therefore the exchange phase should be the same for all the labels,

$$S_i^2 S_{i+1} = S_{i+1}^2 S_i \quad \Rightarrow \quad S_i = \text{const.} = S = \pm 1\,. \tag{2.4}$$

The third relation indicates that distant exchanges do not influence each other and impose no constraint on the exchange phase. Based on these results, we conclude that there are only two exchange phases in symmetry group S_N, which for bosons is $S = +1$ and for fermions $S = -1$. Further we can construct the permutation operator via a sequence of products of the transpositions,

$$\hat{\mathcal{P}}_{i,j} = \prod_{l=j-1}^{i} \hat{S}_l\,. \tag{2.5}$$

However, as the configuration space of braid group B_N is not single-connected (**Sec.** 1.1.1), the elementary operation is now the distinct braidings $\hat{B}_i$ and $\hat{B}_i^{-1}$, and the corresponding relations are

$$\text{Braid inequivalence: } \hat{B}_i^2 \neq 1\,, \tag{2.6a}$$
$$\text{Yang-Baxter: } \hat{B}_i\hat{B}_{i+1}\hat{B}_i = \hat{B}_{i+1}\hat{B}_i\hat{B}_{i+1}\,, \tag{2.6b}$$
$$\text{Locality: } \hat{B}_i\hat{B}_j = \hat{B}_j\hat{B}_i\,,\ \text{for } |i-j| > 1\,. \tag{2.6c}$$

Diagrammatically this can be shown via the strand diagrams below [31], where it's clear that the paths connecting the particles before and after the braiding operations can not coincide:

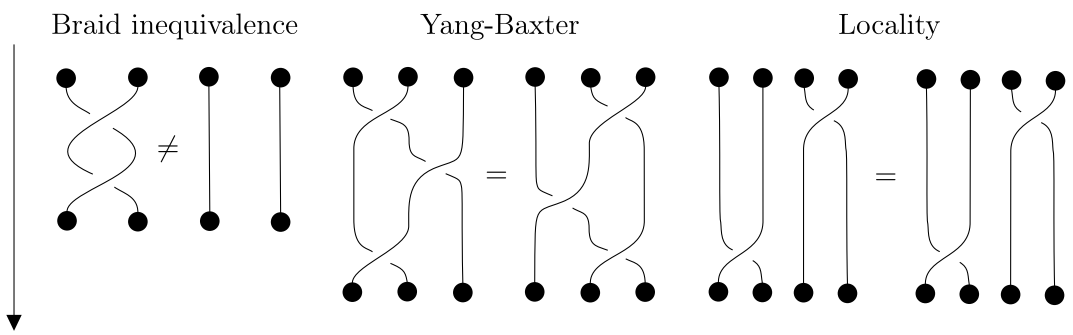

Therefore from (2.6a-2.6b) one can choose the abelian representation

$$\hat{B}_i \left|\Psi\right\rangle = e^{-i\theta} \left|\Psi\right\rangle \,, \tag{2.7}$$

$$\hat{B}_i^{-1} \left|\Psi\right\rangle = e^{i\theta} \left|\Psi\right\rangle \tag{2.8}$$

with $\theta \in [0, 2\pi)$ the arbitrary exchange phase, i.e. the statistic parameter. Further, due to the 2π periodicity of θ and the fact that the time-reversal operation can reflect θ as $\theta \to -\theta$, which comes later from in **Sec.** 2.4 where we discuss the symmetries, we will focus on the range $\theta \in [0, \pi]$ in the following.

As the above discussions use a discretization language, we can implement braiding in a one-dimensional lattice without risk. However, there is a final piece that is missing from the full picture for anyonic algebra. Namely, one could not define a path for particle exchange on the same site. In such case, the self-inverse relation (2.2a) is somehow recovered, and there again, one would have the operator algebra for S_N. The complete braidings is shown in **Fig.** 2.1.

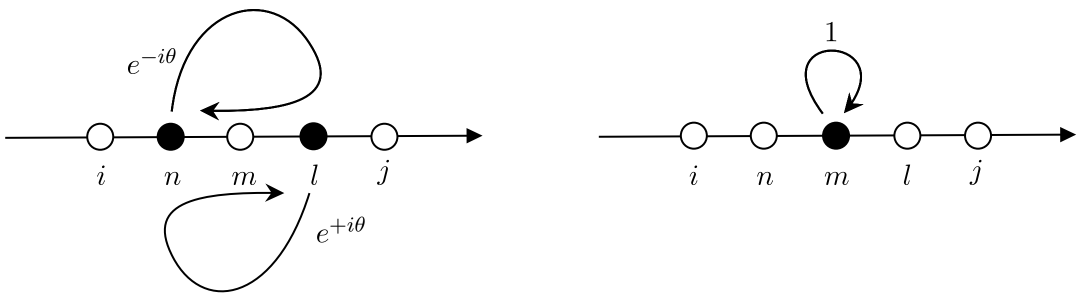

Figure 2.1: Exchange of two anyons in 1D lattice. Left: the cases when the exchange occurs at different lattice sites, the acquired phase is different for clockwise or anticlockwise exchange. Right: the exchange that occurs at the same lattice site leaves the wavefunction unchanged, therefore it's again the bosonic case.

All the given arguments about the braiding in a discrete one dimension correspond to anyonic algebra as given in **Refs.** [46, 64]

$$\hat{a}_i \hat{a}_j^\dagger - k e^{-i\theta \mathrm{sign}(i-j)} \hat{a}_j^\dagger \hat{a}_i = \delta_{i,j} \,, \tag{2.9a}$$

$$\hat{a}_i \hat{a}_j - k e^{i\theta \mathrm{sign}(i-j)} \hat{a}_j \hat{a}_i = 0 \,, \tag{2.9b}$$

$$\hat{a}_i^\dagger \hat{a}_j^\dagger - k e^{i\theta \mathrm{sign}(i-j)} \hat{a}_j^\dagger \hat{a}_i^\dagger = 0 \,. \tag{2.9c}$$

The sign function $\mathrm{sign}(i-j)$ is defined as

$$\mathrm{sign}(i-j) = \begin{cases} +1 \,, & \text{when } i > j \,, \\ -1 \,, & \text{when } i < j \,, \\ 0 \,, & \text{when } i = j \,, \end{cases} \tag{2.10}$$

which embodies the braiding in discrete one dimension, as it explicitly takes into account the relative position of the anyons on the one-dimensional lattice: $\mathrm{sign}(i-j) = +1$ for clockwise braiding, $\mathrm{sign}(i-j) = -1$ for anti-clockwise braiding and $\mathrm{sign}(i-j) = 0$ indicates the on-site exchange. When the index $k = -1$ it implies the anti-commutation with hard-core constraint $(\hat{a}_i)^2 = 0$ on local occupation. When $k = 1$, it corresponds to the commutation relation and imposes no constraint on local occupation. Furthermore, a special remark shall be made to the $i = j$, the on-site case. (2.9a-2.9c) would be reduced to the standard canonical commutation relations

(CCR) for bosons or canonical anti-commutation relations (CAR) for fermions depending on k. This implies that the variation from $\theta = 0$ to $\theta = \pi$ corresponds either to the transmutation of fermions into hard-core bosons, whose local occupation is restricted to one due to the exclusion principle ($k = -1$), or to the transmutation of bosons into so-called pseudo-fermions ($k = 1$), as no exclusion principle applies to these fermions. Therefore pseudo-fermions are on-site bosons and off-site fermions. Also from the relations

$$\begin{aligned} &\hat{a}_i^\dagger \hat{n}_j - \hat{n}_j \hat{a}_i^\dagger = \hat{a}_i^\dagger \hat{a}_j^\dagger \hat{a}_j - \hat{a}_j^\dagger \hat{a}_j \hat{a}_i^\dagger = k e^{i\theta \mathrm{sign}(i-j)} \hat{a}_j^\dagger \hat{a}_i^\dagger \hat{a}_j - \hat{a}_j^\dagger \hat{a}_j \hat{a}_i^\dagger \\ =& k e^{i\theta \mathrm{sign}(i-j)} k^{-1} e^{i\theta \mathrm{sign}(j-i)} \hat{a}_j^\dagger (\hat{a}_j \hat{a}_i^\dagger - \delta_{i,j}) - \hat{a}_j^\dagger \hat{a}_j \hat{a}_i^\dagger = -\delta_{i,j} \hat{a}_i^\dagger \, , \end{aligned} \tag{2.11}$$

$$\begin{aligned} &\hat{a}_i \hat{n}_j - \hat{n}_j \hat{a}_i = \hat{a}_i \hat{a}_j^\dagger \hat{a}_j - \hat{a}_j^\dagger \hat{a}_j \hat{a}_i = (k e^{i\theta \mathrm{sign}(i-j)} \hat{a}_j^\dagger \hat{a}_i + \delta_{i,j}) \hat{a}_j - \hat{a}_j^\dagger \hat{a}_j \hat{a}_i^\dagger \\ =& (k e^{i\theta \mathrm{sign}(i-j)} k^{-1} e^{i\theta \mathrm{sign}(j-i)} \hat{a}_j^\dagger \hat{a}_i + \delta_{i,j}) \hat{a}_j - \hat{a}_j^\dagger \hat{a}_j \hat{a}_i^\dagger = \delta_{i,j} \hat{a}_i \, , \end{aligned} \tag{2.12}$$

that also hold for CCR and CAR, the operator $\hat{n}_j = \hat{a}_j^\dagger \hat{a}_j$ is indeed the local occupation operator for anyons. The non-commutative feature of the relation (2.9c) for off-site particles indicates the non-locality of anyons. Further, when one considers only hopping-like quadratic terms $\hat{a}_i^\dagger \hat{a}_j$, the corresponding commutator would result in [46, 73]

$$\left[\hat{a}_i^\dagger \hat{a}_j, \hat{a}_k^\dagger \hat{a}_l\right]_- = \delta_{j,k} \hat{a}_i^\dagger \hat{a}_l - \delta_{l,i} \hat{a}_k^\dagger \hat{a}_j + \Delta_{i,j,k,l}^k \hat{a}_i^\dagger \hat{a}_k^\dagger \hat{a}_j \hat{a}_l \, . \tag{2.13}$$

where the coefficient $\Delta_{i,j,k,l}^k$ is

$$\Delta_{i,j,k,l}^k = k \left[e^{-i\theta \mathrm{sign}(j-k)} - e^{-i\theta(\mathrm{sign}(l-i) - \mathrm{sign}(i-k) - \mathrm{sign}(l-j))} \right] . \tag{2.14}$$

Compared with the results from CCR and CAR, (2.13) has additionally a quartic term. This is an interaction-like term and makes anyonic algebra drastically differ from CCR and CAR. First of all, the commutation of anyonic quadratic operators generates higher-order contributions and thus is not algebraically closed. It also means that the anyons are intrinsically interacting even in the absence of any inter-particle interaction [46, 73]—the anyonic statistic interaction. Also, there is a widely verified result that the non-interacting anyons are equivalent to interacting bosons or interacting fermions [3, 48, 74]. This motivates us to relate anyons, which are anyhow abstract entities, to conventional particles. To this end, we introduce the fractional Jordan-Wigner transformation. Due to the poorer phenomenology of the $k = -1$ case in (2.9a-2.9c) [46], in the following we focus solely on the $k = 1$ case, which corresponds to the bosons to pseudo-fermions transmutation.

2.3 Fractional Jordan-Wigner Transformation

P. Jordan and E. Wigner introduced in 1928 a non-local mapping from spin-1/2 operators to spinless fermions in one dimension [75, 76]:

$$\hat{\sigma}_j^- = e^{i\pi \sum_{l<j} \hat{c}_j^\dagger \hat{c}_j} \hat{c}_j \, . \tag{2.15}$$

The generalization of such a transformation to the anyonic case is proposed in [64] and one can find the detailed derivation in [46]. The fractional Jordan-Wigner transformation then reads

$$\hat{a}_j = \hat{b}_j \, e^{i\theta \sum_{l<j} \hat{n}_l} \, . \tag{2.16}$$

This transformation (2.16) maps anyons to its parent particle, which are bosons with operators $\hat{b}_j$ and $\hat{b}_j^\dagger$. Also, the mapping binds an additional density-dependent Peierls phase to the bosonic operator. This phase accumulates all particle-filling operators on the left of the j-th lattice site

$1 \leq j$ and thus is a non-local. It is called the density-dependent Peierls phase. Note that the transformation leads to the invariance of the number operator in real space,

$$\hat{n}_j = \hat{a}_j^\dagger \hat{a}_j \overset{(2.16)}{=} \hat{b}_j^\dagger \hat{b}_j \,, \tag{2.17}$$

which again ensured that the anyons could be counted locally. Inserting (2.16) into (2.9a), for the case $i < j$, we have

$$\hat{a}_i \hat{a}_j^\dagger \overset{(2.16)}{=} e^{-i\theta \sum_{i<l<j} \hat{n}_l} \hat{b}_i \hat{b}_j^\dagger e^{-i\theta \hat{n}_i} \tag{2.18a}$$

$$e^{-i\theta} \hat{a}_j^\dagger \hat{a}_i \overset{(2.16)}{=} e^{-i\theta \sum_{i<l<j} \hat{n}_l} e^{-i\theta(\hat{n}_i - 1)} \hat{b}_j^\dagger \hat{b}_i \,, \tag{2.18b}$$

which are combined to

$$\hat{a}_i \hat{a}_j^\dagger - e^{-i\theta} \hat{a}_j^\dagger \hat{a}_i = e^{-i\theta \sum_{i<l<j} \hat{n}_l} \left(\hat{b}_i \hat{b}_j^\dagger e^{-i\theta \hat{n}_i} - e^{-i\theta(\hat{n}_i - 1)} \hat{b}_j^\dagger \hat{b}_i \right) . \tag{2.19}$$

Using the operator identity [77]

$$e^{\xi \hat{A}} \hat{B} e^{-\xi \hat{A}} = \sum_k^\infty \frac{\xi^k}{k!} \underbrace{[\hat{A}, [\hat{A}, \ldots, [\hat{A}}_{k \text{ times}}, \hat{B}] \ldots] \tag{2.20}$$

and the relation

$$[\hat{n}_j, \hat{b}_j]_- = -\hat{b}_j \,, \tag{2.21}$$

we have then

$$e^{i\theta \hat{n}_i} \hat{b}_i e^{-i\theta \hat{n}_i} = \sum_k^\infty \frac{(i\theta)^k \cdot (-1)^k}{k!} \hat{b}_i = e^{-i\theta} \hat{b}_i. \tag{2.22}$$

Multiply (2.22) with $e^{-i\theta \hat{n}_i}$ from the left, we finally have

$$\hat{b}_i e^{-i\theta \hat{n}_i} = e^{-i\theta} e^{-i\theta \hat{n}_i} \hat{b}_i \,, \tag{2.23}$$

then (2.19) is further evaluated to

$$\begin{aligned} \hat{a}_i \hat{a}_j^\dagger - e^{-i\theta} \hat{a}_j^\dagger \hat{a}_i &= e^{-i\theta \sum_{i<l<j} \hat{n}_l} e^{-i\theta(\hat{n}_i + 1)} \left(\hat{b}_i \hat{b}_j^\dagger - \hat{b}_j^\dagger \hat{b}_i \right) \\ &= 0 \,, \end{aligned} \tag{2.24}$$

and we have proven the anyonic commutation relations for $i < j$. Similar steps would lead to the same result for $i > j$ and the case $i = j$ is trivial, therefore complete a full proof that the anyonic algebra can be constructed via the generalized Jordan-Wigner transformation.

One important feature of this transformation is that, although it doesn't affect the open boundary condition [30], the generalized Jordan-Wigner transformation maps the periodic boundary condition for anyons $\hat{a}_{L+1} = \hat{a}_1$ to

$$\hat{b}_{L+1} = \hat{b}_1 \, e^{-i\theta \hat{N}}. \tag{2.25}$$

This means in the bosonic representation of the AHM with periodic boundary conditions, we actually have now a twisted boundary condition that depends on the total particle number

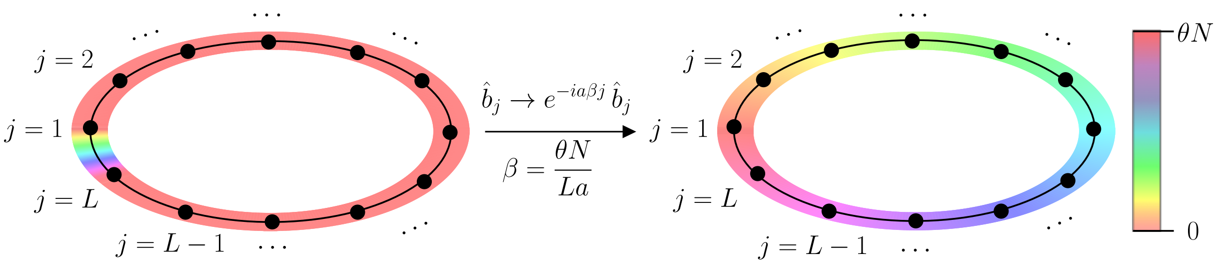

Figure 2.2: Homogenize the twisted phase at the boundary to the overall one-dimensional ring via a local gauge transformation. The colormap represents the phase change that comes from the twisted boundary, indicating that the twist is 'loosened' to the whole 1D chain after such a transformation.

operator $\hat{N}$ and the statistic parameter θ. Therefore we have the bosonic Hamiltonian of AHM as

$$\begin{aligned}\hat{H}^{(\mathrm{B})}_{\mathrm{AHM}} = &- J\sum_{j=1}^{L-1}\left(\hat{b}_j^\dagger\, e^{i\theta\hat{n}_j}\hat{b}_{j+1} + \mathrm{h.c.}\right) - J\left(\hat{b}_L^\dagger\, e^{i\theta\hat{n}_L}\hat{b}_1\, e^{-i\theta\hat{N}} + \mathrm{h.c.}\right)\\ &- \mu\sum_{j=1}^{L}\hat{b}_j^\dagger\hat{b}_j + \frac{U}{2}\sum_{j=1}^{L}\hat{b}_j^\dagger\hat{b}_j^\dagger\hat{b}_j\hat{b}_j\,. \end{aligned} \tag{2.26}$$

One could see that (2.26) has the additional term from the twisted boundary. To circumvent this unwanted twist, we homogenize this term with other in-chain hopping terms. This amounts to a local gauge transformation

$$\hat{b}_j \to e^{-ia\beta j}\hat{b}_j \tag{2.27}$$

that transforms the bosonic Hamiltonian (2.26) to

$$\begin{aligned}\hat{H}^{(\mathrm{B})}_{\mathrm{AHM}} = &- J\sum_{j=1}^{L-1}\left(\hat{b}_j^\dagger\, e^{ia\beta j}e^{i\theta\hat{n}_j}e^{-ia\beta(j+1)}\hat{b}_{j+1} + \mathrm{h.c.}\right) - J\left(\hat{b}_L^\dagger\, e^{i\theta\hat{n}_L}e^{i\left[(L-1)\beta-\theta\hat{N}\right]}\hat{b}_1 + \mathrm{h.c.}\right)\\ &- \mu\sum_{j=1}^{L}\hat{b}_j^\dagger\hat{b}_j + \frac{U}{2}\sum_{j=1}^{L}\hat{b}_j^\dagger\hat{b}_j^\dagger\hat{b}_j\hat{b}_j \end{aligned} \tag{2.28}$$

Note that with the conserved total number of particles, one can simply replace the total particle number operator with its exception value, a scalar $\langle\hat{N}\rangle = N$.

Now, by choosing the gauge

$$\beta = \frac{\theta N}{La}\,, \tag{2.29}$$

we have now the homogenized bosonic Hamiltonian

$$\hat{H}^{(\mathrm{B})}_{\mathrm{AHM}} = -J\sum_{j=1}^{L}\left(\hat{b}_j^\dagger\, e^{i\theta\hat{n}_j}e^{i\frac{\theta N}{L}}\hat{b}_{j+1} + \mathrm{h.c.}\right) - \mu\sum_{j=1}^{L}\hat{b}_j^\dagger\hat{b}_j + \frac{U}{2}\sum_{j=1}^{L}\hat{b}_j^\dagger\hat{b}_j^\dagger\hat{b}_j\hat{b}_j\,, \tag{2.30}$$

As shown in **Fig.** 2.2, meaning the twisted phase (2.29) is sent from the boundary to the overall 1D chain and we have the same twisted phase $e^{i\frac{\theta N}{L}}$ for all hopping terms in (2.30). In such sense, the periodic boundary condition is recovered for the bosonic representation,

$$\hat{b}_j = \hat{b}_{j+L}\,. \tag{2.31}$$

2.4 Symmetry Breaking of the Bosonic Hamiltonian

Now we discuss the symmetry properties of the bosonic Hamiltonian (2.30). In the bosonic limit $\theta \to 0$, (2.30) would reduce to Bose-Hubbard Hamiltonian, which has parity symmetry, time-reversal symmetry and translational invariance under periodic boundary condition. Once goes to the anyonic range $\theta \in (0, \pi)$, the correlated hopping in the Hamiltonian would violate the parity symmetry $\hat{\mathcal{P}}$ and the time-reversal $\hat{\mathcal{T}}$, nevertheless one could have a generalized anyonic inversion symmetry in the Hamiltonian [30, 51, 78], as we shall see in the following.

2.4.1 Parity

The parity operation, i.e. the spatial inversion is simply a mirroring of the spatial coordinates $x \to -x$. In our lattice system, this amounts to a reversed labeling order of the sites, which means $j \to L - j + 1$, and therefore the parity operator acts as

$$\hat{\mathcal{P}}^\dagger \hat{b}_j \hat{\mathcal{P}} = \hat{b}_{L-j+1} \,. \tag{2.32}$$

Correspondingly, the momenta of the particles after the parity operation are also reversed and include additionally a k-dependent gauge phase that originates from the boundary twist

$$\begin{aligned}\hat{\mathcal{P}}^\dagger \hat{b}_k \hat{\mathcal{P}} &= \frac{1}{\sqrt{L}} \sum_j e^{-ikja} \hat{\mathcal{P}}^\dagger \hat{b}_j \hat{\mathcal{P}} = \frac{1}{\sqrt{L}} \sum_j e^{-ikja} \hat{b}_{L-j+1} \\ &= e^{-i(k+\beta)(L+1)a} \hat{b}_{-k} \,.\end{aligned} \tag{2.33}$$

Further, after the spatial inversion, the bosonic Hamiltonian becomes

$$\hat{\mathcal{P}}^\dagger \hat{H}^{(\mathrm{B})}_{\mathrm{AHM}} \hat{\mathcal{P}} = -J \sum_j \left(\hat{b}^\dagger_j \, e^{i\theta \hat{n}_{j+1}} e^{i\frac{\theta N}{L}} \hat{b}_{j+1} + \mathrm{h.c.} \right) - \mu \sum_j \hat{n}_j + \frac{U}{2} \sum_j \hat{n}_j (\hat{n}_j - 1) \tag{2.34}$$

which clearly breaks the parity symmetry as $\hat{\mathcal{P}}^\dagger \hat{H}^{(\mathrm{B})}_{\mathrm{AHM}} \hat{\mathcal{P}} \neq \hat{H}^{(\mathrm{B})}_{\mathrm{AHM}}$, more specially the density-dependent Peierls phase change from $e^{i\theta \hat{n}_i}$ to $e^{-i\theta \hat{n}_{j+1}}$. Also, parity breaking is rooted in the anyonic algebra (2.9a-2.9c) as the $i > j$ is non-equivalent to $i < j$.

2.4.2 Time reversal

The time reversal operation is an operation that reflects the time coordinate $t \to -t$, which also means the reflection in momentum space $k \to -k$ while keeping the spatial coordinate invariant $x \to x$ [30],

$$\hat{\mathcal{T}}^\dagger \hat{b}_j \hat{\mathcal{T}} = \hat{b}_j \,. \tag{2.35}$$

Further, in order to maintain the CCR after the operation, the time-reversal operator is anti-unitary, and therefore $\hat{\mathcal{T}}^\dagger i \hat{\mathcal{T}} = -i$ [30]. Altogether this would result in:

$$\hat{\mathcal{T}}^\dagger \hat{b}_k \hat{\mathcal{T}} = \hat{\mathcal{T}}^\dagger \frac{1}{\sqrt{L}} \sum_j e^{-i(k+\beta)ja} \hat{b}_j \hat{\mathcal{T}} = \hat{b}_{-k} \,. \tag{2.36}$$

Then the bosonic Hamiltonian after the time-reversal operation would be

$$\hat{\mathcal{T}}^\dagger \hat{H}^{(\mathrm{B})}_{\mathrm{AHM}} \hat{\mathcal{T}} = -J \sum_j \left(\hat{b}^\dagger_j \, e^{-i\theta \hat{n}_j} e^{-i\frac{\theta N}{L}} \hat{b}_{j+1} + \mathrm{h.c.} \right) - \mu \sum_j \hat{n}_j + \frac{U}{2} \sum_j \hat{n}_j (\hat{n}_j - 1) \,, \tag{2.37}$$

which again results in $\hat{\mathcal{T}}^\dagger \hat{H}^{(\mathrm{B})}_{\mathrm{AHM}} \hat{\mathcal{T}} \neq \hat{H}^{(\mathrm{B})}_{\mathrm{AHM}}$ and indicates a broken time-reversal symmetry. But we note that

$$\hat{\mathcal{T}}^\dagger \hat{H}^{(\mathrm{B})}_{\mathrm{AHM}}(\theta) \hat{\mathcal{T}} = \hat{H}^{(\mathrm{B})}_{\mathrm{AHM}}(-\theta) \,, \tag{2.38}$$

which means the time-reversal corresponds to $\theta \to -\theta$. In a later chapter, when we derive the asymmetric sound velocities in the long-wavelength limit, we will find that the two species of sound velocities can be interchanged via such inversion of the statistic parameter θ.

2.4.3 Combined symmetry: anyonic parity

Although bosonic Hamiltonian (2.30) breaks parity $\hat{\mathcal{P}}$ and time-reversal $\hat{\mathcal{T}}$, it was shown in **Refs.** [46, 78] that one can combine the $\hat{\mathcal{T}}\hat{\mathcal{P}}$ symmetry with the non-linear gauge transformation,

$$\hat{\mathcal{K}} = e^{i\frac{\theta}{2}\sum_j \hat{n}_j(\hat{n}_j-1)}\hat{\mathcal{T}}\hat{\mathcal{P}} \tag{2.39}$$

then such a combined symmetry operation $\hat{\mathcal{K}}$ leaves the bosonic Hamiltonian (2.30) invariant,

$$\hat{\mathcal{K}}^\dagger \hat{H}^{(\mathrm{B})}_{\mathrm{AHM}} \hat{\mathcal{K}} = \hat{H}^{(\mathrm{B})}_{\mathrm{AHM}} \,. \tag{2.40}$$

Although the operator $\hat{\mathcal{K}}$ is highly non-linear when expressed by the bosonic operators, its physic meaning is clear in the anyonic representation,

$$\hat{\mathcal{K}}^\dagger \hat{a}_j \hat{\mathcal{K}} = \hat{a}_{L-j+1} e^{i\theta\hat{N}} \,. \tag{2.41}$$

Therefore, $\hat{\mathcal{K}}$ can be expressed as a generalized inversion symmetry, as it reverses the labeling order of anyonic operators and further attaches a global density-dependent phase $e^{i\theta\hat{N}}$.

2.5 Experimental realization

As mentioned in **Sec.** 1.2, there are several experimental proposals that try to realize the correlated hopping in the bosonic Hamtilonian of the Anyon-Hubbard Model, i.e. the density-dependent Peierls phase. Up to now the actual realization is done by M. Greiner *et al.* [70] by the Floquet engineering method [68], which applies external periodic drive to a tilted optical lattice [69]. Here below we introduce the basic idea in the **Ref.** [70].

To realize the bosonic Hamiltonian (2.30), one starts with an initial Hamiltonian based on the Bose-Hubbard model

$$\hat{H}_{\mathrm{init}} = -J_0 \sum_j \left(\hat{b}_j^\dagger \hat{b}_{j-1} + \mathrm{h.c.}\right) + \frac{U_0}{2}\sum_j \hat{n}_j(\hat{n}_j - 1) + E\sum_j j\hat{n}_j \,, \tag{2.42}$$

where J_0 is the hopping amplitude and U_0 is the two-body replusive interaction. Additionally, there is a tilted term on each site with an energy offset E, as shown in the left part of **Fig.** 2.3 **(a)**. To include the time dependence, the Hamiltonian (2.42) is mapped to a rotation frame of reference via a unitary transformation

$$\hat{\mathcal{U}} = \exp\left\{ it\left[(U_0 - U)\hat{H}_{\mathrm{init}} + E\sum_j j\hat{n}_j \right] \right\} , \tag{2.43}$$

with U the detuning that corresponds to the effective on-site interaction. The initial Hamiltonian in the rotational frame is

$$\hat{\tilde{H}} = \hat{\mathcal{U}}\hat{H}_{\mathrm{init}}\hat{\mathcal{U}}^\dagger + i\frac{\partial\hat{\mathcal{U}}}{\partial t}\hat{\mathcal{U}}^\dagger \tag{2.44}$$

$$= -J_0\sum_j \left(\hat{b}_j^\dagger e^{it[E+(U_0-U)(\hat{n}_j-\hat{n}_{j-1})]}\hat{b}_{j-1} + \mathrm{h.c.}\right) + \frac{U}{2}\sum_j \hat{n}_j(\hat{n}_j - 1)\,. \tag{2.45}$$

To implement anyons on the tilted lattice with a maximum local occupation of $n_{j,\max} = 2$, one has to engineer the correlated hopping processes that is depicted at the top of **Fig.** 1.9 **(a)** with so-called *three-tone modulation*. The corresponding frequencies as illustrated at the bottom of **Fig.** 1.9 s**(a)** are:

- $\omega_1 = E$ for a particle hops from a single occupied site to an empty site.
- $\omega_2 = E - (U_0 - U)$ corresponds to the hopping from a singly-occupied site to a singly-occupied site.
- $\omega_3 = E + (U_0 - U)$ induces the hopping from a doubly-occupied site to an empty site.

The hopping energy is controlled by modulating the lattice depth V_0 with a perturbation $\delta V \ll V_0$, therefore by Fluoquet engineering of the lattice depth $V(t) = V_0 + \delta V$ with such three-tone modulation, the hopping energy becomes

$$J(t) = J_0 + \sum_{s=1}^{3} \delta J_s \cos(\omega_s t + \theta_s) = J_0 + \sum_{s=1}^{3} \frac{\delta J_s}{2} \left(e^{i(\omega_s t + \theta_s)} + e^{-i(\omega_s t + \theta_s)} \right), \tag{2.46}$$

where θ_s is the phase component of corresponding driving frequencies ω_s. Inserting (2.46) into (2.44), one obtains the effective Hamiltonian

$$\begin{aligned} \hat{H}_{\text{eff}} = &- J_0 \sum_j \left(\hat{b}_j^\dagger e^{it[E+(U_0-U)(\hat{n}_j - \hat{n}_{j-1})]} \hat{b}_{j-1} + \text{h.c.} \right) \\ &- \sum_{s=1}^{3} \frac{\delta J_s}{2} \sum_j \left(\hat{b}_j^\dagger e^{it[E+(U_0-U)(\hat{n}_j - \hat{n}_{j-1}) - \omega_s] - i\theta_s} \hat{b}_{j-1} + \text{h.c.} \right) + \frac{U}{2} \sum_j \hat{n}_j(\hat{n}_j - 1). \end{aligned} \tag{2.47}$$

One further remark is that for the actual realization of a Bose-Hubbard model with density-dependent Peierls phase with $n_{j,\max} = 2$, one additional condition should be fulfilled,

$$J_0 \ll E, \, |E \pm (U_0 - U)|. \tag{2.48}$$

Therefore the hopping energy is $J \simeq \delta J_s/2$, where the amplitude of different components is chosen to be the same, $J_1 = J_2 = J_3$. Then the statistic parameter θ, as shown at the right of **Fig.** 2.3 **(a)**, is realized by the phase difference of the third component to the other two aligned components,

$$\theta = \theta_3 - \theta_1 = \theta_3 - \theta_2. \tag{2.49}$$

The experimental realization procedure of $\hat{H}_{\text{eff}}$ is shown in **Fig.** 2.3 **(b)**. Starting with a two-dimensional Mott insulator at unity-filling of ^{87}Rb atoms in a deep optical lattice with spacing $a = 680\,\text{nm}$ and potential $V_x = V_y = 45E_R$, where $E_R = h \times 1.24\,\text{kHz}$ is the recoil energy. The initial state is prepared with a digital micromirror device (DMD) which allows to project arbitrary potentials with single lattice site resolution [79], therefore can be seen as an optical tweezer that can move particles among the optical lattice. With DMD, two adjacent columns of atoms are confined along y-axis. Afterwards, applying a magnetic field gradient E per site along the x-axis leads to a tilted optical lattice, from which one subsequently applies the three-tone modulation that realizes several quantum walks under the correlated hopping processes. Afterwards, the whole system is projected to number basis for a fluoresces imaging [70].

The experiment as described in **Ref.** [70] realizes anyons in a lattice site with a maximum local occupation $n_{j,\max} = 2$. The difficulty that prevents the current experiments from being extended from two anyons to the many-body case is that for different lattice occupancy numbers, we should add the corresponding driving frequencies to the experimental platform. Then the deconstructing heating effect is inevitable. Nevertheless, this calls for the necessity to extend both experimentally and theoretically the local occupation to arbitrary numbers [80]. In the next chapter, which is the main part of the thesis, we look at the many-body behaviours of anyons in the weak coupling regime on a one-dimensional lattice. In the discussion that follows, we will show that from the modified Bogoliubov theory, there is no local limit, but rather a global limit, which allows for collective behaviours.

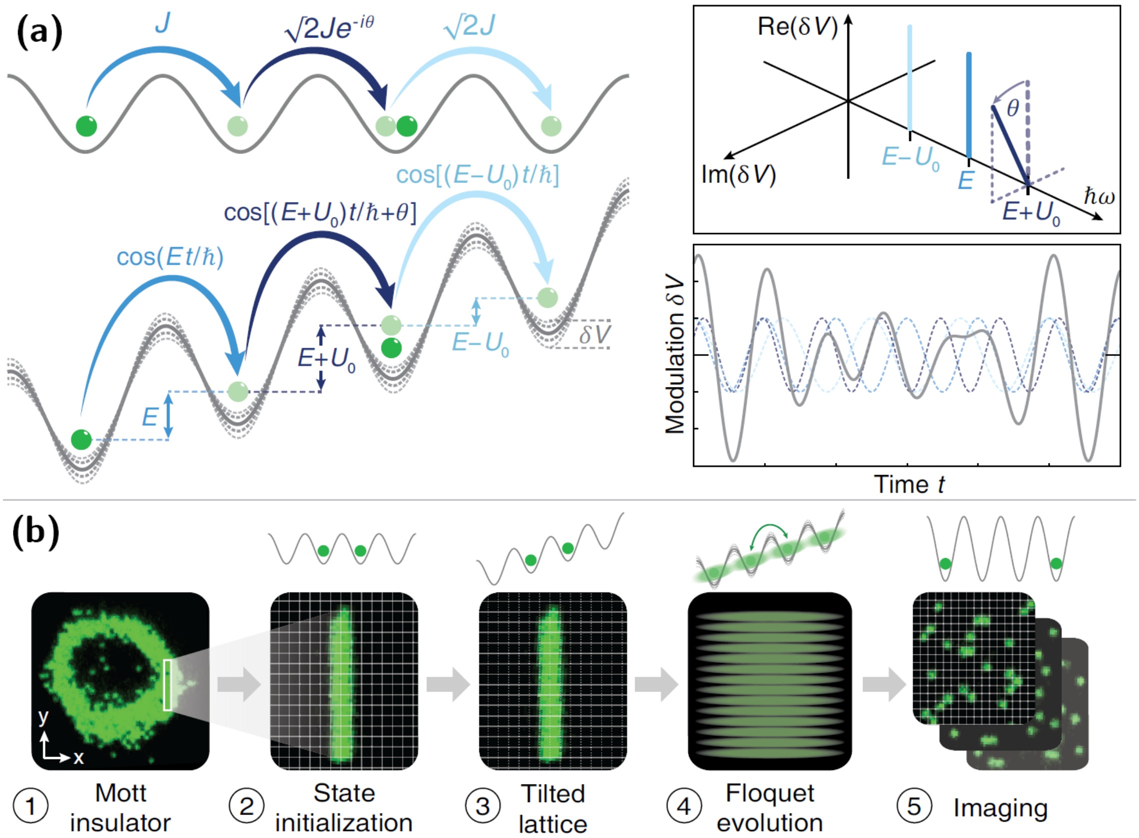

Figure 2.3: The realization of two anyons in 1D [70]. **(a)** is the realization of AHM in a tilted optical lattice with energy offset E per site. The hopping δJ is modulated by the tilted lattice depth δV, and the three different energy gaps correspond to the correlated hopping that depends on the particle number on the site. The statistic parameter θ is the phase difference of the three driving frequencies. The left part shows the three frequencies in the frequency (top) and time (bottom) domain. **(b)** shows the experiment sequence: (1-2) initialize two columns of atoms from a Mott insulator of ^{87}Rb; (3) tilt the lattice such that the lattice depth is lowered in the x-axis for the modulation-induced hopping; (4) apply the three-tone modulation that lead to several independent quantum walk along x; (5) project to the number basis and perform imaging.

Chapter 3

Modified Bogoliubov Theory for Anyons

Having discussed the basic properties of the Anyon-Hubbard model in detail, we derived the corresponding bosonic Hamiltonian with periodic boundary condition (2.30). The fact that one can realize anyons with their parent bosonic particles with correlated hopping gives the insight that anyons can have a macroscopic ground state. Taking inspiration from the success of Bogoliubov theory for bosons in three dimension [72, 81], we want to investigate now the case for anyons in 1D. Although it's a well-known conclusion from the Mermin–Wagner–Hohenberg theorem [82, 83] that states in $d \leq 2$ systems the continuous symmetries can not be spontaneously broken for $T \neq 0$, thus no long-range order can exist and subsequently no true condensate, there are exceptions. The finite-size effect of a one-dimensional lattice suppresses the long-wavelength fluctuations that would destroy the long-range correlations [84]. From the other perspective, the Mermin-Wagner-Hohenberg theory applies only to a quadratic energy-momentum dispersion $E(k) \propto Ak^2$ which corresponds to integer order systems, whereas not the case for a lattice system of anyons that is a fractional order system [85]. Therefore, it is allowed to have quasi-condensate in a low-dimensional system.

This motivates us to work out an analytical approach for the low-energy features of large-N-anyons in a finite-size lattice system in the weak-coupling regime. To this end we propose a modified Bogoliuobv *ansatz* for the bosonic representation of the Anyon-Hubbard model and proceed further to derive the results from the mean-field level and Bogoliubov level. Note that the *ansatz* is an approximation that enforces the existence of condensate, i.e. only a single peak signal in the momentum distribution.

3.1 Generalized Bogoliubov *Ansatz*

To proceed, we remark that normal ordering is crucial for calculating reasonable physical observables as it eliminates the vacuum divergences and results in a physical ground energy [86]. In addition, it simplifies the calculations by reducing the consideration of commutation relations. In the bosonic Hamiltonian, the problem of normal ordering arises in the density-dependent Peierls phase, as it is an exponential of the number operator, $e^{i\theta\hat{n}_j}$. To proceed, one has to use the combinatorial technique called the Stirling number of the second kind $S(q, m)$ [46, 77, 87], which leads to the identity

$$e^{i\theta\hat{n}_j} = \sum_{q=0}^{\infty} \frac{(i\theta)^q}{q!} (\hat{b}_j^\dagger \hat{b}_j)^q = \sum_{q=0}^{\infty} \frac{(i\theta)^q}{q!} \sum_{m=0}^{q} S(q, m)(\hat{b}_j^\dagger)^m (\hat{b}_j)^m \,. \tag{3.1}$$

This normal ordered form on the right-hand side of (3.1) has the physical meaning that the density-dependent Peierls phase can be cast to m-particle interactions and summed to the q-th order. But as the index q is unrestrained in the first summation, the structure of the total summed interactions is highly sophisticated. It is also the statistical interaction. The details for the derivation of (3.1) are included in the **App.** A. Inserting it into the bosonic Hamtionian (2.30), we have then the normal ordered Hamiltonian

$$\begin{aligned} :\hat{H}^{(\mathrm{B})}_{\mathrm{AHM}} := & -Je^{i\frac{\theta N}{L}} \sum_{j=1}^{L} \sum_{q=0}^{\infty} \sum_{m=0}^{q} \left[\frac{(i\theta)^q}{q!} S(q,m) (\hat{b}_j^\dagger)^{m+1} (\hat{b}_j)^m \hat{b}_{j+1} + \text{h.c.} \right] \\ & -\mu \sum_{j=1}^{L} \hat{b}_j^\dagger \hat{b}_j + \frac{U}{2} \sum_{j=1}^{L} \hat{b}_j^\dagger \hat{b}_j^\dagger \hat{b}_j \hat{b}_j \,, \end{aligned} \tag{3.2}$$

where $: \cdots :$ denotes the normal ordering operation. Taking into account the recovered translational invariance in the last chapter (2.27), here we apply the deformed Fourier transformation [88] to the bosonic creation and annihilation operators in (3.2)

$$\hat{b}_j = \frac{1}{\sqrt{L}} \sum_k \hat{b}_k \, e^{-i(k+\beta)ja}, \quad \hat{b}_j^\dagger = \frac{1}{\sqrt{L}} \sum_k \hat{b}_k^\dagger \, e^{i(k+\beta)ja} \,. \tag{3.3}$$

Note that now the restored periodic condition in (2.30) gives the discretized quasi-momentum

$$k = \frac{2\pi n}{La} \quad \begin{cases} n \in \mathbb{Z}_{\neq 0} \cap [-\frac{L}{2}, \frac{L}{2}], & L \text{ is even} \\ n \in \mathbb{Z} \cap [-\frac{L-1}{2}, \frac{L-1}{2}], & L \text{ is odd} \end{cases} \tag{3.4}$$

which is just the standard discretization of momentum space. Yet the twisted boundary would lead to a global and fractional shift of the momentum space with respect to the statistic parameter θ and the total particle number N. Now, combining (3.3) and (3.4) the twisted condition is shown as

$$\begin{aligned} \hat{b}_{j+L} = & \frac{1}{\sqrt{L}} \sum_k \hat{b}_k \, e^{-i(k+\beta)(j+L)a} = \frac{1}{\sqrt{L}} \sum_k \hat{b}_k \, e^{-i(k+\beta)ja} \exp\left[-i \left(\frac{2\pi La}{La} + \frac{\theta N La}{La} \right) \right] \\ = & \, \hat{b}_j \, e^{-i\theta N} \end{aligned} \tag{3.5}$$

From the previous theoretical approach via Gutzwiller mean-field theory and the numerical analysis of density matrix renormalization group (DMRG) [30, 65], as well as the perturbation result from **Ref.** [89], when the statistic parameter is in the anyonic range $\theta \in (0, \theta)$, the quasi-momentum of the ground state is shifted from zero, i.e. $k_0(\theta \neq 0) \neq 0$ [30, 65], which is an exciting feature arising of the broken parity symmetry from the anyonic algebra (2.9a-2.9c), which will lead to many intriguing properties. To investigate this shifted condensate feature, we consider the modified Bogoliubov *ansatz*

$$\begin{aligned} \sum_k \hat{b}_k^\dagger \, e^{i(k+\beta)ja} &= \left(\sqrt{N_{k_0}} + \delta \hat{b}_{k_0}^\dagger \right) \, e^{i(k_0+\beta)ja} + \sum_{k \neq k_0} \hat{b}_k^\dagger \, e^{i(k+\beta)ja} \\ \sum_k \hat{b}_k \, e^{-i(k+\beta)ja} &= \left(\sqrt{N_{k_0}} + \delta \hat{b}_{k_0} \right) \, e^{-i(k_0+\beta)ja} + \sum_{k \neq k_0} \hat{b}_k \, e^{-i(k+\beta)ja} \,, \end{aligned} \tag{3.6}$$

where k_0 denotes the shifted momentum from $k = 0$, and later we will deduce this parameter by finding the minimum of the ground state energy, i.e. the physical one.

Now we treat $: \hat{H}^{(B)}_{\mathrm{AHM}} :$. First insert (3.3) in (3.2), then take into account the *ansatz* (3.6), we obtain a cumbersome expression for the normal ordered Hamiltonian

$$
\begin{aligned}
:\hat{H}^{(B)}_{\mathrm{AHM}} :=& - J\, e^{i\frac{\theta N}{L}} \sum_{j=1}^{L} \sum_{q=0}^{\infty} \sum_{m=0}^{q} \frac{1}{L^{m+1}} \left\{ \frac{(i\theta)^q}{q!} S(q,m) \right. \\
&\times \left[\left(\sqrt{N_{k_0}} + \delta\hat{b}^{\dagger}_{k_0}\right) e^{i(k_0+\beta)ja} + \sum_{k\neq k_0} \hat{b}^{\dagger}_{k}\, e^{i(k+\beta)ja} \right]^{m+1} \\
&\times \left[\left(\sqrt{N_{k_0}} + \delta\hat{b}_{k_0}\right) e^{-i(k_0+\beta)ja} + \sum_{k'\neq k_0} \hat{b}_{k'}\, e^{-i(k'+\beta)ja} \right]^{m} \\
&\times \left. \left[\left(\sqrt{N_{k_0}} + \delta\hat{b}_{k_0}\right) e^{-i(k_0+\beta)(j+1)a} + \sum_{k''\neq k_0} \hat{b}_{k''}\, e^{-i(k''+\beta)(j+1)a} \right] + \mathrm{h.c.} \right\} \\
&- \mu \sum_{j=1}^{L} \frac{1}{L} \left[\left(\sqrt{N_{k_0}} + \delta\hat{b}^{\dagger}_{k_0}\right) e^{i(k_0+\beta)ja} + \sum_{k\neq k_0} \hat{b}^{\dagger}_{k}\, e^{i(k+\beta)ja} \right] \\
&\times \left[\left(\sqrt{N_{k_0}} + \delta\hat{b}_{k_0}\right) e^{-ik_0ja} + \sum_{k'\neq k_0} \hat{b}_{k'}\, e^{-i(k'+\beta)ja} \right] \\
&+ \frac{U}{2} \sum_{j=1}^{L} \frac{1}{L^2} \left[\left(\sqrt{N_{k_0}} + \delta\hat{b}^{\dagger}_{k_0}\right) e^{i(k_0+\beta)ja} + \sum_{k\neq k_0} \hat{b}^{\dagger}_{k}\, e^{i(k+\beta)ja} \right] \\
&\times \left[\left(\sqrt{N_{k_0}} + \delta\hat{b}^{\dagger}_{k_0}\right) e^{i(k_0+\beta)ja} + \sum_{k'\neq k_0} \hat{b}^{\dagger}_{k'}\, e^{i(k'+\beta)ja} \right] \\
&\times \left[\left(\sqrt{N_{k_0}} + \delta\hat{b}_{k_0}\right) e^{-ik_0ja} + \sum_{k''\neq k_0} \hat{b}_{k''}\, e^{-i(k''+\beta)ja} \right] \\
&\times \left[\left(\sqrt{N_{k_0}} + \delta\hat{b}_{k_0}\right) e^{-i(k_0+\beta)ja} + \sum_{k'''\neq k_0} \hat{b}_{k'''}\, e^{-i(k'''+\beta)ja} \right],
\end{aligned}
\tag{3.7}
$$

from which we could successively make a decomposition by following the order of the operators:

$$
:\hat{H}^{(B)}_{\mathrm{AHM}} := \hat{H}_0 + \hat{H}_1 + \hat{H}_2 + \mathcal{O}[(\delta\hat{b}^{(\dagger)}_{k_0})^2] + \mathcal{O}[(\hat{b}^{(\dagger)}_{k\neq k_0})^3]\,, \tag{3.8}
$$

with $\hat{H}_0$ the macroscopic energy, $\hat{H}_1$ the first order fluctuations of macroscopic occupation, $\hat{H}_2$ the contribution of bi-linear operators which represents the fluctuations of the non-condensate states. Then we neglect higher-order fluctuations for macroscopic occupation $\mathcal{O}[(\delta\hat{b}^{(\dagger)}_{k_0})^2]$ and $\mathcal{O}[(\hat{b}^{(\dagger)}_{k\neq k_0})^3]$ the higher-orders fluctuations from the non-condensate states. To actually decompose the Hamiltonian, we need the combination rule

$$
\binom{n}{k} = \frac{n!}{k!(n-k)!} \tag{3.9}
$$

the one-dimensional discrete Fourier transformation from

$$
\sum_{j=1}^{L} e^{ikja} = L\delta_{k,0}\,, \tag{3.10}
$$

and sort the Hamiltonian (3.7) correspondingly. Then the decomposed Hamiltonian of different orders read

$$\hat{H}_0 \equiv E_0 = L\left\{-Jn_{k_0}\sum_{q=0}^{\infty}\sum_{m=0}^{q}\left[\frac{(i\theta)^q}{q!}S(q,m)n_{k_0}^m\, e^{-i(k_0+\beta)a}\, e^{i\frac{\theta N}{L}} + \text{h.c.}\right] - \mu n_{k_0} + \frac{U}{2}n_{k_0}^2\right\}, \tag{3.11}$$

$$\begin{aligned}\hat{H}_1 =& \sqrt{N_{k_0}}\left\{-J\sum_{q=0}^{\infty}\sum_{m=0}^{q}\left[\frac{(i\theta)^q}{q!}S(q,m)(m+1)n_{k_0}^m\, e^{-i(k_0+\beta)a}\, e^{i\frac{\theta N}{L}} + \text{h.c.}\right] - \mu + Un_{k_0}\right\}\\ &\times\left(\delta\hat{b}_{k_0}^\dagger + \delta\hat{b}_{k_0}\right),\end{aligned} \tag{3.12}$$

$$\begin{aligned}\hat{H}_2 =& -J\left\{\sum_{q=0}^{\infty}\sum_{m=0}^{q}\frac{(i\theta)^q}{q!}S(q,m)\, n_{k_0}^m\, e^{i\frac{\theta N}{L}}\sum_{k\neq k_0}\left[(m+1)(me^{-ik_0a}+e^{-ika})\hat{n}_k\right.\right.\\ &\left.\left.+\frac{m(m+1)}{2}\, e^{-ik_0a}\hat{b}_k^\dagger\hat{b}_{2k_0-k}^\dagger + \left(\frac{m(m-1)}{2}e^{-ik_0a} + me^{i(k-2k_0)a}\right)\hat{b}_k\hat{b}_{2k_0-k}\right] + \text{h.c.}\right\}\\ &-\mu\sum_{k\neq k_0}\hat{n}_k + \frac{U}{2}n_{k_0}\sum_{k\neq k_0}\left[4\hat{n}_k + \hat{b}_k^\dagger\hat{b}_{2k_0-k}^\dagger + \hat{b}_k\hat{b}_{2k_0-k}\right]\end{aligned} \tag{3.13}$$

where $n_{k_0} = N_{k_0}/L$ is the marcoscopic occupied particle number density with quasi-momentum k_0.

3.2 Ground state properties

Now we first investigate the ground state properties, which take into account $\hat{H}_0$ and $\hat{H}_1$. To proceed, We could further simplify the summations in the hopping terms of (3.11 - 3.13) with the momentum generating function $G(\theta, n_{k_0})$ for the Stirling numbers of second kind [46, 87]

$$\begin{aligned}\sum_{q=0}^{\infty}\sum_{m=0}^{q}\frac{(i\theta)^q}{q!}S(q,m)n_{k_0}^m &= \sum_{q=0}^{\infty}\frac{(i\theta)^q}{q!}T_q(n_{k_0})\\ &= e^{(e^{i\theta}-1)n_{k_0}} = \langle e^{i\theta\hat{n}}\rangle_{\text{Poisson}} \equiv G(\theta, n_{k_0}),\end{aligned} \tag{3.14}$$

where $T_q(n_{k_0})$ is the Touchard polynomial [46, 87, 90]. Statistically it is the expectation value of the q-th momentum of the Poissonian distribution random variable $\hat{n}_i$ with

$$T_q(n_{k_0}) = \langle\hat{n}_i^q\rangle_{\text{Poisson}} = \sum_{m=0}^{q}S(q,m)n_{k_0}^m. \tag{3.15}$$

From this the summation over q in (3.14) can be interpreted as adding all the moments with the corresponding weight $(i\theta)^q/q!$, and the Poissonian moments also satisfy due to the relation (A.17) the recurrence relation

$$\left\langle\hat{n}_i^{q+1}\right\rangle_{\text{Poisson}} = n_{k_0}(1+\partial_{n_{k_0}})\langle\hat{n}_i^q\rangle_{\text{Poisson}}. \tag{3.16}$$

This then motivates us to define the operator $\hat{D}(n_{k_0}) = n_{k_0}\partial_{n_{k_0}}$, which is useful via [46]

$$\hat{D}(n_{k_0})G(\theta, n_{k_0}) = n_{k_0}\partial_{n_{k_0}}e^{(e^{i\theta}-1)n_{k_0}} = \sum_{q=0}^{\infty}\sum_{m=0}^{q}\frac{(i\theta)^q}{q!}mn_{k_0}^m S(q,m). \tag{3.17}$$

Then apply (3.14) to (3.11, 3.12) we obtain the compact form for different orders of Hamiltonians,

$$\begin{aligned} E_0 &= L\left\{-2J\,\mathrm{Re}\left(G(\theta,n_{k_0})\,e^{-i(k_0+\beta)a}e^{i\frac{\theta N}{L}}\right)n_{k_0} - \mu n_{k_0} + \frac{U}{2}n_{k_0}^2\right\} \\ &= L\left\{-2Je^{-2n_{k_0}\sin^2\frac{\theta}{2}}\cos\left(n_{k_0}\sin\theta - (k_0+\beta)a + \frac{\theta N}{L}\right)n_{k_0} - \mu n_{k_0} + \frac{U}{2}n_{k_0}^2\right\}\,, \end{aligned} \tag{3.18}$$

$$\begin{aligned} \hat{H}_1 &= \sqrt{N_{k_0}}\left\{-2J\left(\hat{D}(n_{k_0})+1\right)\mathrm{Re}\left(G(\theta,n_{k_0})\,e^{-i(k_0+\beta)a}e^{i\frac{\theta N}{L}}\right) - \mu + Un_{k_0}\right\}\left(\delta\hat{b}_{k_0}^\dagger + \delta\hat{b}_{k_0}\right) \\ &= \sqrt{N_{k_0}}\left\{-2Je^{-2n_{k_0}\sin^2\frac{\theta}{2}}\left[\left(1-2n_{k_0}\sin^2\frac{\theta}{2}\right)\cos\left(n_{k_0}\sin\theta-(k_0+\beta)a+\frac{\theta N}{L}\right)\right.\right. \\ &\qquad \left.\left. - n_{k_0}\sin\theta\sin\left(n_{k_0}\sin\theta-(k_0+\beta)a+\frac{\theta N}{L}\right)\right] - \mu + Un_{k_0}\right\}\left(\delta\hat{b}_{k_0}^\dagger + \delta\hat{b}_{k_0}\right)\,. \end{aligned} \tag{3.19}$$

Now we observe $E_0\left(n_{k_0},k_0;\mu,\theta,J,U\right)$ which is the grand-canonical potential at $T=0$. Here μ, θ, J and U are thermodynamic parameters, whereas n_{k_0} and k_0 by definition and compare with the ordinary bosonic Boguoliubov theory, are the two arbitrary parameters included in the complex order parameter. In order to determine the minimum of the ground state energy (3.18), the Hessian matrix

$$\mathrm{Hess}(k_0,n_{k_0}) = \begin{bmatrix} \dfrac{\partial^2 E_0}{\partial k_0^2} & \dfrac{\partial^2 E_0}{\partial k_0 \partial n_{k_0}} \\ \dfrac{\partial^2 E_0}{\partial n_{k_0}\partial k_0} & \dfrac{\partial^2 E_0}{\partial n_{k_0}^2} \end{bmatrix} \tag{3.20}$$

needs to be taken into account. To this end we start with taking first order derivatives of it with respect to k_0 and n_{k_0}, respectively, and demand them to be zero, such that we could determine two implicit expressions for the extreme points $(k_0', n_{k_0'})$

$$\left.\frac{\partial E_0}{\partial k_0}\right|_{k_0',n_{k_0'}} = L\left\{-2Jae^{-2n_{k_0'}\sin^2\frac{\theta}{2}}n_{k_0'}\sin\left(n_{k_0'}\sin\theta-(k_0'+\beta)a-\frac{\theta N}{L}\right)\right\} = 0\,, \tag{3.21}$$

$$\begin{aligned} \left.\frac{\partial E_0}{\partial n_{k_0'}}\right|_{k_0',n_{k_0'}} &= L\left\{-2Je^{-2n_{k_0'}\sin^2\frac{\theta}{2}}\left[\left(1-2n_{k_0'}\sin^2\frac{\theta}{2}\right)\cos\left(n_{k_0'}\sin\theta-(k_0'+\beta)a-\frac{\theta N}{L}\right)\right.\right. \\ &\qquad \left.\left. - n_{k_0'}\sin\theta\sin\left(n_{k_0'}\sin\theta-(k_0'+\beta)a-\frac{\theta N}{L}\right)\right] - \mu + Un_{k_0'}\right\} = 0\,. \end{aligned} \tag{3.22}$$

Noting that the physical quantities L, J, a, $n_{k_0'} > 0$, then (3.21) indicates

$$\sin\left(n_{k_0'}\sin\theta - k_0'a\right) = 0\,, \tag{3.23}$$

and therefore the momentum shift of quasi-momentum is

$$k_0' = \frac{n_{k_0'}\sin\theta + m\pi}{a}\,, \quad m\in\mathbb{Z}\,. \tag{3.24}$$

By inserting (3.24) into (3.22), we could work out the equation of state:

$$n_{k_0'} = \frac{\mu}{U} + 2\frac{J}{U}e^{-2n_{k_0'}\sin^2\frac{\theta}{2}}\left(1-2n_{k_0'}\sin^2\frac{\theta}{2}\right)\cos m\pi\,. \tag{3.25}$$

Now the second-order derivatives lead to

$$\left.\frac{\partial^2 E_0}{\partial k_0^2}\right|_{k_0',n_{k_0'}} = L\cdot 2Ja^2 e^{-2n_{k_0'}\sin^2\frac{\theta}{2}} n_{k_0'}\cos m\pi\,, \tag{3.26}$$

$$\left.\frac{\partial^2 E_0}{\partial n_{k_0}\partial k_0}\right|_{k_0',n_{k_0'}} = \left.\frac{\partial^2 E_0}{\partial k_0\partial n_{k_0}}\right|_{k_0',n_{k_0'}} = L\left\{-2Jae^{-2n_{k_0'}\sin^2\frac{\theta}{2}} n_{k_0'}\sin\theta\cos m\pi\right\}\,, \tag{3.27}$$

$$\left.\frac{\partial^2 E_0}{\partial n_{k_0}^2}\right|_{k_0',n_{k_0'}} = L\Big\{-2Je^{-2n_{k_0'}\sin^2\frac{\theta}{2}}\Big[n_{k_0'}\Big(4\sin^4\frac{\theta}{2}-\sin^2\theta\Big)-4\sin^2\frac{\theta}{2}\Big]\cos m\pi+U\Big\}\,. \tag{3.28}$$

The conditions for a minimum to exist are then

$$\left.\frac{\partial^2 E_0}{\partial k_0^2}\right|_{k_0',n_{k_0'}} > 0 \quad\Rightarrow\quad \cos m\pi = 1 \tag{3.29}$$

$$\det[\mathrm{Hess}(k_0,n_{k_0})]>0 \quad \overset{(3.29)}{\Rightarrow} 8Je^{-2n_{k_0'}\sin^2\frac{\theta}{2}}\sin^2\frac{\theta}{2}\left[1-n_{k_0'}\sin^2\frac{\theta}{2}\right]+U>0\,. \tag{3.30}$$

The first condition (3.29) then confines the mean-field shift of condensate quasi-momentum k_0' to

$$k_0' = \frac{n_{k_0'}\sin\theta}{a}\,, \tag{3.31}$$

Same for the equation of state (3.25),

$$n_{k_0'} = \frac{\mu}{U}+2\frac{J}{U}e^{-2n_{k_0'}\sin^2\frac{\theta}{2}}\Big(1-2n_{k_0'}\sin^2\frac{\theta}{2}\Big)\,. \tag{3.32}$$

One unsound feature of the Bogoliubov theory is the quasi-particle dispersion, as we will derive in the next section, depends on the condensate density n_{k_0}. It shall not be forgotten that in the modified Bogoliubov *ansatz* (3.6), there is a linear decomposition of the macroscopic part $\delta\hat{b}_{k_0}$ that corresponds to the fluctuation of condensate, indicating that the condensate density n_{k_0} is still in the formal sense an operator. The resulting linear Hamiltonian $\hat{H}_1$ (3.12) clearly breaks the conservation of particle number in the condensate as

$$\Big[\delta\hat{b}_j^\dagger\delta\hat{b}_j,\hat{H}_1\Big]_- \neq 0\,. \tag{3.33}$$

However, this problem is safely resolved in the minimization procedure as presented above. Namely the resulting chemical potential μ from (3.32) eliminates the linear Hamiltonian $\hat{H}_1$,

$$\hat{H}_1 \overset{\mu(n_{k_0'},k_0')}{=} 0\,. \tag{3.34}$$

This then leaves n_{k_0} a constant. Later, when taking into account the non-condensate fluctuations $\hat{H}_2$ in **Sec.** 3.3, n_{k_0} would be derived self-consistently.

Since in our model the interaction is considered to be zero or repulsive, i.e. $U \geq 0$, (3.30) leads to the inequality

$$n_{k_0'} < \frac{1}{\sin^2\frac{\theta}{2}}\,, \tag{3.35}$$

which shows now an exciting feature. As plotted in **Fig.** 3.1, for the bosonic case $\theta = 0$, the single-mode occupation $n_{k_0'}$ is unrestrained, so it is allowed to be infinitely large. On the contrary, when we reach the pseudo-fermionic case $\theta=\pi$, $n_{k_0'}$ must be smaller than one, which resembles

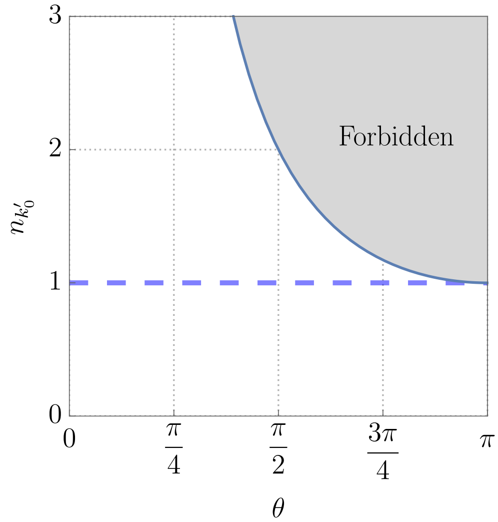

Figure 3.1: The restriction of macroscopic particle density $n_{k_0'}$ due to the statistic angle θ, which resembles a transmutation from Bose-Einstein statistics to Fermi-Dirac statistics. It can also be observed that in order to allow the full anyonic range, one needs $n_{k_0'} < 1$.

the Pauli principle that for fermions we could have at most one particle to occupy each lattice site. This exclusion behaviour on quantum state occupation also corresponds to a generalized Pauli exclusion principle, i.e. the Haldane exclusion principle [55]. Together with the anti-symmetization of the wavefunction as encoded in the anyonic algebra (2.9a), we can conclude that in the current mean-field treatment we have derived a transmutation between the Bose-Einstein statistics and Fermi-Dirac statistics for anyons, which is a function of θ.

If we make a variation to the quasi-condensate momentum $k_0 = k_0' + \delta k_0$ and insert it into (3.18), after an expansion we would have

$$E_0 \approx L \left\{ J e^{-2n_{k_0'} \sin^2 \frac{\theta}{2}} n_{k_0'} \delta k_0^2 a^2 - 2J e^{-2n_{k_0'} \sin^2 \frac{\theta}{2}} n_{k_0'} - \mu n_{k_0'} + \frac{U}{2} n_{k_0'}^2 \right\} , \tag{3.36}$$

from which the effective mass is determined via

$$\frac{\hbar^2 \delta k_0^2}{2m_{\text{eff}}} \overset{!}{=} J e^{-2n_{k_0'} \sin^2 \frac{\theta}{2}} \delta k_0^2 a^2 \tag{3.37}$$

such that

$$m_{\text{eff}} = \frac{\hbar^2}{2Ja^2 e^{-2n_{k_0'} \sin^2 \frac{\theta}{2}}} \, . \tag{3.38}$$

As shown in **Fig.** 3.2, the anyonic effective mass is always heavier than the bosonic mass $m_{\text{eff}}(\theta = 0) = \hbar^2/2Ja^2$, which comes from the enlarged total hopping energy from the bosonic limit to the stable limit (3.35). Specifically, for high condensate density n_{k_0} the effective mass increases more profoundly than the low-density case. The maximum effective mass is limited by the same inequality (3.35), which compares with the bosonic case has the ratio

$$\frac{m_{\text{eff}}(n_{k_0'} = (\sin^2\theta/2)^{-1})}{m_{\text{eff}}(\theta = 0)} = e^2 \, . \tag{3.39}$$

A fast check of letting $\theta = 0$ reduces the effective mass (3.38), chemical potential (3.32) and the

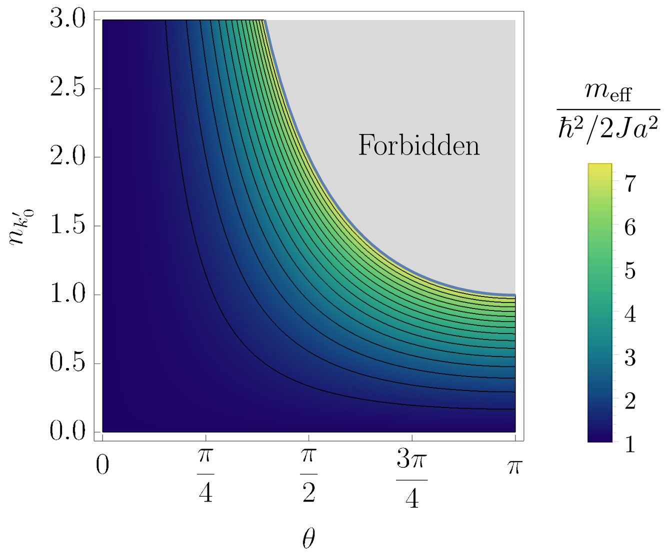

Figure 3.2: The density plot for the ratio of efftive mass m_{eff} and the bosonic mass $\hbar^2/2Ja^2$. As shown, m_{eff} is always larger than the bosonic mass. And the maximum is reached at the stable boundary (3.35).

ground state energy (3.18) to

$$m_{\mathrm{eff}}(\theta = 0) = \frac{\hbar^2}{2Ja^2}\,, \tag{3.40}$$

$$\mu(\theta = 0) = Un_{k'_0=0} - 2J\,, \tag{3.41}$$

$$E_0(\theta = 0) = \left(-2J - \mu + \frac{1}{2}Un_{k'_0=0}\right) N_{k'_0=0}\,, \tag{3.42}$$

which coincides with the bosonic case as mentioned in **Ref.** [72].

The isothermal compressibility for the ground state is a good measure for the statistical interaction, whose definition is

$$\kappa_T = \frac{1}{n_{k'_0}^2} \frac{\partial n_{k'_0}}{\partial \mu}\bigg|_T\,. \tag{3.43}$$

Taking into account the equation of state (3.32) we have

$$\kappa_T = \frac{1}{n_{k'_0}^2}\left[\frac{1}{U} + \frac{8Jn_{k'_0}^2}{U} e^{-2n_{k'_0}\sin^2\frac{\theta}{2}} \left(n_{k'_0}\sin^4\frac{\theta}{2} - \sin^2\frac{\theta}{2}\right)\kappa_T\right]$$

and finally leads to

$$\kappa_T = \left[Un_{k'_0}^2 + 8n_{k'_0}^2 J e^{-2n_{k'_0}\sin^2\frac{\theta}{2}} \sin^2\frac{\theta}{2}\left(1 - n_{k'_0}\sin^2\frac{\theta}{2}\right)\right]^{-1}\,. \tag{3.44}$$

Observing the expression, we can write out the total effective interaction

$$U_{\mathrm{tot}} = \frac{1}{n_{k'_0}^2\kappa_T} = U + U_{\mathrm{stat}}\,, \tag{3.45}$$

where the part from the correlated hopping, i.e. the statistical interaction U_{stat} is

$$U_{\mathrm{stat}} = 8Je^{-2n_{k'_0}\sin^2\frac{\theta}{2}} \sin^2\frac{\theta}{2}\left(1 - n_{k'_0}\sin^2\frac{\theta}{2}\right)\,. \tag{3.46}$$

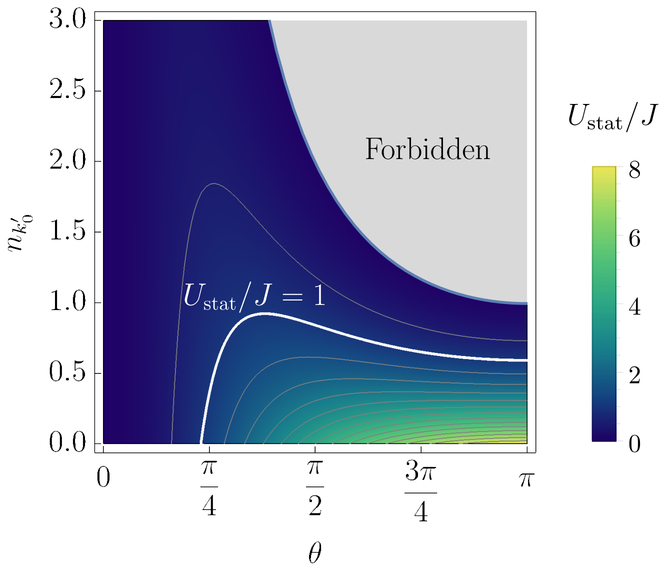

Figure 3.3: The density plot for $U_{\rm stat}/J$. The white contour line denotes the case when the statistical interaction is as strong as the hopping strength. At $\theta = \pi$ and $n_{k'_0} = 0$ the ratio reaches a finite maximum of $U_{\rm stat}/J = 8$ due to the characteristics of the pseudo-fermions.

Thus, we have derived an explicit expression for the statistical interaction on mean-field level. $U_{\rm stat}$ depends on several parameters, $U_{\rm stat}(J, n_{k'_0}, \theta)$, which can be seen as the consequence of the fractional Jordan-Wigner transformation that modifies the hopping term. Thus $U_{\rm stat}$ does not depend on the on-site interaction U. A density plot of the ratio $U_{\rm stat}/J$ is shown in **Fig.** 3.3. The ratio remains zero at the bosonic limit and the boundary (3.35), meaning no statistical interaction exists therein,

$$U_{\rm stat}\Big|_{\theta=0} = 0 = U_{\rm stat}\Big|_{n_{k'_0}\sin^2(\theta/2)=1} . \tag{3.47}$$

However, when one either increases the statistic parameter to the pseudo-fermionic limit or when one reaches the dilute limit $n_{k'_0} \to 0$, the ratio would increase, meaning an enhanced statistic interaction. The former is in accordance with the fact that the effective interaction strength is inversely proportional to the particle density in one dimension, $\gamma \propto 1/n_{k'_0}$ [30, 52]. The latter is the expected result of fermionization [52, 91]. The maximum value of the $U_{\rm stat}$ is then reached with

$$U_{\rm stat}\Big|_{\substack{\theta=\pi \\ n_{k'_0}=0}} = 8J\,, \tag{3.48}$$

which is also visible in **Fig.** 3.3. This limited maximum arises from the fact that pseudo-fermions are on-site bosons and off-site fermions, as encoded in the anyonic algebra (2.9a).

3.3 Higher excitations and Bogoliubov transformation

Now we consider the non-condensate fluctuations on the mean-field basis, which amounts to adding the bi-linear Hamiltonian $\hat{H}_2$ (3.13) to the mean-field energy E_0. To minimize analytical difficulties, again the moment generation function $G(\theta, n_{k_0})$ and the operator $\hat{D}(n_{k_0})$ are needed as in **Sec.** 3.2. Further, it will be very helpful to define $q = k - k'_0$ as the reciprocal momentum vector k is actually symmetric around k'_0. Now the first order Hamiltonian $\hat{H}_1$ (3.13) is first simplified with $\hat{D}(n_{k_0})$ (3.14), which gives

$$\begin{aligned}
\hat{H}_2 =& -J\sum_{q\neq 0}\Bigg\{\left[e^{-ik_0a}(\hat{D}(n_{k_0}))^2+\left(e^{-i(k_0+q)a}+e^{-ik_0a}\right)\hat{D}(n_{k_0})+e^{-i(k_0+q)a}\right]G(\theta,n_{k_0})\hat{n}_{k_0+q}\\
&+\frac{1}{2}\,e^{-ik_0a}\left((\hat{D}(n_{k_0}))^2+\hat{D}(n_{k_0})\right)G(\theta,n_{k_0})\hat{b}^\dagger_{k_0+q}\hat{b}^\dagger_{k_0-q}\\
&+\left[\frac{1}{2}\,e^{-ik_0a}\left((\hat{D}(n_{k_0}))^2-\hat{D}(n_{k_0})\right)+e^{-i(k_0-q)}\hat{D}(n_{k_0})\right]G(\theta,n_{k_0})\hat{b}_{k_0+q}\hat{b}_{k_0-q}+\text{h.c.}\Bigg\}\\
&-\mu\sum_{q\neq 0}\hat{n}_{k_0+q}+\frac{U}{2}n_{k_0}\sum_{q\neq 0}\left[4\hat{n}_{k_0+q}+\hat{b}^\dagger_{k_0+q}\hat{b}^\dagger_{k_0-q}+\hat{b}_{k_0+q}\hat{b}_{k_0-q}\right]\,. \qquad (3.49)
\end{aligned}$$

To apply the standard Bogoliubov transformation to such a cumbersome expression, we note the inverse transformation $q\to -q$ and, for simplicity, define the prefactors for the bi-linear terms

$$\begin{aligned}
A_q =& -J\left\{e^{-ik_0a}\left(\hat{D}(n_{k_0})^2+\hat{D}(n_{k_0})\right)G(\theta,n_{k_0})\right.\\
&\left.+e^{-i(k_0+q)a}\left(\hat{D}(n_{k_0})+1\right)G(\theta,n_{k_0})+\text{h.c.}\right\}-\mu+2\,Un_{k_0}\,, \qquad (3.50)\\
B_q =& -J\Bigg\{\frac{1}{2}\,e^{-ik_0a}\left(\hat{D}(n_{k_0})^2+\hat{D}(n_{k_0})\right)G(\theta,n_{k_0})\\
&+\left[\frac{1}{2}\,e^{ik_0a}\left(\hat{D}(n_{k_0})^2-\hat{D}(n_{k_0})\right)+e^{i(k_0-q)a}\hat{D}(n_{k_0})\right]G^*(\theta,n_{k_0})\Bigg\}+\frac{1}{2}Un_{k_0}\,. \qquad (3.51)
\end{aligned}$$

Evaluate further and define $\varphi = n_{k_0}\sin\theta - k_0a$, we further obtain the explicit forms

$$\begin{aligned}
A_q =& -2Je^{-2n_{k_0}\sin^2\frac{\theta}{2}}\Bigg\{-4n_{k_0}\sin\frac{\theta}{2}\sin\left(\frac{\theta}{2}+\varphi\right)-4n_{k_0}^2\sin^2\frac{\theta}{2}\cos\left(\theta+\varphi\right)\\
&-2n_{k_0}\sin\frac{\theta}{2}\sin\left(\frac{\theta}{2}+\varphi-qa\right)+\cos\left(\varphi-qa\right)\Bigg\}-\mu+2Un_{k_0}\,, \qquad (3.52)\\
B_q =& -Je^{-2n_{k_0}\sin^2\frac{\theta}{2}}\Bigg\{-2n_{k_0}\sin\frac{\theta}{2}\sin\left(\frac{\theta}{2}+\varphi\right)-4n_{k_0}^2\sin^2\frac{\theta}{2}\cos\left(\theta+\varphi\right)\\
&+2i\cdot n_{k_0}\sin\frac{\theta}{2}\cos\left(\frac{\theta}{2}+\varphi\right)+n_{k_0}(e^{-i\theta}-1)\,e^{-i(\varphi+qa)}\Bigg\}+\frac{U}{2}n_{k_0}\,. \qquad (3.53)
\end{aligned}$$

and further we look into the following combination of prefactors

$$
\begin{aligned}
A_q + A_{-q} =& -4Je^{-2n_{k_0}\sin^2\frac{\theta}{2}} \Bigg\{ -4n_{k_0}\sin\frac{\theta}{2}\sin\left(\frac{\theta}{2}+\varphi\right) - 4n_{k_0}^2\sin^2\frac{\theta}{2}\cos\left(\theta+\varphi\right) \\
& - 2n_{k_0}\sin\frac{\theta}{2}\sin\left(\frac{\theta}{2}+\varphi\right)\cos qa + \cos\varphi\cos qa \Bigg\} - 2\mu + 4Un_{k_0}\,, \qquad (3.54) \\
A_q - A_{-q} =& -4Je^{-2n_{k_0}\sin^2\frac{\theta}{2}} \left[n_{k_0} 2\sin\frac{\theta}{2}\cos\left(\frac{\theta}{2}+\varphi\right) + \sin\varphi \right] \sin qa \qquad (3.55) \\
B_q + B_{-q} =& -2Je^{-2n_{k_0}\sin^2\frac{\theta}{2}} \Bigg\{ -2n_{k_0}\sin\frac{\theta}{2}\sin\left(\frac{\theta}{2}+\varphi\right) - 4n_{k_0}^2\sin^2\frac{\theta}{2}\cos\left(\theta+\varphi\right) \\
& + 2i\cdot n_{k_0}\sin\frac{\theta}{2}\cos\left(\frac{\theta}{2}+\varphi\right) + n_{k_0}\cos qa(e^{-i\theta}-1)\,e^{-i\varphi} \Bigg\} + Un_{k_0} \qquad (3.56) \\
2\mathrm{Re}\left[B_q + B_{-q}\right] =& -4Je^{-2n_{k_0}\sin^2\frac{\theta}{2}} \Bigg\{ -2n_{k_0}\sin\frac{\theta}{2}\sin\left(\frac{\theta}{2}+\varphi\right) - 4n_{k_0}^2\sin^2\frac{\theta}{2}\cos\left(\theta+\varphi\right) \\
& - 2n_{k_0}\sin\frac{\theta}{2}\sin\left(\frac{\theta}{2}+\varphi\right)\cos qa \Bigg\} + 2Un_{k_0} \qquad (3.57)
\end{aligned}
$$

which will be useful for later calculations. Note the identity $\sum_{q\neq 0} f(q) = \sum_{q\neq 0} f(-q)$, now we are working with the total Hamiltonian

$$
:\hat{H}_{\mathrm{AHM}}^{(\mathrm{B})}: \approx E_0 + \frac{1}{2}\sum_{q\neq 0}\Big[\left(A_q\,\hat{n}_{k_0+q} + A_{-q}\hat{n}_{k_0-q}\right) + \Big(\left(B_q + B_{-q}\right)\hat{b}^\dagger_{k_0+q}\hat{b}^\dagger_{k_0-q} + \mathrm{h.c.} \Big) \Big]\,, \qquad (3.58)
$$

modify to the symmetric form

$$
\begin{aligned}
:\hat{H}_{\mathrm{AHM}}^{(\mathrm{B})}: \approx& E_0 - \frac{1}{2}\sum_{q\neq 0} A_{-q} \\
&+ \frac{1}{2}\sum_{q\neq 0}\Big[\Big(A_q\,\hat{b}^\dagger_{k_0+q}\hat{b}_{k_0+q} + A_{-q}\hat{b}_{k_0-q}\hat{b}^\dagger_{k_0-q} \Big) + \Big(\left(B_q + B_{-q}\right)\hat{b}^\dagger_{k_0+q}\hat{b}^\dagger_{k_0-q} + \mathrm{h.c.} \Big) \Big]\,,
\end{aligned} \qquad (3.59)
$$

Bogoliubov Transformation

In order to diagonalize the Hamiltonian, we apply the bosonic Bogoliubov transformation [92]

$$
\hat{b}_{k_0+q} = \cosh\alpha_q\,\hat{d}_{k_0+q} - \sinh\alpha_q\,\hat{d}^\dagger_{k_0-q}\,, \qquad (3.60)
$$

$$
\hat{b}^\dagger_{-q} = -\sinh\alpha_q\,\hat{d}_{k_0+q} + \cosh\alpha_q\,\hat{d}^\dagger_{k_0-q}\,, \qquad (3.61)
$$

where we denote that with the hyperbolic trigonometric identity

$$
\cosh^2\alpha_q - \sinh^2\alpha_q = 1\,, \qquad (3.62)
$$

the bosonic commutation relation is maintained for the transformed field operators $\hat{d}_q$ and $\hat{d}^\dagger_q$,

$$
\left[\hat{d}_{k_0+q},\,\hat{d}^\dagger_{k_0+q'}\right]_- = \delta_{q,q'}\,. \qquad (3.63)
$$

Therefore the transformed field operators represent the quasi-bosons and its antiparticle, which come from the linear combination of the original boson and its antiparticle. Now, by defining $\cosh\alpha_q = u_q$ and $\sinh\alpha_q = v_q$, we insert the Bogoliubov transformations (3.60) and (3.61) into the symmetric Hamiltonian (3.59). By sorting the terms with regard to the quadratic quasi-boson operator terms, we have

$$\begin{aligned}
:\hat{H}^{(\mathrm{B})}_{\mathrm{AHM}}:\approx & E_0 - \frac{1}{2}\sum_{q\neq 0} A_{-q} + \frac{1}{2}\sum_{q\neq 0}\left[A_q u_q^2 + A_{-q}v_q^2 - (B_q + B_q^*)u_q v_q\right]\hat{d}^\dagger_{k_0+q}\hat{d}_{k_0+q} \\
& + \left[A_q v_q^2 + A_{-q}u_q^2 - (B_q + B_q^*)u_q v_q\right]\hat{d}_{k_0-q}\hat{d}^\dagger_{k_0-q} \\
& + \left[(B_q + B_{-q})u_q^2 + (B_q^* + B_{-q}^*)v_q^2 - (A_q + A_{-q})u_q v_q\right]\hat{d}^\dagger_{k_0+q}\hat{d}^\dagger_{k_0-q} \\
& + \left[(B_q^* + B_{-q}^*)u_q^2 + (B_q + B_{-q})v_q^2 - (A_q + A_{-q})u_q v_q\right]\hat{d}_{k_0+q}\hat{d}_{k_0-q}\,.
\end{aligned} \tag{3.64}$$

The diagonalization procedure simply corresponds to the demand that the off-diagonal terms $\hat{b}^\dagger_{k_0+q}\hat{b}^\dagger_{k_0-q}$ and $\hat{b}_{k_0+q}\hat{b}_{k_0-q}$ should vanish in the resulting Hamiltonian, which corresponds to

$$\begin{cases} (B_q + B_{-q})u_q^2 + (B_q^* + B_{-q}^*)v_q^2 - (A_q + A_{-q})u_q v_q \overset{!}{=} 0 \\ (B_q^* + B_{-q}^*)u_q^2 + (B_q + B_{-q})v_q^2 - (A_q + A_{-q})u_q v_q \overset{!}{=} 0 \end{cases}. \tag{3.65}$$

Adding the two equations together we have the result for the Bogoliubov angle α_q [81]

$$\frac{2\mathrm{Re}\,(B_q + B_{-q})}{A_q + A_{-q}} = \frac{2u_q v_q}{u_q^2 + v_q^2} = \frac{2\cosh\alpha_q\,\sinh\alpha_q}{\cosh^2\alpha_q + \sinh^2\alpha_q} = \tanh 2\alpha_q\,. \tag{3.66}$$

Further with the trigonometric identities [93] we obtain

$$\cosh^2\alpha_q = \frac{1}{2}(\cosh 2\alpha_q + 1) = \frac{1}{2}\left(\frac{1}{\sqrt{1-\tanh^2 2\alpha_q}} + 1\right) \tag{3.67}$$

where leads to

$$\cosh^2\alpha_q = \frac{1}{2}\left(\frac{A_q + A_{-q}}{\sqrt{(A_q + A_{-q})^2 - (2\mathrm{Re}\,[B_q + B_{-q}])^2}} + 1\right) \tag{3.68}$$

and consequently follow (3.62),

$$\sinh^2\alpha_q = \frac{1}{2}\left(\frac{A_q + A_{-q}}{\sqrt{(A_q + A_{-q})^2 - (2\mathrm{Re}\,[B_q + B_{-q}])^2}} - 1\right)\,. \tag{3.69}$$

This then gives the diagonalized Hamiltonian as

$$\hat{H}_{\mathrm{diag}} \approx E_0 + \frac{1}{2}\sum_{q\neq 0} E_q - A_q + \frac{1}{2}\sum_{q\neq 0}\left(E_q \hat{d}^\dagger_{k_0+q}\hat{d}_{k_0+q} + E_{-q}\hat{d}^\dagger_{k_0-q}\hat{d}_{k_0-q}\right)\,. \tag{3.70}$$

The diagonalized Hamiltonian $\hat{H}_{\mathrm{diag}}$ represents the non-interacting Hamiltonian for the bosonic Landau quasi-paricles $\hat{d}^{(\dagger)}_{k_0+q}$ [81, 92]. Those particles are quasi in the sense that they are the linear combinations of the real bosons $\hat{b}^\dagger_{k_0+q}$ and their anti-particles $\hat{b}_{k_0+q}$ [86, 94]. $\hat{H}_{\mathrm{diag}}$ consists of three parts: the ground-state energy E_0, the quantum corrections in the second term, and the operator-valued elementary excitations in the third term. The elementary excitation spectrum of the quasi-bosons, i.e. the Bogoliubov dispersions E_q has the expression by the diagonal terms in (3.64)

$$E_q = A_q \cosh^2\alpha_q + A_{-q}\sinh^2\alpha_q - 2\mathrm{Re}\,(B_q + B_{-q})\cosh\alpha_q\sinh\alpha_q\,. \tag{3.71}$$

Taking into account the Bogoliubov amplitudes $\cosh \alpha_q$ (3.68) $\sinh \alpha_q$ (3.69), we have

$$E_q = \frac{1}{2}\sqrt{(A_q + A_{-q})^2 - [2\mathrm{Re}\,(B_q + B_{-q})]^2} + \frac{1}{2}(A_q - A_{-q})\,, \tag{3.72}$$

which is evaluated further with (3.54-3.57) as

$$\begin{aligned} E_q = & \left\{ (C_1 - \mu + U n_{k_0})^2 + 2U n_{k_0} (C_1 - \mu + U n_{k_0}) - C_2^2 - 2U n_{k_0} C_2 \right\}^{\frac{1}{2}} \\ & - 2J e^{-2n_{k_0} \sin^2 \frac{\theta}{2}} \left[2n_{k_0} \sin\frac{\theta}{2} \cos\left(\frac{\theta}{2} + \varphi\right) + \sin\varphi \right] \sin qa\,, \end{aligned} \tag{3.73}$$

with the coefficients

$$\begin{aligned} C_1 = & - 2J e^{-2n_{k_0} \sin^2 \frac{\theta}{2}} \left\{ - 4n_{k_0} \sin\frac{\theta}{2} \sin\left(\frac{\theta}{2} + \varphi\right) - 4n_{k_0}^2 \sin^2\frac{\theta}{2} \cos(\theta + \varphi) \right. \\ & \left. - 2n_{k_0} \sin\frac{\theta}{2} \sin\left(\frac{\theta}{2} + \varphi\right) \cos qa + \cos\varphi \cos qa \right\}, \end{aligned} \tag{3.74}$$

$$\begin{aligned} C_2 = & - 2J e^{-2n_{k_0} \sin^2 \frac{\theta}{2}} \left\{ - 2n_{k_0} \sin\frac{\theta}{2} \sin\left(\frac{\theta}{2} + \varphi\right) - 4n_{k_0}^2 \sin^2\frac{\theta}{2} \cos(\theta + \varphi) \right. \\ & \left. - 2n_{k_0} \sin\frac{\theta}{2} \sin\left(\frac{\theta}{2} + \varphi\right) \cos qa \right\}. \end{aligned} \tag{3.75}$$

3.4 Anyonic Bogoliubov Dispersion

As a reminder, we have to deal with two parameters in the complex order parameter. If we follow the analysis for bosons and the Popov approximation, it means the condensate density is determined via a self-consistent calculation [95]. In our case, this will lead to two inter-correlated self-consistent equations for k_0 and n_{k_0}, respectively. This would cause huge analytic difficulties. Also, the linear Hamiltonian can lead to non-physical results as discussed in **Sec.** 3.2. To circumvent those artefacts, we consider the mean-field result k_0 (3.24), which means then $\varphi = 0$. Subsequently with the mean-field chemical potential (3.32) that let $\hat{H}_1 = 0$. In this way, the Bogoliubov dispersion (3.73) becomes

$$\begin{aligned} E_q = & \left\{ 4J^2 e^{-4n_{k_0} \sin^2 \frac{\theta}{2}} \left[(1 - \cos qa)^2 + 4\sin^2\frac{\theta}{2} \left(n_{k_0}(1 + \cos qa) + 2n_{k_0}^2 \cos\theta \right) (1 - \cos qa) \right] \right. \\ & \left. + 4JU n_{k_0} e^{-2n_{k_0} \sin^2 \frac{\theta}{2}} (1 - \cos qa) \right\}^{\frac{1}{2}} - 2J e^{-2n_{k_0} \sin^2 \frac{\theta}{2}} n_{k_0} \sin\theta \sin qa \end{aligned} \tag{3.76}$$

The anyonic Bogoliubov dispersion, as shown in (3.76), is rather hard to handle and in essence would become complex for several ranges of θ, q, n_{k_0} and U/J, which leads to the failure of Bogoliubov theory and the stability would be broken, rather than the emergence of new phases in our framework. Then it's crucial to find a stable ranges for our theory.

To check on that, we need to look into the diagonalizablity requirement of the Bogoliubov-De-Gennes matrix. This then amounts to look at the radiant of the even part in the anyonic dispersion (3.73). When it is smaller than zero, we cannot diagonalize the Hamiltonian anymore, and thus, Bogoliubov theory fails in this region. In order to obtain a Bogoliubov theory for the whole momentum space $q \in [-\pi/a, \pi/a]$ (by taking into account the periodicity of the first

Bouillon zone due to low-energy consideration) and the full anyonic range $\theta \in [0, \pi]$, we first investigate the inequality

$$(A_q + A_{-q})^2 - \left(B_q + B_{-q} + B_q^* + B_{-q}^*\right)^2 \geqslant 0. \tag{3.77}$$

Work this out for the on-site interaction to hopping ratio U/J, we have at first

$$\frac{U}{J} \geqslant -\frac{e^{-2n_{k_0}\sin^2\frac{\theta}{2}}}{n_{k_0}}\left[1 - \cos qa + 4\sin^2\frac{\theta}{2}n_{k_0}(1+\cos qa) + 8n_{k_0}^2\sin^2\frac{\theta}{2}\cos\theta\right], \tag{3.78}$$

where we recall that the Hubbard interaction U is always larger than zero. Then this amounts to check when the bracket on the r.h.s. of (3.78) becomes negative and therefore a nonzero repulsive interaction would be required. We check first the long-wavelength limit, which leads to

$$q \to 0: \quad \frac{U}{J} \geqslant -8e^{-2n_{k_0}\sin^2\frac{\theta}{2}}\sin^2\frac{\theta}{2}\left(1 + n_{k_0}\cos\theta\right). \tag{3.79}$$

This then indicates one has to choose $n_{k_0} \leqslant 1$ to have the full range of statistical parameter θ, which is in agreement with the mean-field result (3.35).

When one goes to the boundary of the first Brillouin zone, the inequality becomes

$$q \to \pm\pi: \quad \frac{U}{J} \geqslant -\frac{2e^{-2n_{k_0}\sin^2\frac{\theta}{2}}}{n_{k_0}}\left[1 + 4n_{k_0}^2\sin^2\frac{\theta}{2}\cos\theta\right], \tag{3.80}$$

which leads

$$\theta = \pi \quad \Rightarrow \quad 1 - 4n_{k_0}^2 \leqslant 0 \quad \Rightarrow \quad n_{k_0} \leqslant 0.5\,. \tag{3.81}$$

Therefore to have a stable dispersion regardless of the interaction strength along the whole low-energy regime that spares only the first Brillouin zone, and in the whole range of the statistical parameter, one has to choose $n_{k_0} \leqslant 0.5$.

3.5 Anyonic Quantum Depletion

Before going into some plots of the anyonic Bogoliubov dispersion (3.76), it is important to remark that in the modified Bogoliubov *ansatz* (3.6) we have the macroscopic part dressed by the non-condensate part. The physical significance of this is that quantum fluctuations are always present even at zero temperature due to interactions between the actual bosons, which causes the condensate to be depleted [81]. This further suggests that the controllable parameter of the system is the total number of particles put into the system, and subsequently the total particle density $n = N/L$. It can be defined as the summation of all the particles spanning the full momentum space [72], i.e.

$$n = \frac{1}{L}\sum_q \langle \hat{b}_{k_0+q}^\dagger \hat{b}_{k_0+q}\rangle_{\hat{H}_{\text{diag}}} = n_{k_0} + \frac{1}{L}\sum_{q\neq 0}\langle \hat{b}_{k_0+q}^\dagger \hat{b}_{k_0+q}\rangle_{\hat{H}_{\text{diag}}} \tag{3.82}$$

where $\langle\,\bullet\,\rangle_{\hat{H}_{\text{diag}}}$ denotes the expectation value under the diagonalized Hamiltonian, i.e. the vacuum state for the quasi-bosons. Taking into account the Bogoliubov transformations (3.60, 3.61), the quantum correction under the quasi-bosons representation is

$$\begin{aligned}\langle \hat{b}_{k_0+q}^\dagger \hat{b}_{k_0+q}\rangle_{\hat{H}_{\text{diag}}} &= \left(\cosh^2\alpha_q + \sinh^2\alpha_q\right)\langle \hat{d}_{k_0+q}^\dagger \hat{d}_{k_0+q}\rangle_{\hat{H}_{\text{diag}}} \\ &\quad + \sinh^2\alpha_q + \cosh\alpha_q\sinh\alpha_q\Big[\underbrace{\langle \hat{d}_{k_0+q}^\dagger \hat{d}_{k_0-q}^\dagger\rangle_{\hat{H}_{\text{diag}}} - \langle \hat{d}_{k_0+q}\hat{d}_{k_0-q}\rangle_{\hat{H}_{\text{diag}}}}_{=0}\Big].\end{aligned} \tag{3.83}$$

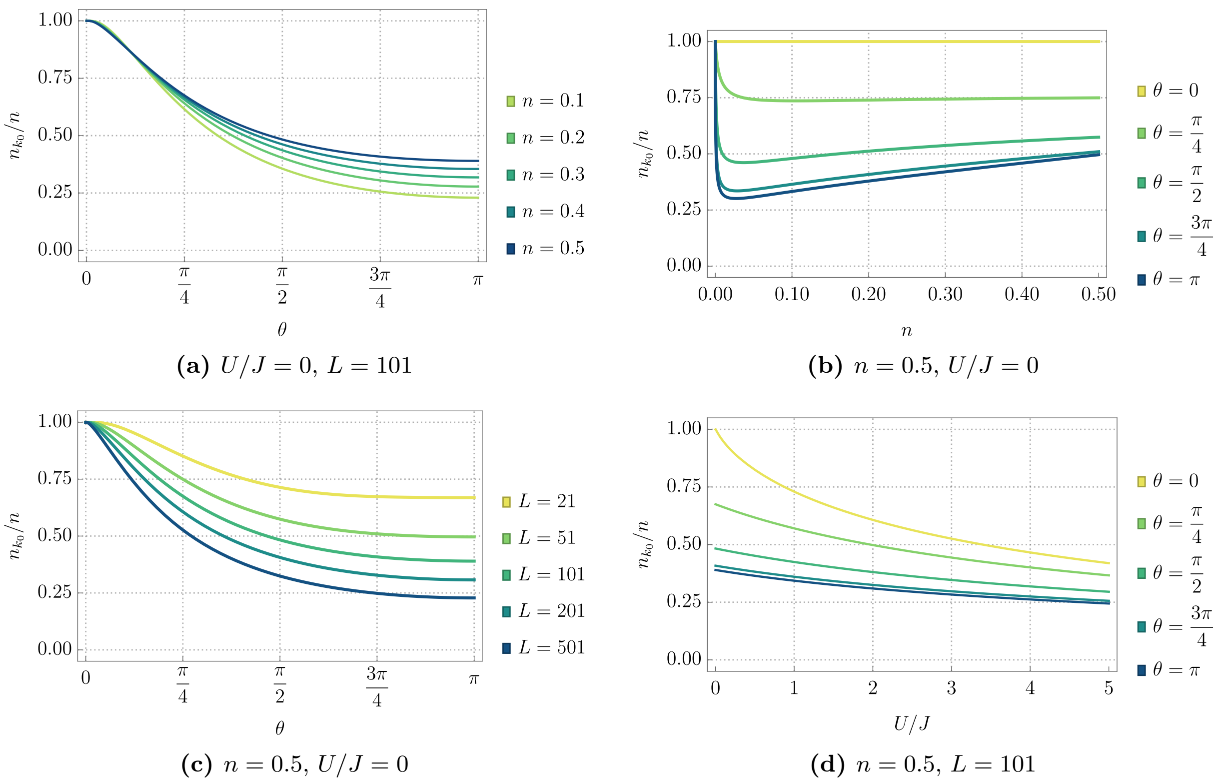

(a) $U/J = 0$, $L = 101$

(b) $n = 0.5$, $U/J = 0$

(c) $n = 0.5$, $U/J = 0$

(d) $n = 0.5$, $L = 101$

Figure 3.4: Anyonic quantum depletion. Four scenarios are shown here. **(a)** Depletion comes purely from the fractional statistics as $U/J = 0$. The reduced total density n leads to larger depletion due to the peculiarity of interaction in one dimension [30]; **(b)** The correspondence of **(a)**, showing the non-linear impact of the total particle density. **(c)** investigates the finite-size effect and **(d)** the influence of the Hubbard interaction U as a comparison with **(a)**, showing the statistics-induced depletion is comparable to strong on-site interaction.

Inserting the Bogoliubov angle α_q (3.66) into (3.83) leads to the total number density

$$n = n_{k_0} + \frac{1}{L}\sum_{q\neq 0}\frac{1}{2}\left[\frac{A_q + A_{-q}}{2E_q - (A_q - A_{-q})} - 1\right] + \frac{1}{L}\sum_{q\neq 0}\frac{A_q + A_{-q}}{2E_q - (A_q - A_{-q})}\frac{1}{e^{\beta E_q} - 1}\,, \tag{3.84}$$

which is decomposed into three parts, namely the macroscopic occupation, the quantum fluctuations and thermal fluctuations. As our focus is on the quantum effect, the thermal part is neglected. Therefore

$$n \overset{T=0}{=} n_{k_0} + \frac{1}{L}\sum_{q\neq 0}\frac{1}{2}\left[\frac{A_q + A_{-q}}{2E_q - (A_q - A_{-q})} - 1\right]\,, \tag{3.85}$$

where the quantum fluctuations part is given explicitly from the previously calculated coefficients (3.54-3.57) as

$$\begin{aligned} \frac{1}{2}\left[\frac{A_q + A_{-q}}{2E_q - (A_q - A_{-q})} - 1\right] &= -\frac{1}{2} \\ &+ \frac{2n_{k_0}\sin^2\frac{\theta}{2}(1 + \cos qa + 2\cos\theta) + (1 - \cos qa) + \frac{Un_{k_0}}{2J}e^{2n_{k_0}\sin^2\frac{\theta}{2}}}{2\sqrt{(1 - \cos qa)^2 + (1 - \cos qa)\left\{4n_{k_0}\sin^2\frac{\theta}{2}\left[1 + \cos qa + 2n_{k_0}\cos\theta\right] + \frac{Un_{k_0}}{J}e^{2n_{k_0}\sin^2\frac{\theta}{2}}\right\}}}\,. \end{aligned} \tag{3.86}$$

Note that in the expression (3.86) the particle density is the condensate density n_{k_0}, together

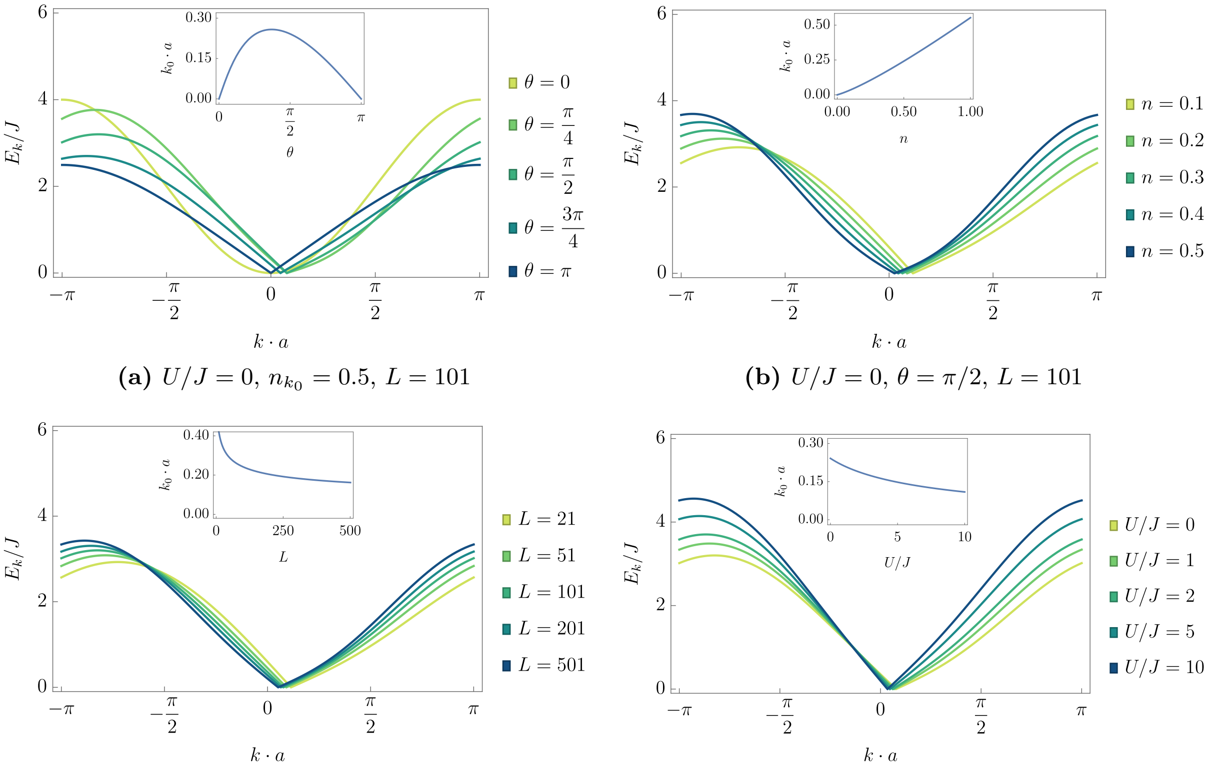

(a) $U/J = 0,\ n_{k_0} = 0.5,\ L = 101$

(b) $U/J = 0,\ \theta = \pi/2,\ L = 101$

(c) $U/J = 0,\ \theta = \pi/2,\ n_{k_0} = 0.5$

(d) $n_{k_0} = 0.5,\ \theta = \pi/2,\ L = 101$

Figure 3.5: Bogoliubov dispersion for anyons in units of hopping strength J. (**a**) The dispersions for different statistical parameters θ, where the bosonic and pseudo-fermionic dispersion have vanishing quasi-momentum, while the anyonic one is shifted from zero. Also the anyonic dispersions are asymmetric around k_0, showing the breaking of spatio-temporal inversion symmetry. The inset shows how the condensate quasi-momentum shifts with θ. (**b**) The increased total particle density leads to further shifted k_0 and larger amplitude. **(c)** The larger lattice size would repress k_0 but enlarge the amplitude, as the fluctuations are enhanced. **(d)** the on-site interaction reduces k_0 but amplifies the overall dispersion.

with the fact that the experimental parameter is the total particle density $n = N/L$. Thus, in the equation (3.85), the quasi-condensate n_{k_0} is determined self-consistently. This is the Popov approximation, which is more accurate when the depletion is relatively large, compared to the Bogoliubov approximation where $n \simeq n_{k_0}$ [81, 96, 97].

The resulting condensate density n_{k_0} is schematically represented in the **Fig.** 3.4a-3.4d as the condensate fraction n_{k_0}/n. **Fig.** 3.4a shows how the condensate is depleted solely from the statistical interaction, since the on-site interaction $U = 0$. The depletion is enhanced by approaching the pseudo-fermionic limit. The maximum depletion at $\theta = \pi$ is comparable to a strong on-site interaction $U/J = 5$ as the bosonic limit $\theta = 0$ in **Fig.** 3.4d. Then the impact of total particle density is depicted together with **Fig.** 3.4b a stronger depletion caused by smaller n. This aligns implicitly with the discussion about the mean-field statistical interaction U_{stat} (3.46), that a reduced density would lead to stronger interaction in one dimension, which is also characteristic in one-dimensional Bose gases [30, 71]. The finite-size effect is shown in **Fig,** 3.4c that a larger lattice would lead to stronger depletion for a constant total density n. This can be simply understood as that a larger lattice size leads to more allowed quasi-momentum modes with the spacing $\Delta k = 2\pi/La$ in the first Bouillon zone and therefore summing over the modes would lead to larger quantum fluctuations.

Now we can also discuss the dispersion in detail. As shown in Fig. 3.5a, again in the case of

$\theta = 0$, as $k_0(\theta = 0) = 0$, $q = k$, the anyonic Bogoliubov dispersion changes to the standard bosonic case in the finite-size lattice system as noted in [72],

$$E_k^{\theta=0} = \sqrt{4J^2(1-\cos ka)^2 + 4Un_0J(1-\cos ka)}\,. \tag{3.87}$$

On the other hand, the Bogoliubov dispersion for pseudo-fermion, depicted in **Fig,** 3.5a, has the form

$$E_k^{\theta=\pi} = \sqrt{4J^2e^{-4n_{k_0}}\left[(1-\cos ka)^2 + 4n_{k_0}(1-\cos^2 ka)\right] + 4JUn_{k_0}e^{-2n_{k_0}}(1-\cos ka)}\,. \tag{3.88}$$

Compare with $E_k^{\theta=0}$, $E_k^{\theta=\pi}$ is also symmetric, and the minimum located at the center of the Bouillon zone $k = 0$, but with a more complicated analytic structure in the radiant. Within the anyonic range $\theta \in (0, \pi)$, the minimum of the dispersion would shift from $k = 0$ due to the mean-field relation $k_0a = n_{k_0}\sin\theta$, as can be seen from the inset of **Fig,** 3.5a. But as we now take into account the quantum depletion, the $k_0 - \theta$ relation is in general not symmetric from $\theta = \pi/2$. Also, it can be seen that the dispersions are not symmetric around k_0 due to the $\sin qa$ term in E_k (3.76). This clearly breaks both the parity and time-reversal symmetries, which is a consequence rooted in the anyonic algebra (2.9a). Then **Fig.** 3.5b-3.5d describe the impact of the $\theta = \pi/2$ dispersion from the n, L and U/J. First of all, as all the parameters have an effect on the quantum depletion as discussed above, therefore it subsequently impacts also the condensate quasi-momentum k_0, whose behaviours can be seen in the insets and can be related to those in **Fig.** 3.4a-3.4d. Applying the same reasoning to enhanced quantum depletions which correspond to either enlarged on-site or statistical interactions, we can observe a consistent trend with increasing dispersion amplitude.

3.6 Asymmetric Two-Mode Sound Velocities

3.6.1 Weak coupling-Bogoliubov velocities

To investigate now the long-wavelength behaviours of the elementary excitations, we expand E_q in the limit $q \to 0$. The resulting non-vanishing coefficient starts from the linear term:

$$\begin{aligned} E_q \overset{q\cdot a\to 0}{=} & -2Jn_{k_0'}\,e^{-2n_{k_0'}\sin^2\frac{\theta}{2}}\sin\theta\cdot qa + \left\{2J^2n_{k_0'}e^{-4n_{k_0'}\sin^2\frac{\theta}{2}}\left[8\sin^2\frac{\theta}{2} + n_{k_0'}8\sin^2\frac{\theta}{2}\cos\theta\right]\right. \\ & \left. + 2JUn_{k_0'}e^{-2n_{k_0'}\sin^2\frac{\theta}{2}}\right\}^{\frac{1}{2}}|qa| + \mathcal{O}\left((qa)^2\right)\,, \end{aligned} \tag{3.89}$$

where we identify two linear dispersions that correspond to two different sound mode velocities for $\theta \in (0, \pi)$ for $q > 0$ and $q < 0$, which differs from each other with two times the coefficient before $|qa|$. This corresponds then again to the breaking of the parity in the anyonic algebra (2.9a) and the bosonic Hamiltonian (2.30).

The two species of sound velocities are

$$\begin{aligned} c^{>/<} = \frac{1}{\hbar}\frac{\partial E_q}{\partial q}\bigg|_{q\to 0^\pm} = \frac{Ja}{\hbar}\Bigg\{ & -2n_{k_0'}\,e^{-2n_{k_0'}\sin^2\frac{\theta}{2}}\sin\theta \\ & \pm\left[e^{-4n_{k_0'}\sin^2\frac{\theta}{2}}\left(16n_{k_0'}\sin^2\frac{\theta}{2} + 16n_{k_0'}^2\sin^2\frac{\theta}{2}\cos\theta\right) + 2\frac{U}{J}n_{k_0'}e^{-2n_{k_0'}\sin^2\frac{\theta}{2}}\right]^{\frac{1}{2}}\Bigg\}\,, \end{aligned} \tag{3.90}$$

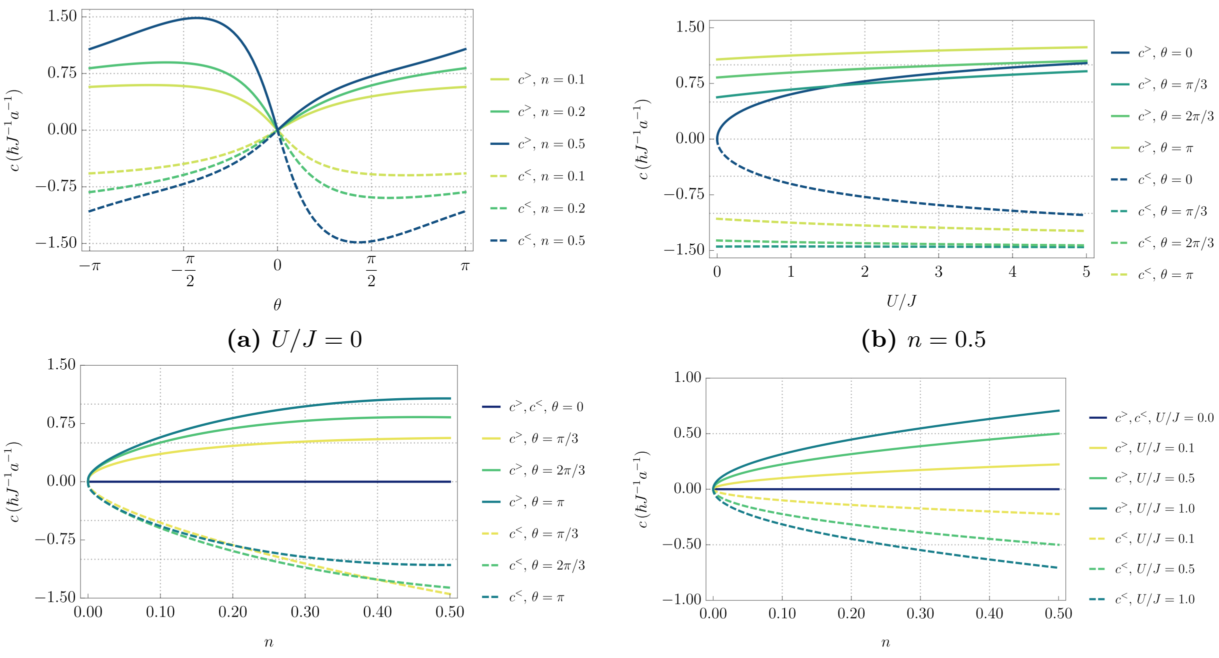

(a) $U/J = 0$ **(b)** $n = 0.5$

(c) $U/J = 0$ **(d)** $\theta = 0$

Figure 3.6: Behaviours of sound velocities with respect to statistical and ordinary interactions, as well as its density dependence for $L = 101$. According to **Eq.** (3.90) we see that the statistical interactions modulates of the density and are in-homogeneously amplifying the sound velocities. **(a)** Change of sound velocities with respect to purely statistical interactions, i.e. $U = 0$, for different values of the density n. **(b)** Change of sound velocities with respect to the on-site interaction U under different values of θ. **(c)** the impact of n with different θ that correspond to the respective statistical interactions and $U/J = 0$. **(d)** Change of sound velocities with respect to density for pure on-site interactions, i.e. $\theta = 0$.

where $c^>$ denotes right-propagating sound velocity (positive-valued) and $c^<$ the left-propagating one (negative valued). The bosonic velocity at $\theta = 0$ is given as

$$c^0 = \sqrt{\frac{2Ja^2}{\hbar^2} U n_{k_0}}\,, \tag{3.91}$$

which with the definition of effective mass (3.38) we can rewrite as

$$c^0 = \sqrt{\frac{U n_{k_0}}{m_{\text{eff},\,\theta=0}}} \tag{3.92}$$

Also note that the square root in (3.90) leads to a valid U/J range:

$$\frac{U}{J} \geqslant -8e^{-2n_{k_0'} \sin^2 \frac{\theta}{2}} \sin^2 \frac{\theta}{2} \left[1 + n_{k_0'} \cos\theta \right]. \tag{3.93}$$

which also gives $n_{k_0'} \leqslant 1$ as the long-wave limit result (3.79). In **Fig.** 3.6a-3.6d the behaviour of sound velocities are investigated. The asymmetry of the two sound modes is visible in **Fig.** 3.6a with vanishing on-site interaction $U = 0$, when one compares the right-propagating spices $c^>$ with the left-propagating spices $c^<$ for the same total particle density n. Then a very important feature is that a reversed statistical parameter $\theta \to -\theta$ leads to the interchanged behaviour between $c^>$ and $c^<$

$$|c^>(\theta)| = |c^<(-\theta)|\,. \tag{3.94}$$

This corresponds also to the temporal inversion $\hat{\mathcal{T}}$ as we mentioned in **Sec.** 2.4. Then the increasing of on-site interaction U enlarges both spices $c^{>/<}$ in a monotonous and parabolic manner, whereas the impact of statistical interaction via $\theta \to \pm\pi$ is rather non-linear. A larger total particle density n also leads to larger sound velocities, as shown in both **Fig.** 3.6c and 3.6d. The two figures also compare the effects of statistical interactions and field interactions accordingly, showing again that statistical interaction would break the parity. It should also be mentioned that such parity breaking feature is also implicitly indicated experimentally, i.e. the imbalanced transport of two anyons on optical lattice [70], as discussed in **Sec.** 2.5 and seen in **Fig.** 1.9. Then, with the asymmetry of sound velocities, we conclude that such imbalanced features can also appear in experiments for the many-body cases.

3.6.2 Estimation between Bogoliubov and Luttinger theory

It's the right place to remind about what Bogoliubov theory is as we have already proceeded: based on the mean-field theory, one can further include the fluctuating part of the wavefunction; then by diagonalizing the two-body interaction Hamiltonian via transformation of the bosonic particle operators to a new set of bosonic landau quasiparticle - the collective excitations, we have now a non-interacting system with those quasiparticles. The validity of this theory relies on the **diluteness condition** [52, 81]

$$|a_s| \ll d\,, \tag{3.95}$$

where a_s is the s-wave scattering length and $d = n^{-1/D}$ is the average distance between particles with D the dimensionality. a_s, as in standard scattering theory, characterizes the property of interactions. Then this smallness of a_s (3.95) now implies that we are working among a weak bare interacting regime, which allows the Bogoliubov-Popov theory, as now the quasiparticle has rather long lifetime.

In our anyonic context, other than the Hubbard interaction U, there is also the statistic interaction which is implicitly encoded in the density-dependent Peierls phase from (2.30). On the other hand, for the strong interacting systems in one dimension, Haldane [98] proposed the effective low-energy Tomonaga-Luttinger liquid (TLL) theory which characterizes the system with $\hat{H}_{\text{TLL}}\{K, u\}$, where K is the Luttinger parameter and u the fermi velocity [52, 91]. Bonkhoff then extended the TLL theory to the anyonic version by including the statistical parameter θ [51]. Then it's valuable to make quantitative comparisons between the Bogoliubov theory and extended TLL theory now under the anyonic context. To this end we make a round routine, namely first we estimate the sound velocities from the extended TLL (eTLL) theory and compare them with the Bogoliubov theory. Inversely we try to estimate the parameters in the eTLL theory from the Bogoliubov theory.

From Luttinger to Bogoliubov

Based on **Ref.** [51], we have the eTLL Hamiltonian in diagonalized form (Also see **App.** C for the derivation):

$$\hat{H}_{\text{cont.}} \approx \sum_{q\neq 0} u \left[1 + \frac{\Delta}{2}\text{sign}(q)\right] |q| \hat{\beta}^\dagger \hat{\beta}\,, \tag{3.96}$$

Then in the long-wave limit we have the sound velocities for the eTLL theory, in the natural unit

$$c^{\pm}_{\text{TLL, NU}} = -\frac{u \cdot \Delta}{2} \pm u \tag{3.97}$$

Taking into account the Luttinger parameter K

$$K = \sqrt{\frac{\pi^2 \rho_0}{V_2(\theta) + c + 3\rho_0 V_3(\theta)}}\,, \tag{3.98}$$

the Fermi velocity u

$$u = \frac{2\pi\rho_0}{K}\,, \tag{3.99}$$

and the parity-breaking interaction Δ

$$\Delta = \frac{8\rho_0 V_J(\theta)}{u}\,, \tag{3.100}$$

this leads then

$$c^{\pm}_{\text{TLL, NU}} = -4\rho_0 \sin\theta \pm 2\pi\rho_0 \sqrt{\frac{V_2(\theta) + c + 3\rho_0 V_3(\theta)}{\pi^2\rho_0}} \tag{3.101}$$

where we could further insert the coefficients for the interactions (C.7 C.10) and the normalized coefficient $c = U/2Ja$ and obtain

$$c^{\pm}_{\text{TLL, NU}} = -4\rho_0 \sin\theta \pm 2\pi\rho_0 \sqrt{\frac{\frac{2}{a}(1-\cos\theta) + \frac{U}{2Ja} - 3\rho_0(1 - 2\cos\theta + \cos 2\theta)}{\pi^2\rho_0}}\,. \tag{3.102}$$

In order to make a quantitative comparison, we have to proceed as follows: first, we denote the different definitions for particle density in continuous and discrete space, which gives the relation $\rho_0 = \frac{N_0}{La} = \frac{n_0}{a}$. Then, as the eTLL theory is valid only for low-density, such a framework excludes even a quasi-condensate description. Nevertheless, quantitatively, it is allowed to correspond n_0 to the average macroscopic occupation number n_{k_0} in the Bogoliubov context. Therefore the sound velocities in eTLL theory are expressed with Bogoliubov notions:

$$c^{\pm}_{\text{eTLL, NU}} = -\frac{4n_{k_0}}{a}\sin\theta \pm \frac{2}{a}\sqrt{2n_{k_0}(1-\cos\theta) - 3n_{k_0}^2(1 - 2\cos\theta + \cos 2\theta) + \frac{U}{2J}}\,. \tag{3.103}$$

Then, as we are yet working with natural units and the scaled $Ja^2 = 1$, one has to go through a dimensional analysis to translate the TLL sound velocities into SI units via

$$c^{\pm}_{\text{TLL}} = (Ja^2)^{\alpha}\hbar^{\beta} c^{\pm}_{\text{TLL, NU}}\,, \tag{3.104}$$

which amounts then to find the coefficients α, β.

The SI units of the sound velocity are known to everyone, as how long the distance is translated per second:

$$\dim\,\left[c^{\pm}_{\text{Bog.}}\right] = T^{-1}L\,, \tag{3.105}$$

and the dimension of the sound velocities for the eTLL theory (3.103) we have so far is

$$\dim\,\left[c^{\pm}_{\text{TLL, NU}}\right] = \dim\,\left[\frac{1}{a}\right] = L^{-1}\,. \tag{3.106}$$

Then the dimensions of the scaling factors are

$$\begin{cases} \dim\,\left[Ja^2\right] = T^{-2}L^2M \cdot L^2 = T^{-2}L^4M \\ \dim\,\left[\hbar\right] = \dim\,\left[E/\omega\right] = T^{-2}L^2M/T^{-1} = T^{-1}L^2M \end{cases}, \tag{3.107}$$

therefore we could determine the coefficients via comparing the power of the corresponding unit,

$$T^{-1}L = \left[T^{-2}L^4M\right]^{\alpha}\left[T^{-1}L^2M\right]^{\beta}L^{-1}\,, \tag{3.108}$$

which leads to

$$\alpha = 1\,,\ \beta = -1\,. \tag{3.109}$$

Now, together with the trigonometric identities

$$1-\cos\theta = 2\sin^2\frac{\theta}{2}\,,\quad 1-2\cos\theta+\cos 2\theta = -4\sin^2\frac{\theta}{2}\cos\theta\,, \tag{3.110}$$

we finally obtain the sound velocities for the eTLL theory in SI units,

$$c_{\text{eTLL}}^{>/<} = \frac{Ja}{\hbar}\left\{-4n_{k_0}\sin\theta \pm \left[\left(16n_{k_0}\sin^2\frac{\theta}{2}+48n_{k_0}^2\sin^2\frac{\theta}{2}\cos\theta\right)+\frac{2Un_{k_0}}{J}\right]^{\frac{1}{2}}\right\}, \tag{3.111}$$

Compare now the eTLL sound velocities $c_{\text{eTLL}}^{>/<}$ with the Bogoliubov sound velocities $c^{>/<}$ (3.90), we can observe that they share the same structure, but with different coefficients. This is in accordance with the conslusions in **Ref.** [91] that at low-energy and long-wavelength regime, Bogoliubov theory coincide with Luttinger liquid theory. Those coefficients play an important role in the stability of the sound velocities, namely, from the demand of making the radiant in (3.111) real, we have

$$\frac{U}{J} \geqslant -8e^{-2n_{k_0}\sin^2\frac{\theta}{2}}\sin^2\frac{\theta}{2}\left[1+3n_{k_0}\cos\theta\right]. \tag{3.112}$$

Compare (3.112) with (3.93), the eTLL theory would have either a more dilute system, meaning for the non-negative interaction $U/J \geq 0$, and full statistical range $\theta \in [0,\pi]$, in the low-energy limit $q \to 0$,

$$\begin{cases}\text{Bog.:} & n_{k_0} \leqslant 1\\ \text{eTLL:} & n_{k_0} \leqslant \dfrac{1}{3}\end{cases}, \tag{3.113}$$

or it requires a larger interaction strength U/J when taking into account the $\theta \to \pi$, in the low-energy limit $q \to 0$

$$\begin{cases}\text{Bog.:} & \dfrac{U}{J} \geqslant e^{-2n_{k_0}}\left(n_{k_0}-1\right)\\ \text{eTLL:} & \dfrac{U}{J} \geqslant e^{-2n_{k_0}}\left(3n_{k_0}-1\right)\end{cases}, \tag{3.114}$$

as it is a theory for the strong-coupling regime. One can also compare the ratios of the velocities between the two theories, as shown in **Fig.** 3.7 and **Fig.** 3.8. One can see that for both plots the eTLL ratio is smaller than the Bogoliubov one for the same parameter set, meaning a stronger parity breaking, which corresponds to the fact that the extended Tomonaga-Luttinger liquid theory works also in the strong-coupling regime.

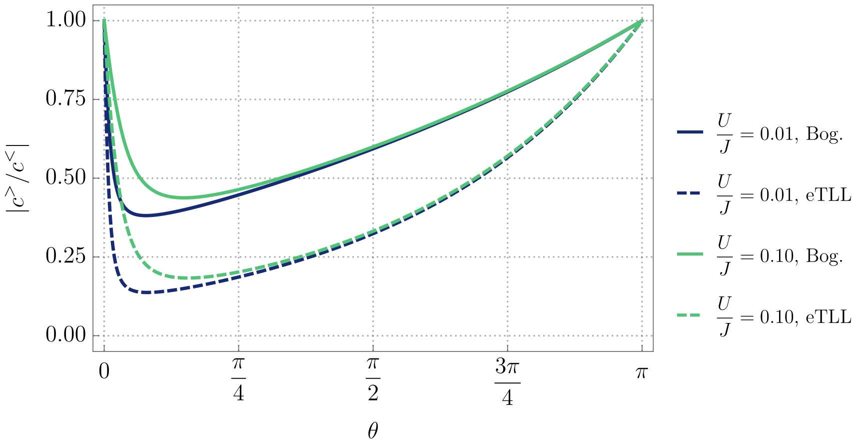

Figure 3.7: Absolute ratio between the sound velocities of the right- and left-propagating species for two theories. Here condensate density per site is $n_{k_0'} = 0.3$.

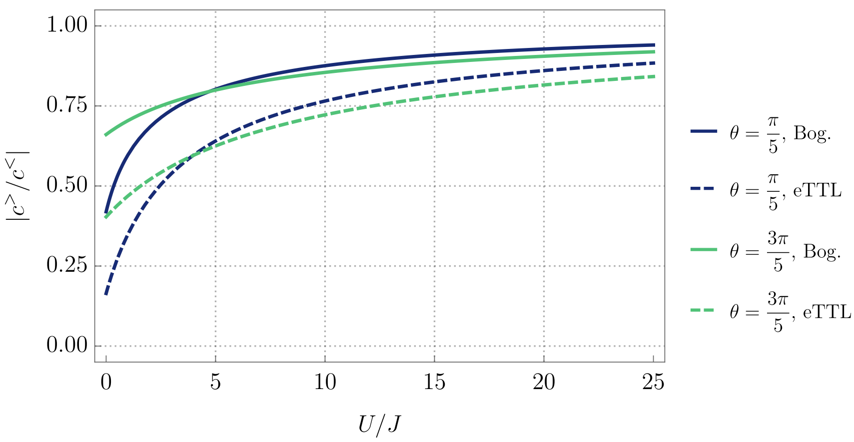

Figure 3.8: Absolute ratio between the sound velocities of the right- and left-propagating species for two theories. Here condensate density per site is $n_{k_0} = 0.3$.

From Bogoliubov to Luttinger

Finally, we try to estimate the Luttinger parameters in the Bogoliubov theory. From the expression of the extended TLL sound velocities (3.97), we could simply scale the Bogoliubov sound velocities (3.90) with $Ja^2/\hbar$ and compare them respectively, therefore we could obtain the equation

$$-\frac{u_{\text{Bog.}}\cdot\Delta_{\text{Bog.}}}{2}\pm u_{\text{Bog.}}=-\frac{2n_{k_0}\,e^{-2n_{k_0}\sin^2\frac{\theta}{2}}\sin\theta}{a}$$
$$\pm\left[\frac{e^{-4n_{k_0}\sin^2\frac{\theta}{2}}}{a^2}\left(16n_{k_0}\sin^2\frac{\theta}{2}+16n_{k_0}^2\sin^2\frac{\theta}{2}\cos\theta\right)+\frac{2U}{Ja^2}n_{k_0}e^{-2n_{k_0}\sin^2\frac{\theta}{2}}\right]^{\frac{1}{2}} \tag{3.115}$$

and the Fermi velocity (3.99) in the Bogoliubov theory could be directly read off as

$$u_{\text{Bog.}}=\left[\frac{e^{-4n_{k_0}\sin^2\frac{\theta}{2}}}{a^2}\left(16n_{k_0}\sin^2\frac{\theta}{2}+16n_{k_0}^2\sin^2\frac{\theta}{2}\cos\theta\right)+\frac{2U}{Ja^2}n_{k_0}e^{-2n_{k_0}\sin^2\frac{\theta}{2}}\right]^{\frac{1}{2}}. \tag{3.116}$$

From the definition of the parity-breaking interaction (3.100) in eTLL theory, the first term on both sides of (3.115) could be evaluated as

$$\frac{4n_{n_{k_0}}V_{J,\,\text{Bog.}}(\theta)}{a}=\frac{2n_{k_0}\,e^{-2n_{k_0}\sin^2\frac{\theta}{2}}\sin\theta}{a}, \tag{3.117}$$

therefore the current interaction strength in Bogoliubov theory is

$$V_{J,\,\text{Bog.}}(\theta)=\frac{1}{2}e^{-2n_{k_0}\sin^2\frac{\theta}{2}}\sin\theta\,. \tag{3.118}$$

Then the parity-breaking interaction in Bogoliubov theory is

$$\Delta_{\text{Bog.}}=\frac{8n_{k_0}V_{J,\,\text{Bog.}}(\theta)}{u_{\text{Bog.}}a}\,. \tag{3.119}$$

From the definition of the Fermi velocity (3.99) we could deduce now the Luttinger parameter

$$K_{\text{Bog.}}=\frac{2\pi n_{k_0}}{u_{\text{Bog.}}a}=\left[\frac{\pi^2 n_{k_0}}{e^{-4n_{k_0}\sin^2\frac{\theta}{2}}\left(4\sin^2\frac{\theta}{2}+4n_{k_0}\sin^2\frac{\theta}{2}\cos\theta\right)+\frac{U}{2J}e^{-2n_{k_0}\sin^2\frac{\theta}{2}}}\right]^{\frac{1}{2}}, \tag{3.120}$$

compare with the definition of the Luttinger parameter from eTLL theory (3.98),

$$K=\sqrt{\frac{\pi^2\rho_0}{V_2(\theta)+c+3\rho_0V_3(\theta)}}=\left[\frac{\pi^2 n_{k_0}}{4\sin^2\frac{\theta}{2}+12n_{k_0}\sin^2\frac{\theta}{2}\cos\theta+\frac{U}{2J}}\right]^{\frac{1}{2}}, \tag{3.121}$$

we have the Bogoliubov versions of the interaction strength and coefficient

$$V_{2,\,\text{Bog.}}(\theta)=\frac{2(1-\cos\theta)}{a}\,e^{-4n_{k_0}\sin^2\frac{\theta}{2}}, \tag{3.122}$$

$$V_{3,\,\text{Bog.}}(\theta)=\frac{-(1-2\cos\theta+\cos2\theta)}{3}\,e^{-4n_{k_0}\sin^2\frac{\theta}{2}}, \tag{3.123}$$

$$c_{\text{Bog.}}=\frac{U}{2Ja}\,e^{-2n_{k_0}\sin^2\frac{\theta}{2}}\,. \tag{3.124}$$

This again implies a correspondence between Bogoliubov theory and Luttinger liquid theory. Using the so-called bosonization technique, the one-dimensional bosonic gas is mapped onto the Luttinger liquid model [91]. The Bogoliubov phonons then correspond to the collective excitations in the Luttinger liquid theory.

Chapter 4

Correlation Functions

Having a complete analysis of the anyonic Bogoliubov dispersion, especially the stable parameter range, gives then hints about the experimentally accessible observables that can unveil the anyonic properties. The correlation functions are the natural framework for characterizing our system both experimentally and theoretically [99]. For example, the absorption images after the time-of-flight (TOF) can measure the expansion of a trapped atomic cloud by turning off the trap and imaging the expanded cloud, so that its momentum distribution can be mapped to the the density distribution of the TOF images [100]. This is also how the momentum distribution of the first realized BEC was measured in **Ref.** [6], also shown in **Fig.** 1.1. The quantum gas microscope, first proposed by M. Greiner *et al.* in **Ref.** [79], is an advanced imaging system that can observe and manipulate individual ultracold atoms trapped in optical lattice with single-atom and single-site resolutions. It is also used to detecting the anyons in the Floquet engineering realization introduced in **Sec.** 2.5. With quantum gas microscope the anyonic Hanbury Brown-Twiss effect, i.e. the transmutation from the bunching of bosons to the anti-bunching of pseudo-fermions, is also observed via detect the density-density correlation [70]. Nowadays, the two techniques are the two of most widely used tools in determining the correlations in ultracold quantum systems. Both of the two can detect the single-particle density matrix and pair particle matrix in momentum space; Thus, it is valuable to investigate those correlations. To this end we start from their definitions and derive the corresponding detailed expressions.

4.1 Spatial Coherence for Bosons

To start, we would like to investigate the spatial correlations for single bosonic particles[1],

$$G_{ij}^{(1)} = \langle \hat{b}_i^\dagger \hat{b}_j \rangle \,, \tag{4.1}$$

this amounts first to Fourier transform the bi-linear term $\hat{b}_i^\dagger \hat{b}_j$,

$$\hat{b}_i^\dagger \hat{b}_j = \frac{1}{L} \sum_{k,k'} \hat{b}_k^\dagger \hat{b}_{k'}\, e^{i(ki-k'j)a} e^{i\beta(i-j)a} \,. \tag{4.2}$$

Inserting the modified Bogoliubov *ansatz* (3.6) leads to

$$\begin{aligned}\hat{b}_i^\dagger \hat{b}_j \approx \frac{1}{L}\Bigg\{ &\left|\sqrt{N_{k_0}} + \delta\hat{b}_{k_0}^\dagger\right|^2 e^{ik_0(i-j)a} e^{i\beta(i-j)a} + \Bigg[\left(\sqrt{N_{k_0}} + \delta\hat{b}_{k_0}^\dagger\right) e^{i(k_0+\beta)ia} \sum_{k\neq k_0} \hat{b}_k\, e^{-i(k+\beta)ja} \\ &+ \left(\sqrt{N_{k_0}} + \delta\hat{b}_{k_0}\right) e^{-i(k_0+\beta)ja} \sum_{k\neq k_0} \hat{b}_k^\dagger\, e^{i(k+\beta)ja}\Bigg] + \sum_{k,k'\neq k_0} \hat{b}_k^\dagger \hat{b}_{k'}\, e^{i(ki-k'j)a} e^{i\beta(i-j)a}\Bigg\}\,,\end{aligned} \tag{4.3}$$

[1]We drop from now on the suffix for the expectation value, $\langle \bullet \rangle_{\hat{H}_{\rm diag}} \to \langle \bullet \rangle$.

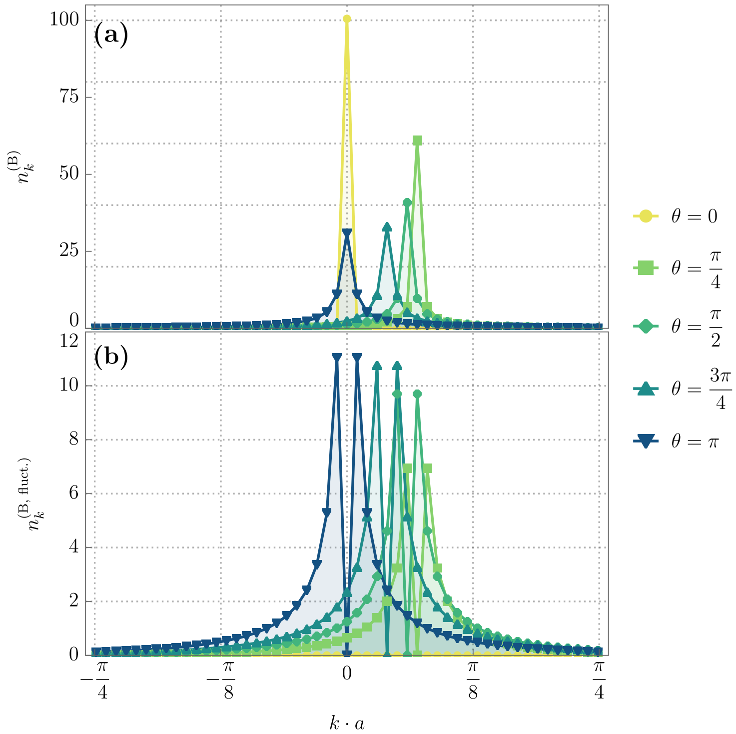

Figure 4.1: Quasi momentum distribution for bosons **Eq.** (4.7) with the total particle density $n = 0.5$, number of lattice sites $L = 201$ and without Hubbard interaction, $U/J = 0$. **(a)** is the total distribution, **(b)** demonstrates the fluctuation part of **(a)**: two peaks located symmetrically around the quasi-condensate, with the same height. The quasi-momentum distribution shifts reversely to the results in **Ref.** [30, 65, 89] due to the definition of the Fourier transformation. Otherwise the shift direction is the same.

Taking into account the Bogoliubov transformation (3.60, 3.61), we know the exception value for single particle operators vanish, $\langle(\delta)\hat{b}_j^{(\dagger)}\rangle = 0$ due to $\langle\hat{d}_j^{(\dagger)}\rangle = 0$. Therefore the spatial correlation is given as

$$G_{ij}^{(1)} \approx \frac{e^{i\beta(i-j)a}e^{ik_0(i-j)a}}{L}\left\{N_{k_0} + \sum_{q\neq k_0}\langle\hat{b}^{\dagger}_{k_0'+q}\hat{b}_{k_0'+q}\rangle\, e^{iq(i-j)a}\right\} \tag{4.4}$$

4.2 Quasi-momentum Distribution for Bosons

The quasi-momentum distribution for bosons is defined via the deformed Fourier transformation of its spatial correlation,

$$\langle\hat{n}_k^{\mathrm{B}}\rangle = \frac{1}{L}\sum_{ij}\langle\hat{b}_i^{\dagger}\hat{b}_j\rangle_{\hat{H}_{\mathrm{diag}}}\, e^{-ik(i-j)a}e^{-i\beta(i-j)a}\,. \tag{4.5}$$

Taking into account (4.5), this leads to

$$\langle\hat{n}_k^{\mathrm{B}}\rangle = \sum_{ij}\left\{\frac{n_{k_0}}{L}\, e^{-i(k-k_0)(i-j)a} + \frac{e^{-ik(i-j)a}}{L^2}\sum_{q'\neq 0}\langle\hat{b}^{\dagger}_{k_0+q'}\hat{b}_{k_0+q'}\rangle\, e^{i(q'+k_0)(i-j)a}\right\}. \tag{4.6}$$

The double summation $\sum_{ij}$ in (4.6) can be decomposed into single summations $\sum_i$ and $\sum_j$ free of risk, from which one can further use the one-dimensional Fourier transformation of Kronecker delta function (B.5), which finally leads to simply form,

$$\langle\hat{n}_k^{\mathrm{B}}\rangle = N_{k_0}\delta_{k,k_0} + (1-\delta_{k,k_0})\langle\hat{b}_k^{\dagger}\hat{b}_k\rangle\,. \tag{4.7}$$

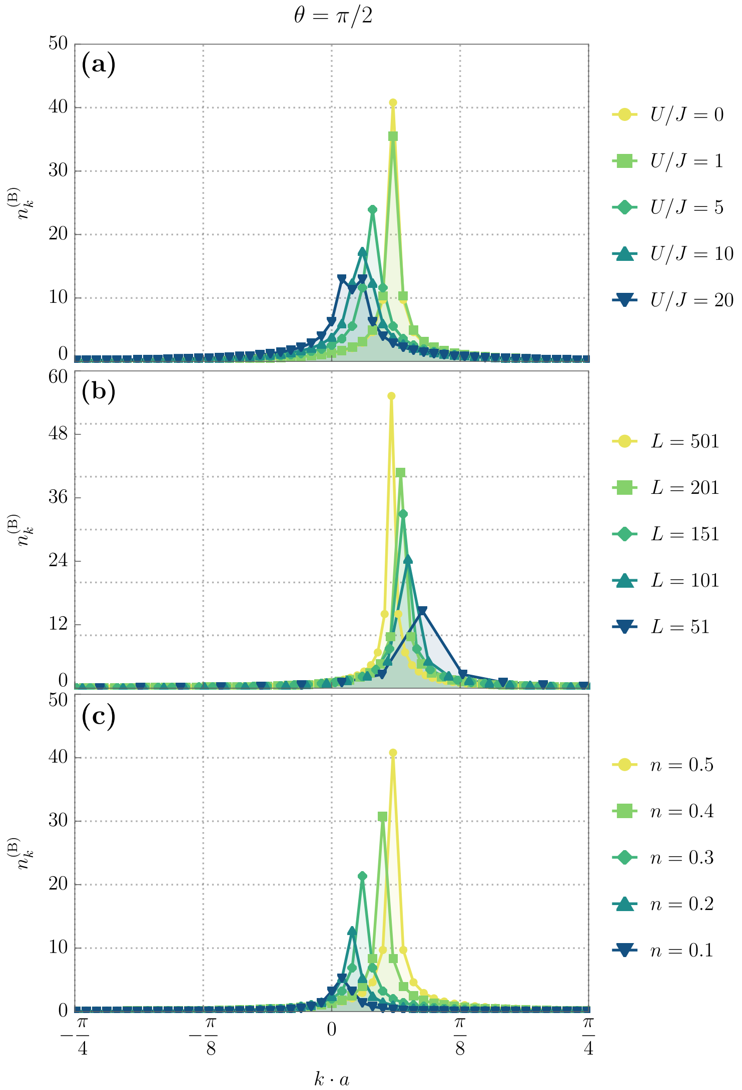

Figure 4.2: Quasi momentum distribution for bosons **Eq.** (4.7) with the statistic parameter $\theta = \pi/2$, and compare the change of other parameters. **(a)** compare the effect of the Hubbard interaction with $L = 201$ and $n = 0.5$; **(b)** compares the impact of the number of lattice sites, with $U/J = 0$ and $n = 0.5$. **(c)** then compares the effect of the total particle density on-site, with $L = 201$ and $U/J = 0$.

Note that due to the discretization of the momentum space, the quasi-momentum of the condensate should also be quantized in units of $\Delta k = 2\pi/L$. Then the actual k_0 is rounded to it's nearest permitted integer unit, which is also indicated in the Kronecker delta δ_{k,k_0} in the expression of $\langle \hat{n}_k^{\mathrm{B}} \rangle$. The first term in (4.7) is the macroscopic occupation, i.e. the quasi-condensate that shifted in the momentum space with k_0 as indicated by the Kronecker delta δ_{k,k_0}. This is rather an expression for true condensate than the quasi-condensate in one dimension, whose momentum distribution should be broadened, which comes from the mean-field assumption in the modified Bogoliubov *ansatz* that the macroscopic state occupies only k_0 mode. The second part denotes the quantum fluctuations that come from both the on-site interaction U and the statistical one, with a highly sophisticated structure as in (3.86).

The corresponding schematic of $\langle \hat{n}_k^{\mathrm{B}} \rangle$ is given in **Fig.** 4.1. The broken spatial and temporal symmetries are significantly visible in the quasi-momentum distribution, which aligns with the previous Gutzwiller and DMRG results from **Ref.** [30, 65, 89], when taking into account the reversed definition for the Fourier transformations. Also, as the statistical parameter goes from the bosonic limit to the pseudo-fermionic limit, the macroscopic part is depleted to the fluctuations, as the peak of the distribution is lower, and the fluctuation part is enlarged in amplitude and also broadened. It is also notable that the fluctuations are symmetric around the macroscopic occupation, as shown in **Fig.** 4.1 **(b)**.

Then the **Fig.** 4.2 investigates the effect of different parameters. A very large on-site interaction U also leads to a broadened distribution; the fluctuations are enhanced such that they would even exceed the amplitude of the macroscopic part. The finite-size effect would lead to higher peak amplitude and shortened distribution with increased L that approaches the δ function. A broadened distribution is shown with reduced total particle density n, meaning an enhanced statistical interaction as expected from previous results in the ground state (3.46) and in the quantum depletion part.

4.3 Pair Correlation for Bosons

In the field of quantum gases, pair correlation is the fundamental tool to investigate the particle interactions, quantum statstics and many-body phenomena [91, 101]. The un-normalized $G^{(2)}$ function is defined as

$$G_{ij}^{(2)} = \langle \hat{b}_i^\dagger \hat{b}_j^\dagger \hat{b}_i \hat{b}_j \rangle = \frac{1}{L^2} \sum_{k_1,k_2,k_3,k_4} e^{i\left[(k_1-k_3)i+(k_2-k_4)j\right]a} \langle \hat{b}_{k_1}^\dagger \hat{b}_{k_2}^\dagger \hat{b}_{k_3} \hat{b}_{k_4} \rangle \,. \tag{4.8}$$

It quantifies the possibility to find two particles at two lattice sites i and j simultaneously. Now again we insert the modified Bogoliubov *ansatz* (3.6), which leads to

$$\begin{aligned}
G_{ij}^{(2)} \overset{q=k-k_0}{=} \frac{1}{L^2} \Bigg\langle & N_{k_0}^2 + N_{k_0}^{\frac{3}{2}} \sum_{q_1 \neq 0} \left[\hat{b}_{k_0+q_1}^\dagger \, e^{iq_1ia} + \hat{b}_{k_0+q_1} \, e^{-iq_1ia} + \hat{b}_{k_0+q_1}^\dagger \, e^{iq_1ja} + \hat{b}_{k_0+q_1} \, e^{-iq_1ja} \right] \\
& + N_{k_0} \sum_{q_1,q_2 \neq 0} \left[\hat{b}_{k_0+q_1}^\dagger \hat{b}_{k_0+q_2} \left(e^{i(q_1-q_2)ia} + e^{i(q_1-q_2)ja} \right) + \hat{b}_{k_0+q_1}^\dagger \hat{b}_{k_0+q_2} \, e^{i(q_1i-q_2j)a} \right. \\
& \left. + \hat{b}_{k_0+q_1}^\dagger \hat{b}_{k_0+q_2} \, e^{-i(q_1i-q_2j)a} + \left(\hat{b}_{k_1}^\dagger \hat{b}_{k_2}^\dagger \, e^{i(q_1i+q_2j)a} + \text{h.c.} \right) \right] \\
& + N_{k_0}^{\frac{1}{2}} \sum_{q_1,q_2,q_3 \neq 0} \left[\hat{b}_{k_0+q_1}^\dagger \hat{b}_{k_0+q_2}^\dagger \hat{b}_{k_0+q_3} \, e^{i[(q_1-q_3)i+q_2j]a} + \hat{b}_{k_0+q_1}^\dagger \hat{b}_{k_0+q_2}^\dagger \hat{b}_{k_0+q_3} \, e^{i[(q_2-q_3)j+q_1i]a} \right. \\
& \left. + \hat{b}_{k_0+q_1}^\dagger \hat{b}_{k_0+q_2} \hat{b}_{k_0+q_3} \, e^{i[(q_1-q_3)j-q_3i]a} + \hat{b}_{k_0+q_1}^\dagger \hat{b}_{k_0+q_2} \hat{b}_{k_0+q_3} \, e^{i[(q_1-q_2)i-q_3i]a} \right] \\
& + \sum_{q_1,q_2,q_3,q_4 \neq 0} \hat{b}_{k_0+q_1}^\dagger \hat{b}_{k_0+q_2}^\dagger \hat{b}_{k_0+q_3} \hat{b}_{k_0+q_4} \, e^{i[(q_1-q_3)i+(q_2-q_4)j]a} \Bigg\rangle \,.
\end{aligned} \tag{4.9}$$

Similar to the case that expectation value would vanish for single particle operators, the tri-linear terms also do not contribute in (4.9). This then leads to the expression after combining the terms according to their order,

$$\begin{aligned}
G_{ij}^{(2)} = \frac{1}{L^2} \Bigg\{ & N_{k_0}^2 + N_{k_0} \sum_{q \neq 0} \Big[(2 + 2\cos[q(i-j)a]) \langle \hat{b}_{k_0+q}^\dagger \hat{b}_{k_0+q} \rangle \\
& + \left(\langle \hat{b}_{k_0+q}^\dagger \hat{b}_{k_0-q}^\dagger \rangle e^{iq(i-j)a} + \text{h.c.} \right) \Big] \\
& + \sum_{q_1,q_2,q_3,q_4 \neq 0} \langle \hat{b}_{k_0+q_1}^\dagger \hat{b}_{k_0+q_2} \hat{b}_{k_0+q_3}^\dagger \hat{b}_{k_0+q_4} \rangle \, e^{i[(q_1-q_2)i+(q_3-q_4)j]a} \Bigg\} \,.
\end{aligned} \tag{4.10}$$

The first term denotes the macroscopic-macroscopic correlation, with the second part describing the macroscopic-fluctuation correlation, together they are also called the disconnected part of the correlation [102, 103],

$$G_{ij}^{(2,0)} = n_{k_0}^2 \,, \tag{4.11}$$

$$G_{ij}^{(2,1)} = \frac{N_{k_0}}{L^2} \sum_{q\neq 0} \Big[(2 + 2\cos[q(i-j)a]) \langle \hat{b}^\dagger_{k_0+q} \hat{b}_{k_0+q} \rangle_{\hat{H}_{\text{diag}}} + \Big(\langle \hat{b}^\dagger_{k_0+q} \hat{b}^\dagger_{k_0-q} \rangle_{\hat{H}_{\text{diag}}} e^{iq(i-j)a} + \text{h.c.} \Big) \Big] \,. \tag{4.12}$$

The third term in (4.10) is then the connected part, which denotes the fluctuation-fluctuation correlation

$$G_{ij}^{(2,2)} = \frac{1}{L^2} \sum_{q_1,q_2,q_3,q_4 \neq 0} \langle \hat{b}^\dagger_{k_0+q_1} \hat{b}^\dagger_{k_0+q_2} \hat{b}_{k_0+q_3} \hat{b}_{k_0+q_4} \rangle_{\hat{H}_{\text{diag}}} e^{i[(q_1-q_3)i+(q_2-q_4)j]a} \tag{4.13}$$

$G_{ij}^{(2,2)}$ contains a four-point correlator $\langle \hat{b}^\dagger_{k_0+q_1} \hat{b}^\dagger_{k_0+q_2} \hat{b}_{k_0+q_3} \hat{b}_{k_0+q_4} \rangle$, which is in general not contractible. However, as we have done the Bogoliubov transformations (3.60-3.61), the resulting diagonalized Hamiltonian leads to a Gaussian density matrix for the quasi-bosonic operators, which allows to safely use the Wick's theorem [104] for the contraction for bosonic particle operators:

$$\langle \hat{A}_1 \ldots \hat{A}_{2m} \rangle = \sum_{\sigma} \langle \hat{A}_{i_1} \hat{A}_{i_2} \rangle \langle \hat{A}_{i_3} \hat{A}_{i_4} \rangle \ldots \langle \hat{A}_{i_{2m-1}} \hat{A}_{i2m} \rangle \,, \tag{4.14}$$

where σ denotes all the permutations for exchanging the order of the bosonic operators $\hat{A}_i$ from $1, 2, \ldots, 2m$ to $i_1, i_2, \ldots, i_{2m}$. To this end we first insert the Bogoliubov transformations in $\langle \hat{b}^\dagger_{k_0+q_1} \hat{b}^\dagger_{k_0+q_2} \hat{b}_{k_0+q_3} \hat{b}_{k_0+q_4} \rangle$,

$$\begin{aligned} \langle \hat{b}^\dagger_{k_0+q_1} \hat{b}^\dagger_{k_0+q_2} \hat{b}_{k_0+q_3} \hat{b}_{k_0+q_4} \rangle = \Big\langle & \Big(\cosh\alpha_{q_1} \, \hat{d}^\dagger_{k_0+q_1} - \sinh\alpha_{q_1} \, \hat{d}_{k_0-q_1} \Big) \\ & \times \Big(\cosh\alpha_{q_2} \, \hat{d}^\dagger_{k_0+q_2} - \sinh\alpha_{q_2} \, \hat{d}_{k_0-q_2} \Big) \\ & \times \Big(\cosh\alpha_{q_3} \, \hat{d}_{k_0+q_3} - \sinh\alpha_{q_3} \, \hat{d}^\dagger_{k_0-q_3} \Big) \\ & \times \Big(\cosh\alpha_{q_4} \, \hat{d}_{k_0+q_4} - \sinh\alpha_{q_4} \, \hat{d}^\dagger_{k_0-q_4} \Big) \Big\rangle \,, \end{aligned} \tag{4.15}$$

which would lead to six non-vanishing four-point correlators for the quasi-particles,

$$\begin{aligned} \langle \hat{b}^\dagger_{k_0+q_1} \hat{b}^\dagger_{k_0+q_2} \hat{b}_{k_0+q_3} \hat{b}_{k_0+q_4} \rangle = \; & \cosh\alpha_{q_1} \cosh\alpha_{q_2} \cosh\alpha_{q_3} \cosh\alpha_{q_4} \Big\langle \hat{d}^\dagger_{k_0+q_1} \hat{d}^\dagger_{k_0+q_2} \hat{d}_{k_0+q_3} \hat{d}_{k_0+q_4} \Big\rangle \\ & + \cosh\alpha_{q_1} \sinh\alpha_{q_2} \sinh\alpha_{q_3} \cosh\alpha_{q_4} \Big\langle \hat{d}^\dagger_{k_0+q_1} \hat{d}_{k_0-q_2} \hat{d}^\dagger_{k_0-q_3} \hat{d}_{k_0+q_4} \Big\rangle \\ & + \cosh\alpha_{q_1} \sinh\alpha_{q_2} \cosh\alpha_{q_3} \sinh\alpha_{q_4} \Big\langle \hat{d}^\dagger_{k_0+q_1} \hat{d}_{k_0+q_2} \hat{d}_{k_0-q_3} \hat{d}^\dagger_{k_0-q_4} \Big\rangle \\ & + \sinh\alpha_{q_1} \cosh\alpha_{q_2} \sinh\alpha_{q_3} \cosh\alpha_{q_4} \Big\langle \hat{d}_{k_0-q_1} \hat{d}^\dagger_{k_0+q_2} \hat{d}^\dagger_{k_0-q_3} \hat{d}_{k_0+q_4} \Big\rangle \\ & + \sinh\alpha_{q_1} \cosh\alpha_{q_2} \cosh\alpha_{q_3} \sinh\alpha_{q_4} \Big\langle \hat{d}_{k_0-q_1} \hat{d}^\dagger_{k_0+q_2} \hat{d}_{k_0+q_3} \hat{d}^\dagger_{k_0-q_4} \Big\rangle \\ & + \sinh\alpha_{q_1} \sinh\alpha_{q_2} \sinh\alpha_{q_3} \sinh\alpha_{q_4} \Big\langle \hat{d}_{k_0-q_1} \hat{d}_{k_0-q_2} \hat{d}^\dagger_{k_0-q_3} \hat{d}^\dagger_{k_0-q_4} \Big\rangle \,. \end{aligned} \tag{4.16}$$

Using the CCR for bosonic operators and the Wick's theorem (4.14), this leads to for the first term

$$\begin{aligned}\left\langle \hat{d}^\dagger_{k_0+q_1}\hat{d}^\dagger_{k_0+q_2}\hat{d}_{k_0+q_3}\hat{d}_{k_0+q_4}\right\rangle =& \left\langle \hat{d}^\dagger_{k_0+q_1}\hat{d}_{k_0+q_3}\right\rangle\left\langle \hat{d}^\dagger_{k_0+q_2}\hat{d}_{k_0+q_4}\right\rangle + \left\langle \hat{d}^\dagger_{k_0+q_1}\ \hat{d}_{k_0+q_4}\right\rangle\left\langle \hat{d}^\dagger_{k_0+q_2}\hat{d}_{k_0+q_3}\right\rangle \\ &+ \left\langle \hat{d}^\dagger_{k_0+q_1}\hat{d}^\dagger_{k_0+q_2}\right\rangle\left\langle \hat{d}_{k_0+q_3}\hat{d}_{k_0+q_4}\right\rangle \\ =& \,\delta_{q_1,q_3}\delta_{q_2,q_4}\langle \hat{n}^d_{k_0+q_1}\rangle\langle \hat{n}^d_{k_0+q_2}\rangle + \delta_{q_1,q_4}\delta_{q_2,q_3}\langle \hat{n}^d_{k_0+q_1}\rangle\langle \hat{n}^d_{k_0+q_3}\rangle\,.\end{aligned} \tag{4.17}$$

Apply the same for the rest five terms, and combine all of them, we would have

$$\begin{aligned}\langle \hat{b}^\dagger_{k_0+q_1}\hat{b}_{k_0+q_2}\hat{b}^\dagger_{k_0+q_3}\hat{b}_{k_0+q_4}\rangle_{\hat{H}_{\rm diag}} =& \sinh\alpha_{q_1}\cosh\alpha_{q_2}\cosh\alpha_{q_3}\sinh\alpha_{q_4}(\delta_{q_1,-q_2}\delta_{q_3,-q_4}) \\ &+ \sinh\alpha_{q_1}\sinh\alpha_{q_2}\sinh\alpha_{q_3}\sinh\alpha_{q_4}(\delta_{q_1,q_4}\delta_{q_2,q_3}+\delta_{q_1,q_3}\delta_{q_2,q_4})\,.\end{aligned} \tag{4.18}$$

Therefore the connected part of the pair correlation (4.8) is

$$\begin{aligned}G^{(2,2)}_{ij} =& \frac{1}{L^2}\sum_{q_1,q_2\neq 0}\left(1+e^{i[(q_1-q_2)(i-j)]a}\right)\sinh^2\alpha_{q_1}\sinh^2\alpha_{q_2} \\ &+ \sinh\alpha_{q_1}\cosh\alpha_{q_1}\sinh\alpha_{q_2}\cosh\alpha_{q_4}\,e^{i[(q_1-q_2)(i-j)]a}\end{aligned} \tag{4.19}$$

and we have the full expression for the un-normalized pair correlation function

$$\begin{aligned}G^{(2)}_{ij} =& G^{(2,0)}_{ij} + G^{(2,1)}_{ij} + G^{(2,2)}_{ij} \\ =& \frac{1}{L^2}\Bigg\{ N^2_{k_0} + N_{k_0}\sum_{q\neq 0}\Big[(2+2\cos(q(i-j)a))\sinh^2\alpha_q - 2\cos(q(i-j)a)\sinh\alpha_q\cosh\alpha_q\Big] \\ &+ \sum_{q_1,q_2\neq 0}\Bigg[\left(1+e^{i[(q_1-q_2)(i-j)]a}\right)\sinh^2\alpha_{q_1}\sinh^2\alpha_{q_2} \\ &+ \sinh\alpha_{q_1}\cosh\alpha_{q_1}\sinh\alpha_{q_2}\cosh\alpha_{q_4}\,e^{i[(q_1-q_2)(i-j)]a}\Bigg]\,,\end{aligned} \tag{4.20}$$

4.4 Structure Factor

In solid state physics, the structure factor gives the structural information of a crystal lattice by characterizing the scattering momentum of the incoming and outcoming quanta that is external to the system [103]. In cold atom systems, it is also relevant in experimentally unveiling the low-energy and collective behaviours, for example the dispersion relation of anyons [78] and the superfluid in optical lattice via momentum-resolved Bragg spectroscopy [105].

Mathematically, the static structure factor is defined as the Fourier transform of the connected part of the pair correlation (4.20), i.e. [103]

$$S(k) = \frac{1}{N}\sum_{i,j} e^{ik(i-j)a}\left[G^{(2)}_{ij} - G^{(1)}_{ii}G^{(1)}_{jj}\right]. \tag{4.21}$$

With the results for the spatial coherence (4.4) and the pair correlation (4.20), this leads to

$$S(k) = \frac{1}{N}\sum_{i,j} e^{-ik(i-j)a}\frac{1}{L^2}\Bigg\{N_{k_0}\sum_{q\neq 0} 2\cos\left(q(i-j)a\right)\left(\sinh^2\alpha_q - \sinh\alpha_q\cosh\alpha_q\right)$$
$$+\sum_{q_1,q_2\neq 0} e^{i(q_1-q_2)(i-j)a}\left[\sinh^2\alpha_{q_1}\cosh^2\alpha_{q_2} + \sinh\alpha_{q_1}\cosh\alpha_{q_1}\sinh\alpha_{q_2}\cosh\alpha_{q_2}\right]\Bigg\}. \tag{4.22}$$

Using now again the one-dimensional discrete Fourier transformation of the delta function (B.5) as we did for the quasi-momentum distribution for bosons, we have

$$S(k) = \frac{1}{N}\Bigg\{2N_{k_0}(1-\delta_{k,0})\left(\sinh^2\alpha_k - \sinh\alpha_k\cosh\alpha_k\right)$$
$$+\sum_{q_1\neq 0,\, q_1\neq k}\left(\sinh^2\alpha_{q_1}\cosh^2\alpha_{q_1-k} + \sinh\alpha_{q_1}\cosh\alpha_{q_1}\sinh\alpha_{q_1-k}\cosh\alpha_{q_1-k}\right)\Bigg\}. \tag{4.23}$$

Note that the discretization of k_0 is again taken into account. In **Fig.** 4.3 the effects of different parameters are investigated. The overall structure can be understood from the Fourier transformation of the δ function [103]. If the particles are un-correlated, a vanishing signal is expected. While constant and periodic modulated pair correlations lead to single peak and multiple peaks, respectively. The reduced peak signal from $\theta = 0$ to $\theta = \pi$ can be seen as the effect of statistical interaction that repulses the two particles from occupying the same quantum state. The effect of total density and on-site interaction follows the same argument. The behaviour of increasingly sharp signals for larger lattice size is the same as the δ function in a lattice.

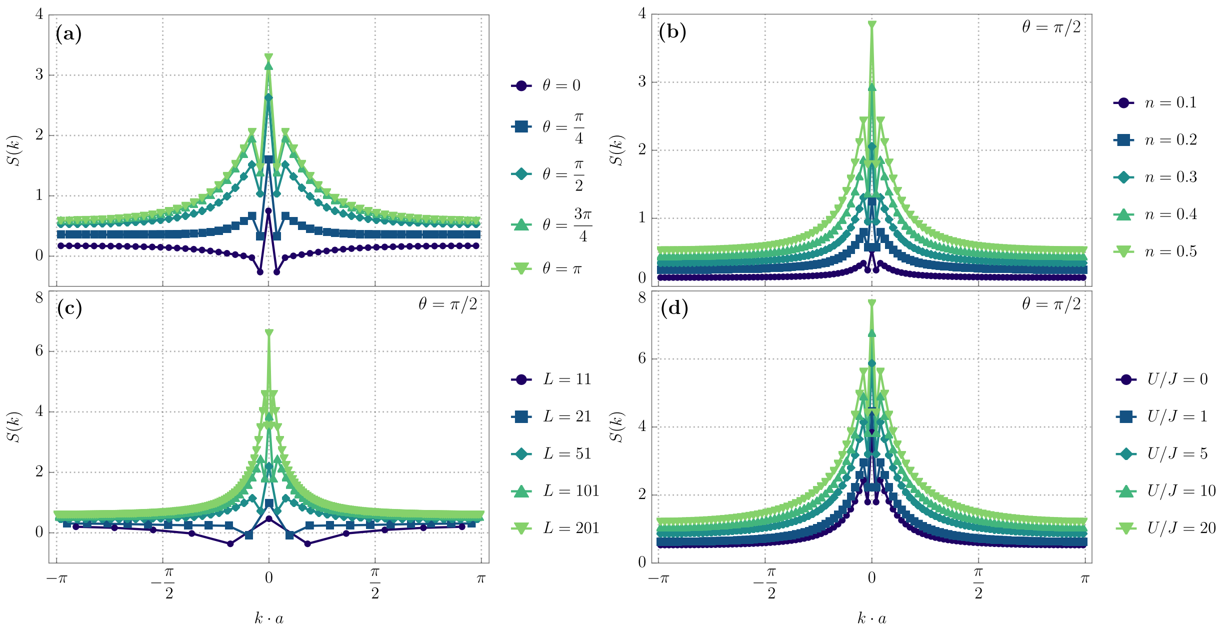

Figure 4.3: Static structure factors, **(a)** with $L = 101$, $n = 0.5$ and $U/J = 1$. The peak value gets higher when approaching the pseudo-fermionic limit. **(b)** concerns the difference of total particle density with $U/J = 0$ and $L = 101$; **(c)** then compares the impact of finite-size effect with $n = 0.5$ and $U/J = 0$. **(d)** shows the impact of Hubbard interaction with $L = 101$ and $n = 0.5$.

Chapter 5

Conclusion and Outlook

At the end of the thesis, it's valuable to recapitulate the key points. First of all, although fractional statistics does not appear naturally in one-dimension as its two-dimensional counterpart where the braid group is fundamental, one can nevertheless construct it *a priori* and define the anyonic algebra (2.9a-2.9c) on the one-dimensional lattice. The Anyon-Hubbard model (2.1), as is proposed in a lattice, is not only an apt theoretical playground but is also of importance as one can relate anyons to bosons via the fractional Jordan-Wigner transformation, therefore sheds light on possible experimental realization.

The breaking of spatial and temporal symmetries is essential for the Anyon-Hubbard model, expressed either in the anyonic algebra (2.9a) or the bosonic Hamiltonian (2.30). The parity breaking is also the reason for the non-zero minimum of quasi-momentum distribution from the Gutzwiller mean-field theory and DMRG simulation results from **Refs.** [30, 65], and this motivated us to propose the modified Bogoliubov *ansatz* such that the macroscopic part captures the non-vanishing k_0. This further leads to an asymmetric Bogoliubov dispersion and subsequently two types of sound velocities that can be mediated via the temporal inversion, which is also equivalent to the inversion of the statistic parameter $\theta \to -\theta$. The existence of two-mode sound velocities can also be observed implicitly from the imbalanced transport of two anyons in experiment [70]. The same feature is also seen in the extended Tomonaga-Luttinger liquid theory, and a quantitative comparison shows that the results of sound velocities from the weak-coupling, discretized Bogoliubov theory and the strong-coupling, low-density, continuous extended Tomonaga-Luttinger theory, share the same analytic structure under the low-energy and dilute limits.

Another crucial perspective is the anyonic statistical interaction. Although deriving an explicit form for such statistical interaction is generally highly non-trivial, in this thesis, we have approached it from different indirect ways. From the modified Bogoliubov theory, on the mean-field level we had the salient result that for vanishing and repulsive two-body interaction U, the allowed quasi-condensate density is limited by the statistical parameter θ and therefore resembles the Haldane exclusion principle and the transmutation from Bose-Einstein statistics to Fermi-Dirac statistics. Based on this, the effective mass and isothermal compressibility are correspondingly investigated, and from the latter we succeed in deriving an explicit form for statistical interaction. When approaching the pseudo-fermionic limit and the dilute limit, the statistical interaction reaches a finite maximum value that depends on the hopping strength (**Fig.** 3.3). Also, statistics-induced quantum depletion is an important sign of statistical interaction, which is determined in a self-consistent manner. From there also the range of stability for the Bogoliubov theory among the full range $\theta \in [0, \pi]$ and non-negative Hubbard interaction U is discussed, which provides a suitable parameter set for future experiments. We also worked out several correlation functions, which are experimentally feasible, for example with quantum gas microscopy [106].

As a concluding remark, we want to mention two interesting conceptions from different contexts that enrich the idea of anyons: one is the renowned *more is different* principle by P. W. Anderson in quantum many-body physics [107]. The other is somehow a pure philosophical framework, *A Thousand Plateaus* by philosophers G. Deleuze [108]. Anyons, as the generalized concept of identical particles, reside in the lower-dimensional space. But they can have richer many-body physics even than bosons and fermions in the daily three-dimensional world, which embodies the emergence of complexity and demands also a generalization of the current theoretical framework. This can also be corresponded to the *de-territorialization* and *re-territorialization* processes in Deleuze's work, which means that the breaking down of a fixed structures or boundaries is the condition for the emergence of newer and broader configurations. The Deleuze's rhizomatic structure—

> *"Rhizome has no beginning or end; it is always in the middle, between things, interbeing, intermezzo."[108]*

—is also quite general. It can be a reflection on the non-local interactions of the one-dimensional anyons due to the generalized commutation relations (2.9a-2.9c), or even on the intertwine between different theories, like statistics and topology. Another hot-off-press example is that the Nobel Prize in Physics 2024 is just devoted to the area of artificial neural networks [109]. This is then also the situation for the present research on anyons; the exploration of the Anyon-Hubbard model is still in its early stages, but we believe that new theories will emerge from the interweaving of knowledge from different backgrounds. This will then also facilitate the progress of corresponding experiments. Due to the time constraints of this thesis, numerous topics remain to be addressed. In the following, we will highlight some of these worthy topics.

Correlations for anyons

Although the correlations are discussed extensively in the main text, all the derivations and discussions went with bosons under the parameter θ. Although it was debated that the quasi-momentum distribution for anyons is not experimentally feasible as in this case the Fourier transformation is no longer canonical under the generalized anyonic algebra, one can still look at the spatial coherence for anyons,

$$\left\langle \hat{a}_i^\dagger \hat{a}_j \right\rangle = \left\langle \hat{b}_i^\dagger \, e^{i\theta\left(\sum_{l<1}^{i} - \sum_{l<1}^{j}\right)\hat{n}_l} \hat{b}_j \right\rangle = \begin{cases} 1).\ i = j & \Rightarrow \quad \left\langle \hat{a}_i^\dagger \hat{a}_i \right\rangle = \left\langle \hat{b}_i^\dagger \hat{b}_i \right\rangle = G_{ii}^{(1)} \\ 2).\ i < j & \Rightarrow \quad \left\langle \hat{b}_i^\dagger \, e^{i\theta \hat{n}_i} \displaystyle\prod_{l=i+1}^{j-1} e^{i\theta \hat{n}_l} \hat{b}_j \right\rangle \\ 3).\ i > j & \Rightarrow \quad \left\langle \hat{b}_i^\dagger \displaystyle\prod_{l=j+1}^{i-1} e^{-i\theta \hat{n}_l} e^{-i\theta \hat{n}_j} \hat{b}_j \right\rangle \end{cases} \tag{5.1}$$

which is measurable in quantum gas microscopy [79]. There are results from Gutzwiller mean-field theory, DMRG [30, 65] and perturbation method [89]. A Bogoliubov persective will further enrich this scenario.

Maxwell relation

From the literature [110], in a quantum many-body system, there exists a Maxwell relation between the pair correlation—a two-body observable, and the entropy—a macroscopic thermodynamic quantity. This is shown in the Lieb-Liniger model [47]

$$\hat{H} = -\frac{\hbar^2}{2m} \int dx \, \hat{\Psi}^\dagger \frac{\partial^2 \hat{\Psi}}{\partial x^2} + \frac{\chi}{2} \int dx \, \hat{\Psi}^\dagger \hat{\Psi}^\dagger \hat{\Psi} \hat{\Psi} \,, \tag{5.2}$$

where $\hat{\Psi}^\dagger(x)$ and $\hat{\Psi}(x)$ are the bosonic field operators and $\chi > 0$ characterize the strength of repulsive two-body interaction, which is determined via the $s-$wave scattering length a_s. The unnormalized pair correlation is defined as $\bar{G}^{(2)} \equiv \int dx \left\langle \hat{\Psi}^\dagger \hat{\Psi}^\dagger \hat{\Psi} \hat{\Psi} \right\rangle$. The Maxwell relation between the pair correlation and entropy $S(T, L, N, \chi)$ is evaluated as

$$\left(\frac{\partial S}{\partial \chi}\right)_{T,L,N} = -\frac{1}{2}\left(\frac{\partial \bar{G}^{(2)}}{\partial T}\right)_{L,N,\chi}, \tag{5.3}$$

with which one can measure the entropy via the pair correlation. As the relation is held in the context of two-body interacting Bose gas in one dimension, it would be meaningful to generalize it to the anyonic case and investigate the respective entropy for anyons.

Dynamics

In the thesis, we discussed the static structure factor, which is used to describe a system in equilibrium, i.e. the situation in this thesis. Experimentally the dynamic structure factor [103]

$$S(k,\omega) \equiv \frac{1}{N}\sum_{i,j}\int dt\, e^{-ik(i-j)a+i\omega t}\Big[\left\langle \hat{n}_i(t)\hat{n}_j(0)\right\rangle - \left\langle \hat{n}_i(t)\right\rangle \left\langle \hat{n}_j(0)\right\rangle\Big] \tag{5.4}$$

is more feasible and should be done in such respect. There is iDMRG numerical result in **Ref.** [78] and it is already largely discussed in the extended Tomonaga-Luttinger liquid theory **Ref.** [53], but still missing in the weak-coupling regime. To this end, one should consider the temporal dependence on the operators. This can be done by solving the time-dependent Gross-Pitavevski equation, from which we might again discover the Bogoliubov dispersion (3.76). Also, based on that, the anyonic superfluidity would be particularly interesting, on one side the asymmetric sound modes from the broken parity might lead to somehow a multi-component superfluid that propagates on the ring; on the other side, one usually introduces artificially a vanishing twist in the lattice in the calculation for superfluid for the bosonic case [111]. However, a twist already exists in the bosonic Hamiltonian of the Anyon-Hubbard model (2.30), in the hopping term.

Open system

Although the theoretical framework for isolated quantum systems is well established, real-world systems are inevitably coupled to their surrounding environment [112]. To date, most open quantum systems involving either bosonic or fermionic particles coupled to bosonic or fermionic baths have been extensively studied. However, anyons remain absent from these scenarios, as highlighted in **Tab.** 5.1.

System \ Bath	Bosonic	Anyonic	Fermionic
Bosonic	$\surd$	?	$\surd$
Anyonic	?	?	?
Fermionic	$\surd$	?	$\surd$

Table 5.1: The different types of open systems that could be taken into account regarding the types of particles in the system and bath.

It would also be interesting to consider the transport problem of 1D anyons in the open system, as shown in **Fig.** 5.1, the two ending sites of a 1D chain are connected to two baths with the same species of anyonic particles, differing from the chemical potential $\mu_L < \mu_R$. In the case of bosonic baths, this would lead to asymmetric transport that the particles from the hot bath can hop incoherently toward the cold bath, and more particles will nest in the finite boundary region that connects to the cold bath with a staggered density profile. This is the so-called bosonic skin effect [113]. Due to the broken spatial inversion symmetry, the transport of anyons is more complicated. Things would be even more intriguing if we consider a disorder on the chain.

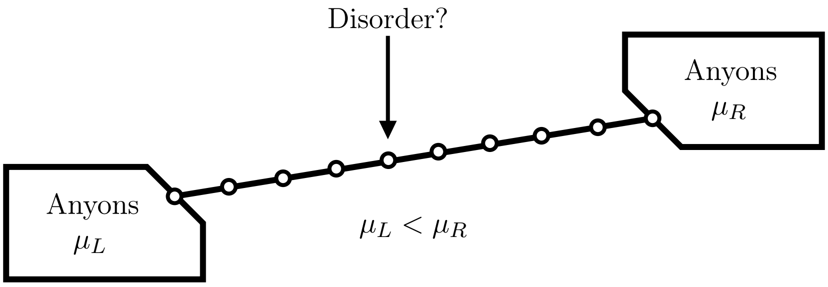

Figure 5.1: The schematic description for the transport problem of 1D anyons in the open-dissipative system.

Chapter 6

Acknowledgement

First of all I would like to express my profound gratitude to my supervisor Priv. Doz. Dr. Axel Pelster, for offering me opportunities to work in his working group and to complete my master's thesis. His unwavering enthusiasm for physics has been a constant source of motivation for me. During our weekly discussions, he has always been patient and supportive in addressing the details, while continually offering numerous inspiring ideas that have expanded my knowledge in the field of cold atoms and physics in general. In addition, under his generous support, I had the chance to attend various academic conferences, seminars and schools. His invaluable guidance has enabled me to delve deeper into the kaleidoscopic world of physics.

Special thanks to Martin Bonkhoff, who always patiently explained details about the subject of this thesis to me and cleared up my trivial and childish confusions. Without his insightful comments, the quality of this thesis could have been greatly diminished.

I would also like to thank Prof. Dr. Michael Fleischhauer for allowing me to participate in his group seminar and being the second reviewer.

Additionally, I am grateful for my colleagues Sejung Yong, Nikolai Kaschewski, and Joshua Krauß, as well as the people from Prof. Dr. Sebastian Eggert's working group, for various discussions and support during my studies. Also, I would like to thank all my friends for always being there for me and encouraging me.

Finally, I would like to thank my parents, without their support and understanding, I would not be where I am now.

Chapter 7

Bibliography

1. Pathria, R. K. *Statistical Mechanics* 3rd (Academic Press; Feb. 2011).
2. Huang, K. *Statistical Mechanics* 2nd ed. (John Wiley & Sons, Apr. 1987).
3. Khare, A. *Fractional statistics and quantum theory* 2. ed (World Scientific, Singapore, 2005).
4. Pauli, W. The Connection Between Spin and Statistics. *Physical Review* **58,** 716–722. https://link.aps.org/doi/10.1103/PhysRev.58.716 (Oct. 1940).
5. Bose. Plancks Gesetz und Lichtquantenhypothese. *Zeitschrift für Physik* **26,** 178–181. https://doi.org/10.1007/BF01327326 (Dec. 1924).
6. Anderson, M. H., Ensher, J. R., Matthews, M. R., Wieman, C. E. & Cornell, E. A. Observation of Bose-Einstein Condensation in a Dilute Atomic Vapor. *Science* **269,** 198–201. https://www.jstor.org/stable/2888436 (1995).
7. Cornell, E. Very cold indeed: The nanokelvin physics of Bose-Einstein condensation. *Journal of Research of the National Institute of Standards and Technology* **101,** 419. https://nvlpubs.nist.gov/nistpubs/jres/101/4/j4cornel.pdf (July 1996).
8. Davis, K. B. *et al.* Bose-Einstein Condensation in a Gas of Sodium Atoms. *Physical Review Letters* **75,** 3969–3973. https://link.aps.org/doi/10.1103/PhysRevLett.75.3969 (Nov. 1995).
9. Ketterle, W. & Zwierlein, M. W. Making, probing and understanding ultracold Fermi gases. *La Rivista del Nuovo Cimento* **31,** 247–422. https://doi.org/10.1393/ncr/i2008-10033-1 (July 2008).
10. Pauli, W. Über den Zusammenhang des Abschlusses der Elektronengruppen im Atom mit der Komplexstruktur der Spektren. *Zeitschrift für Physik* **31,** 765–783. https://doi.org/10.1007/BF02980631 (Feb. 1925).
11. Bardeen, J., Cooper, L. N. & Schrieffer, J. R. Theory of Superconductivity. *Physical Review* **108,** 1175–1204. https://link.aps.org/doi/10.1103/PhysRev.108.1175 (Dec. 1957).
12. Onnes, H. K. Further experiments with liquid helium. C. On the change of electric resistance of pure metals at very low temperatures etc. IV. The resistance of pure mercury at helium temperatures. *commun. phys. lab., Leiden University*. https://link.springer.com/chapter/10.1007/978-94-009-2079-8_15 (1911).
13. Meissner, W. & Ochsenfeld, R. Ein neuer Effekt bei Eintritt der Supraleitfähigkeit. *Naturwissenschaften* **21,** 787–788. https://doi.org/10.1007/BF01504252 (Nov. 1933).
14. Sigrist, M. & Ueda, K. Phenomenological theory of unconventional superconductivity. *Reviews of Modern Physics* **63,** 239–311. https://link.aps.org/doi/10.1103/RevModPhys.63.239 (Apr. 1991).

15. Mermin, N. D. & Lee, D. M. Superfluid helium-3. English. *Sci. Am.; (United States)* **235:6.** https://www.osti.gov/biblio/7227626 (Dec. 1976).

16. Cooper, L. N. Bound Electron Pairs in a Degenerate Fermi Gas. *Physical Review* **104,** 1189–1190. https://link.aps.org/doi/10.1103/PhysRev.104.1189 (Nov. 1956).

17. Sá de Melo, C. A. R. When fermions become bosons: Pairing in ultracold gases. *Physics Today* **61,** 45–51. https://doi.org/10.1063/1.3001867 (Oct. 2008).

18. Yong, S. *Hartree–Fock–Bogoliubov Mean-Field Theory for trapped fermionic atoms* MA thesis (Rheinland-Pfälzischen Technischen Universität Kaiserslautern-Landau, Mar. 2024). http://www.physik.fu-berlin.de/~pelster/Theses/yong-master.pdf.

19. Gänger, B., Phieler, J., Nagler, B. & Widera, A. A versatile apparatus for fermionic lithium quantum gases based on an interference-filter laser system. *Review of Scientific Instruments* **89,** 093105. https://doi.org/10.1063/1.5045827 (Sept. 2018).

20. Chin, C., Grimm, R., Julienne, P. & Tiesinga, E. Feshbach resonances in ultracold gases. *Reviews of Modern Physics* **82,** 1225–1286. https://link.aps.org/doi/10.1103/RevModPhys.82.1225 (Apr. 2010).

21. Leinaas, J. M. & Myrheim, J. On the theory of identical particles. *Il Nuovo Cimento B (1971-1996)* **37,** 1–23. https://doi.org/10.1007/BF02727953 (Jan. 1977).

22. Greiter, M. & Wilczek, F. Fractional Statistics. *Annual Review of Condensed Matter Physics* **15,** 131–157. https://www.annualreviews.org/content/journals/10.1146/annurev-conmatphys-040423-014045 (Mar. 2024).

23. Wilczek, F. Magnetic Flux, Angular Momentum, and Statistics. *Physical Review Letters* **48,** 1144–1146. https://link.aps.org/doi/10.1103/PhysRevLett.48.1144 (Apr. 1982).

24. Wilczek, F. & Zee, A. Linking Numbers, Spin, and Statistics of Solitons. *PHYSICAL REVIEW LETTERS* **51** (1983).

25. Wilczek, F. Quantum Mechanics of Fractional-Spin Particles. *Physical Review Letters* **49,** 957–959. https://link.aps.org/doi/10.1103/PhysRevLett.49.957 (Oct. 1982).

26. Wilczek, F. Quanta of the Third Kind. *Inference* **6.** https://inference-review.com/article/quanta-of-the-third-kind (Nov. 2021).

27. Wächter, S. *Proseminar on Algebra, Topology & Group theory in physics: The Aharonov-Bohm effect* en. in (Zürich, 2018).

28. Abbott, E. A. *Flatland: A romance of many dimensions* (1884).

29. Zatloukal, V. *Basic properties of anyons* in Proceedings of International School— *Anyon Physics of Ultracold Atomic Gases* (2013). http://users.physik.fu-berlin.de/~pelster/Anyon1/index.html.

30. Bonkhoff, M. *Interacting Anyons in a One-Dimensional Optical Lattice* PhD thesis (TU Kaiserslautern, Dec. 2016).

31. Naegels, D. An introduction to Goldstone boson physics and to the coset construction. arXiv:2110.14504 [cond-mat, physics:hep-ph, physics:hep-th, physics:math-ph]. http://arxiv.org/abs/2110.14504 (Oct. 2021).

32. Fadell, E. & Neuwirth, L. Configuration Spaces. *MATHEMATICA SCANDINAVICA* **10,** 111–118. https://www.mscand.dk/article/view/10517 (June 1962).

33. Nagies, S., Wang, B., Knapp, A. C., Eckardt, A. & Harshman, N. L. Beyond braid statistics: Constructing a lattice model for anyons with exchange statistics intrinsic to one dimension. *SciPost Physics* **16,** 086. https://scipost.org/SciPostPhys.16.3.086 (Mar. 2024).

34. Klitzing, K. V., Dorda, G. & Pepper, M. New Method for High-Accuracy Determination of the Fine-Structure Constant Based on Quantized Hall Resistance. *Physical Review Letters* **45,** 494–497. https://link.aps.org/doi/10.1103/PhysRevLett.45.494 (Aug. 1980).

35. Pachos, J. K. *Introduction To Topological Quantum Computation* (Cambridge University Press, 2012).

36. Tsui, D. C., Stormer, H. L. & Gossard, A. C. Two-Dimensional Magnetotransport in the Extreme Quantum Limit. *Physical Review Letters* **48,** 1559–1562. https://link.aps.org/doi/10.1103/PhysRevLett.48.1559 (May 1982).

37. Laughlin, R. B. Anomalous Quantum Hall Effect: An Incompressible Quantum Fluid with Fractionally Charged Excitations. *Physical Review Letters* **50,** 1395–1398. https://link.aps.org/doi/10.1103/PhysRevLett.50.1395 (May 1983).

38. Halperin, B. I. Statistics of Quasiparticles and the Hierarchy of Fractional Quantized Hall States. *Physical Review Letters* **52,** 1583–1586. https://link.aps.org/doi/10.1103/PhysRevLett.52.1583 (Apr. 1984).

39. Jain, J. K. Composite-fermion approach for the fractional quantum Hall effect. *Physical Review Letters* **63,** 199–202. https://link.aps.org/doi/10.1103/PhysRevLett.63.199 (July 1989).

40. Sanz Ruiz, M. *Tensor Networks in Condensed Matter* PhD thesis (Technische Universität München, 2011). https://mediatum.ub.tum.de/1070963.

41. Tsukazaki, A. *et al.* Observation of the fractional quantum Hall effect in an oxide. *Nature Materials* **9,** 889–893. https://tohoku.elsevierpure.com/en/publications/observation-of-the-fractional-quantum-hall-effect-in-an-oxide (Nov. 2010).

42. Laughlin, R. B. Superconducting Ground State of Noninteracting Particles Obeying Fractional Statistics. *Physical Review Letters* **60,** 2677–2680. https://link.aps.org/doi/10.1103/PhysRevLett.60.2677 (June 1988).

43. Hasan, M. Z. & Kane, C. L. Colloquium: Topological insulators. *Reviews of Modern Physics* **82,** 3045–3067. https://link.aps.org/doi/10.1103/RevModPhys.82.3045 (Nov. 2010).

44. Kitaev, A. Y. Unpaired Majorana fermions in quantum wires. *Physics-Uspekhi* **44,** 131. https://dx.doi.org/10.1070/1063-7869/44/10S/S29 (Oct. 2001).

45. Posske, T., Trauzettel, B. & Thorwart, M. Second quantization of Leinaas-Myrheim anyons in one dimension and their relation to the Lieb-Liniger model. *Physical Review B* **96,** 195422. https://link.aps.org/doi/10.1103/PhysRevB.96.195422 (Nov. 2017).

46. M. Bonkhoff. *Advances in Luttinger Liquid Theory: Applications to Lattice Anyons and Finite Spin Chains* http://users.physik.fu-berlin.de/~pelster/Theses/bonkhoff-phd.pdf. PhD thesis (Rheinland-Pfälzischen Technischen Universität Kaiserslautern-Landau, 2022).

47. Lieb, E. H. & Liniger, W. Exact Analysis of an Interacting Bose Gas. I. The General Solution and the Ground State. *Physical Review* **130,** 1605–1616. https://link.aps.org/doi/10.1103/PhysRev.130.1605 (May 1963).

48. Wilczek, F. *Fractional statistics and anyon superconductivity* (World Scientific, Singapore; Teaneck, NJ, 1990).

49. Kundu, A. Exact Solution of Double δ Function Bose Gas through an Interacting Anyon Gas. *Physical Review Letters* **83,** 1275–1278. https://link.aps.org/doi/10.1103/PhysRevLett.83.1275 (Aug. 1999).

50. Batchelor, M. T., Guan, X.-W. & Oelkers, N. One-Dimensional Interacting Anyon Gas: Low-Energy Properties and Haldane Exclusion Statistics. *Physical Review Letters* **96,** 210402. https://link.aps.org/doi/10.1103/PhysRevLett.96.210402 (June 2006).

51. Bonkhoff, M. *et al.* Bosonic Continuum Theory of One-Dimensional Lattice Anyons. *Physical Review Letters* **126.** https://link.aps.org/doi/10.1103/PhysRevLett.126.163201, 163201 (Apr. 2021).

52. Giamarchi, T. *Quantum Physics in One Dimension* (Clarendon Press, 2003).

53. Jung, P. *Impurities and Dynamical Structure Factor of an Anyonic Luttinger Liquid* MA thesis (Rheinland-Pfälzischen Technischen Universität Kaiserslautern-Landau, July 2023).

54. Frölian, A. *et al.* Realizing a 1D topological gauge theory in an optically dressed BEC. *Nature* **608,** 293–297. https://www.nature.com/articles/s41586-022-04943-3 (Aug. 2022).

55. Haldane, F. D. M. "Fractional statistics" in arbitrary dimensions: A generalization of the Pauli principle. *Physical Review Letters* **67,** 937–940. https://link.aps.org/doi/10.1103/PhysRevLett.67.937 (Aug. 1991).

56. Shastry, B. S. Exact solution of an S=1/2 Heisenberg antiferromagnetic chain with long-ranged interactions. *Physical Review Letters* **60,** 639–642. https://link.aps.org/doi/10.1103/PhysRevLett.60.639 (Feb. 1988).

57. Polychronakos, A. P. *Generalized Statistics in One Dimension* in *Aspects topologiques de la physique en basse dimension. Topological aspects of low dimensional systems* (Springer, Berlin, Heidelberg, 1999), 415–471.

58. Pasquier, V. *Integrable Models and Strings: Proceedings of the 3rd Baltic Rim Student Seminar Held at Helsinki, Finland, 13–17 September 1993* Softcover reprint of the original 1st ed. 1994 edition, 36–48 (Springer, Nov. 2013).

59. Chisholm, C. S. *et al.* Encoding a one-dimensional topological gauge theory in a Raman-coupled Bose-Einstein condensate. *Physical Review Research* **4,** 043088. https://link.aps.org/doi/10.1103/PhysRevResearch.4.043088 (Nov. 2022).

60. Rabello, S. J. A gauge theory of one-dimensional anyons. *Physics Letters B* **363,** 180–183. https://www.sciencedirect.com/science/article/pii/0370269395012620 (Nov. 1995).

61. Aglietti, U., Griguolo, L., Jackiw, R., Pi, S.-Y. & Seminara, D. Anyons and Chiral Solitons on a Line. *Physical Review Letters* **77,** 4406–4409. https://link.aps.org/doi/10.1103/PhysRevLett.77.4406 (Nov. 1996).

62. Griguolo, L. & Seminara, D. Chiral solitons from dimensional reduction of Chern-Simons gauged non-linear Schrödinger equation: classical and quantum aspects. *Nuclear Physics B* **516,** 467–498. https://www.sciencedirect.com/science/article/pii/S0550321397008109 (1998).

63. Vitoriano, C. & Coutinho-Filho, M. D. Fractional Statistics and Quantum Scaling Properties of the Hubbard Chain with Bond-Charge Interaction. *Physical Review Letters* **102,** 146404. https://link.aps.org/doi/10.1103/PhysRevLett.102.146404 (Apr. 2009).

64. Keilmann, T., Lanzmich, S., McCulloch, I. & Roncaglia, M. Statistically induced phase transitions and anyons in 1D optical lattices. *Nature Communications* **2.** https://www.nature.com/articles/ncomms1353, 361 (June 2011).

65. Tang, G., Eggert, S. & Pelster, A. Ground-state properties of anyons in a one-dimensional lattice. *New Journal of Physics* **17.** http://arxiv.org/abs/arXiv:1509.01888, 123016 (2015).

66. Dutta, O. *et al.* Non-standard Hubbard models in optical lattices: a review. *Reports on Progress in Physics* **78,** 066001. https://dx.doi.org/10.1088/0034-4885/78/6/066001 (May 2015).

67. Longhi, S. & Della Valle, G. Anyons in one-dimensional lattices: a photonic realization. *Optics Letters* **37,** 2160. https://opg.optica.org/abstract.cfm?URI=ol-37-11-2160 (June 2012).

68. Sträter, C., Srivastava, S. C. L. & Eckardt, A. Floquet realization and signatures of one-dimensional anyons in an optical lattice. *Physical Review Letters* **117,** 205303. http://arxiv.org/abs/1602.08384 (Nov. 2016).

69. Eckardt, A. Colloquium: Atomic quantum gases in periodically driven optical lattices. *Reviews of Modern Physics* **89,** 011004. https://link.aps.org/doi/10.1103/RevModPhys.89.011004 (Mar. 2017).

70. Kwan, J. *et al.* Realization of 1D Anyons with Arbitrary Statistical Phase. http://arxiv.org/abs/2306.01737 (June 2023).

71. Greschner, S. & Santos, L. Anyon Hubbard Model in One-Dimensional Optical Lattices. *Physical Review Letters* **115,** 053002. https://link.aps.org/doi/10.1103/PhysRevLett.115.053002 (July 2015).

72. Van Oosten, D., van der Straten, P. & Stoof, H. Quantum phases in an optical lattice. *Physical Review A* **63.** https://link.aps.org/doi/10.1103/PhysRevA.63.053601, 053601 (2001).

73. Tosta, A. D. C., Galvão, E. F. & Brod, D. J. Gaussian optical networks for one-dimensional anyons. *Physical Review A* **104,** 022604. https://link.aps.org/doi/10.1103/PhysRevA.104.022604 (Aug. 2021).

74. Kitaev, A. Anyons in an exactly solved model and beyond. *Annals of Physics* **321,** 2–111. https://linkinghub.elsevier.com/retrieve/pii/S0003491605002381 (Jan. 2006).

75. Jordan, P. & Wigner, E. Über das Paulische Äquivalenzverbot. *Zeitschrift für Physik* **47,** 631–651. https://doi.org/10.1007/BF01331938 (Sept. 1928).

76. Batista, C. D. & Ortiz, G. Algebraic Approach to Interacting Quantum Systems. *Advances in Physics* **53,** 1–82. http://arxiv.org/abs/cond-mat/0207106 (Jan. 2004).

77. Louisell, W. *Quantum statistical properties of radiation* https://books.google.de/books?id=NRlRAAAAMAAJ (Wiley, 1973).

78. Lange, F., Ejima, S. & Fehske, H. Anyonic Haldane Insulator in One Dimension. *Physical Review Letters* **118,** 120401. https://link.aps.org/doi/10.1103/PhysRevLett.118.120401 (Mar. 2017).

79. Bakr, W. S., Gillen, J. I., Peng, A., Fölling, S. & Greiner, M. A quantum gas microscope for detecting single atoms in a Hubbard-regime optical lattice. en. *Nature* **462,** 74–77. https://www.nature.com/articles/nature08482 (Nov. 2009).

80. Bonkhoff, M. private communication. Oct. 2024.

81. Pitaevskiĭ, L. P. & Stringari, S. *Bose-Einstein condensation and superfluidity* First edition. en (Oxford University Press, Oxford, United Kingdom, 2016).

82. Mermin, N. D. & Wagner, H. Absence of Ferromagnetism or Antiferromagnetism in One- or Two-Dimensional Isotropic Heisenberg Models. *Physical Review Letters* **17,** 1133–1136. https://link.aps.org/doi/10.1103/PhysRevLett.17.1133 (Nov. 1966).

83. Hohenberg, P. C. Existence of Long-Range Order in One and Two Dimensions. *Physical Review* **158,** 383–386. https://link.aps.org/doi/10.1103/PhysRev.158.383 (June 1967).

84. Halperin, B. I. On the Hohenberg–Mermin–Wagner Theorem and Its Limitations. *Journal of Statistical Physics* **175,** 521–529. http://link.springer.com/10.1007/s10955-018-2202-y (May 2019).

85. Dartora, C. A. The breaking of Mermin-Wagner-Hohenberg's theorem for fractional systems. *Physics Letters A* **496,** 129318. https://www.sciencedirect.com/science/article/pii/S0375960124000136 (Feb. 2024).

86. Pelster, A. Lecture Manuscript: Quantum Field Theory. https://www-user.rhrk.uni-kl.de/~apelster/Vorlesungen/WS2021/qft.html (2021).

87. Blasiak, P., Horzela, A., Penson, K. A., Solomon, A. I. & Duchamp, G. H. Combinatorics and Boson normal ordering: A gentle introduction. *American Journal of Physics* **75.** https://arxiv.org/abs/0704.3116, 639–646 (2007).

88. De Pasquale, A. & Facchi, P. *XY* model on the circle: Diagonalization, spectrum, and forerunners of the quantum phase transition. *Physical Review A* **80,** 032102. https://link.aps.org/doi/10.1103/PhysRevA.80.032102 (Sept. 2009).

89. Lange, F., Ejima, S. & Fehske, H. Strongly repulsive anyons in one dimension. en. *Physical Review A* **95,** 063621. http://link.aps.org/doi/10.1103/PhysRevA.95.063621 (June 2017).

90. Rennie, B. & Dobson, A. On stirling numbers of the second kind. en. *Journal of Combinatorial Theory* **7,** 116–121. https://linkinghub.elsevier.com/retrieve/pii/S0021980069800451 (Sept. 1969).

91. Cazalilla, M. A. Bosonizing one-dimensional cold atomic gases. *Journal of Physics B: Atomic, Molecular and Optical Physics* **37,** S1. https://dx.doi.org/10.1088/0953-4075/37/7/051 (Mar. 2004).

92. Bogoljubov, N., Tolmachov, V. V. & Širkov, D. A new method in the theory of superconductivity. *Fortschritte der physik* **6.** https://doi.org/10.1002/prop.19580061102, 605–682 (1958).

93. Mattern, P. *BEC in Optical Lattices: Beyond the Bogoliubov Approximation, Diploma thesis, Freie Universität Berlin* en. http://users.physik.fu-berlin.de/~pelster/Theses/mattern.pdf. May 2012.

94. Mattuck, R. D. *A guide to Feynman diagrams in the many-body problem* 2nd. en. https://www.amazon.de/-/en/Richard-D-Mattuck/dp/0486670473 (Dover Publications, INC., 1992).

95. Pelster, A. *Lecture notes in Bose-Einstein Kondenzation* de. Essen, July 2004. http://www-user.rhrk.uni-kl.de/~apelster/Manuscripts/bec.pdf.

96. Popov, V. N. *Functional Integrals and Collective Excitations* https://www.cambridge.org/core/books/functional-integrals-and-collective-excitations/2F86C7457298EF428E481690 (Cambridge University Press, Cambridge, 1988).

97. Popov, V. N. *Functional Integrals in Quantum Field Theory and Statistical Physics* 1st ed. https://link.springer.com/book/9789027714718 (Springer Dordrecht, 2001).

98. Haldane, F. D. M. 'Luttinger liquid theory' of one-dimensional quantum fluids. I. Properties of the Luttinger model and their extension to the general 1D interacting spinless Fermi gas. *Journal of Physics C: Solid State Physics* **14,** 2585. https://dx.doi.org/10.1088/0022-3719/14/19/010 (July 1981).

99. Altman, E., Demler, E. & Lukin, M. D. Probing many-body states of ultracold atoms via noise correlations. *Physical Review A* **70,** 013603. https://link.aps.org/doi/10.1103/PhysRevA.70.013603 (July 2004).

100. Li, S. *Quantum correlations of ultracold atoms in optical lattices* en. PhD thesis (University of Colorado, Colorado, 2014).

101. Bloch, I., Dalibard, J. & Zwerger, W. Many-body physics with ultracold gases. en. *Reviews of Modern Physics* **80,** 885–964. https://link.aps.org/doi/10.1103/RevModPhys.80.885 (July 2008).

102. Altland, A. & Simons, B. *Condensed Matter Field Theory* 3rd ed. en. https://www.cambridge.org/core/product/identifier/9781108781244/type/book (Cambridge University Press, Sept. 2023).

103. Yukalov, V. I. Structure factor of Bose-condensed systems. *Journal of Physical Studies* **11,** 55–62. http://physics.lnu.edu.ua/jps/2007/1/abs/a055-062.html (2007).

104. Wick, G. C. The Evaluation of the Collision Matrix. *Physical Review* **80,** 268–272. https://link.aps.org/doi/10.1103/PhysRev.80.268 (Oct. 1950).

105. Ernst, P. T. *et al.* Probing superfluids in optical lattices by momentum-resolved Bragg spectroscopy. en. *Nature Physics* **6,** 56–61. https://www.nature.com/articles/nphys1476 (Jan. 2010).

106. Gross, C. & Bakr, W. S. Quantum gas microscopy for single atom and spin detection. *Nature Physics* **17,** 1316–1323. https://www.nature.com/articles/s41567-021-01370-5 (Dec. 2021).

107. Anderson, P. W. More Is Different. *Science* **177,** 393–396. https://www.science.org/doi/10.1126/science.177.4047.393 (Aug. 1972).

108. Deleuze, G. & Guattari, F. *Thousand Plateaus: Capitalism and Schizophrenia* 002 edition. English (UNIV OF MINNESOTA PR, Minneapolis, Dec. 1987).

109. *The Nobel Prize in Physics 2024* Accessed: 2024-10-11. https://www.nobelprize.org/prizes/physics/2024/press-release/.

110. Watson, R. S., Coleman, C. & Kheruntsyan, K. V. Maxwell Relation between Entropy and Atom-Atom Pair Correlation. *Physical Review Letters* **133,** 100403. https://link.aps.org/doi/10.1103/PhysRevLett.133.100403 (Sept. 2024).

111. Rey, A. M. *et al.* Bogoliubov approach to superfluidity of atoms in an optical lattice. *Journal of Physics B: Atomic, Molecular and Optical Physics* **36,** 825. https://dx.doi.org/10.1088/0953-4075/36/5/304 (2003).

112. Szańkowski, P. Introduction to the theory of open quantum systems. *SciPost Physics Lecture Notes,* 068. https://scipost.org/10.21468/SciPostPhysLectNotes.68 (Apr. 2023).

113. Garbe, L., Minoguchi, Y., Huber, J. & Rabl, P. The bosonic skin effect: Boundary condensation in asymmetric transport. *SciPost Physics* **16,** 029. https://scipost.org/10.21468/SciPostPhys.16.1.029 (Jan. 2024).

114. Peskin, M. E. & Schroeder, D. V. *An Introduction To Quantum Field Theory* 1st edition. English (Westview Press, Boca Raton London New York, Oct. 1995).

115. Katriel, J. Combinatorial aspects of boson algebra. en. *Lettere al Nuovo Cimento (1971-1985)* **10,** 565–567. https://doi.org/10.1007/BF02784783 (July 1974).

116. Gerry, C. C. & Knight, P. L. *Introductory Quantum Optics* 2nd edition. English (Cambridge University Press, Cambridge New York, NY Port Melbourne, VIC New Delhi Singapore, Feb. 2024).

117. Wilcox, R. M. Exponential Operators and Parameter Differentiation in Quantum Physics. *Journal of Mathematical Physics* **8,** 962–982. https://doi.org/10.1063/1.1705306 (Apr. 1967).

118. Rössler, U. *Solid State Theory: An Introduction* en. https://link.springer.com/10.1007/978-3-540-92762-4 (Springer Berlin Heidelberg, Berlin, Heidelberg, 2009).

Appendix A

Combinatorics and Normal Ordering

Normal ordering is a fundamental technique in quantum field theory that historically resolved the problem of ultraviolet divergence, as the vacuum expectation value of the normal ordered Hamiltonian vanishes [86]. For example for the particle number operator

$$\langle 0| \hat{b}_j^{\dagger}\hat{b}_j |0\rangle = 0\,. \tag{A.1}$$

Further, the above expression implies that by setting the vacuum expectation value of the Hamiltonian to zero due to $\hat{b}_j |0\rangle = 0$, normal ordering aligns the theoretical ground state energy with the physical expectation that the vacuum should not contribute to measurable energy. This is also related to the renormalizations group [114].

Back to our problem, based on **Ref.** [115] here below we show how to normal order the density-dependent Peierls phase $e^{i\theta\hat{n}_j}$, from two ways around. The first uses solely combinatorial identities and the second uses combinatorial identities and the recurrence relations. For simplicity, we drop here the suffix of the operator $\hat{b}_j \to \hat{b}$ and thus $[\hat{b}, \hat{b}^{\dagger}]_- = 1$.

To start, we note the basic actions of bosonic operators on the Fock state, i.e. the number basis $|n\rangle$ [116],

$$\hat{b}\,|n\rangle = \sqrt{n}\,|n-1\rangle\ , \tag{A.2}$$

$$\hat{b}^{\dagger}\,|n\rangle = \sqrt{n+1}\,|n+1\rangle\ , \tag{A.3}$$

$$\hat{n}\,|n\rangle = \sqrt{n}\,|n\rangle\ . \tag{A.4}$$

Therefore for a complex number λ we can have

$$(\lambda+1)^{\hat{n}}\,|N\rangle = (\lambda+1)^{l}\,|N\rangle\ , \tag{A.5}$$

which further leads to the binomial decomposition

$$(\lambda+1)^{N}\,|N\rangle = \sum_{m=0}^{\infty}\binom{N}{m}\lambda^m\,|N\rangle = \sum_{m=0}^{\infty}\frac{N!}{m!(N-m)!}\lambda^m\,|N\rangle\ , \tag{A.6}$$

which with (A.2, A.3) can be written as

$$\sum_{m=0}^{\infty}\frac{\lambda^m}{m!}(\hat{b}^{\dagger})^m\hat{b}^m\,|N\rangle = \sum_{m=0}^{\infty}\frac{N!}{m!(N-m)!}\lambda^m\,|N\rangle\ . \tag{A.7}$$

Therefore we have the equation

$$(\lambda+1)^{\hat{n}}\,|N\rangle = \sum_{m=0}^{\infty}\frac{\lambda^m}{m!}(\hat{b}^{\dagger})^m\hat{b}^m\,|N\rangle\ . \tag{A.8}$$

Letting $e^{\xi} = 1 + \lambda$, we have the operator identity [77]

$$e^{\xi \hat{b}^\dagger \hat{b}} = \sum_m^\infty \frac{(e^{\xi} - 1)^m}{m!} (\hat{b}^\dagger)^m \hat{b}^m \,. \tag{A.9}$$

Now expand both sides, where for right-hand side we have [117]

$$(e^{\xi} - 1)^m = \sum_{l=0}^{m} \frac{(-1)^{m-l} m! e^{l\xi}}{l!(m-l)!} \,. \tag{A.10}$$

Therefore compare the corresponding coefficients on both sides of (A.9) leads to [115]

$$(\hat{b}^\dagger \hat{b})^q = \sum_{m=0}^{q} S(q,m) (\hat{b}^\dagger)^m \hat{b}^m \tag{A.11}$$

with the explicit form of the Stirling number of second kind $S(q,m)$ [87, 115]

$$S(q,m) = \frac{1}{m!} \sum_{l=1}^{m} \binom{m}{j} l^q (-1)^{m-l} \,. \tag{A.12}$$

The second way to normal ordering $(\hat{b}^\dagger \hat{b})^q$ is to find a recurrence relation, from which we first assume the normal ordered form of $(\hat{b}^\dagger \hat{b})^q$ is

$$(\hat{b}^\dagger \hat{b})^q = \sum_{m=1}^{q} C_m^q (\hat{b}^\dagger)^m \hat{b}^m \,, \tag{A.13}$$

where the coefficient $C_0^q = 0$ for $q > 0$ due to $\langle 0 | (\hat{b}^\dagger \hat{b})^q | 0 \rangle = \delta_{0,q}$. Then correspondingly for $(\hat{b}^\dagger \hat{b})^{q+1}$ we have

$$(\hat{b}^\dagger \hat{b})^{q+1} = \left(\sum_{m=1}^{q} C_m^q (\hat{b}^\dagger)^m \hat{b}^m \right) \hat{b}^\dagger \hat{b} \,. \tag{A.14}$$

Using repeatedly the commutation relation for bosons leads to

$$\left(\sum_{m=1}^{q} C_m^q (\hat{b}^\dagger)^m \hat{b}^m \right) \hat{b}^\dagger \hat{b} = \sum_{m=1}^{q+1} (C_{m-1}^q + m C_m^q) (\hat{b}^\dagger)^m \hat{b}^m \,, \tag{A.15}$$

from which follows the recurrence relation

$$C_m^{q+1} = C_{m-1}^q + m C_m^q \tag{A.16}$$

This is exactly the recurrence relation for the Stirling numbers of second kind:

$$S(q+1, m) = S(q, m-1) + m S(q, m) \,. \tag{A.17}$$

Therefore we identify the normal ordering coefficients C_m^q with the Stirling numbers of second kind $S(q,m)$ and complete the normal ordering procedure for (3.1) in the main text.

Appendix B

Periodic Boundary Condition

Here we demonstrate the discretization of a one-dimensional lattice under periodic boundary condition (PBC) based on **Ref.** [118].

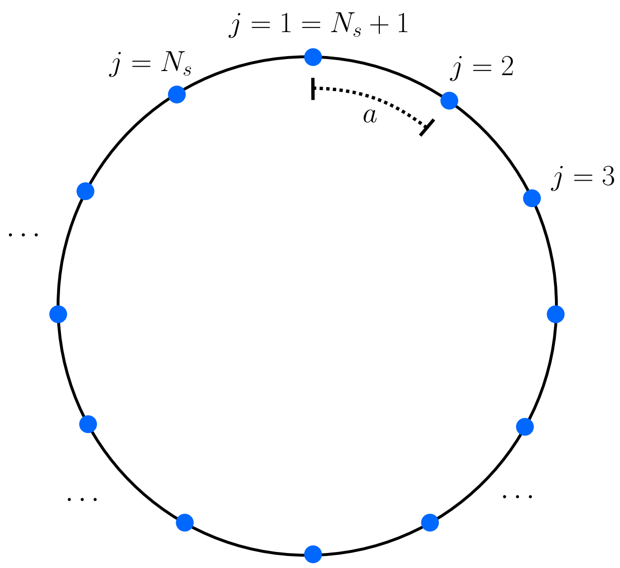

Figure B.1: Ring presentation of 1d lattice under PBC.

B.1 Discretization of momentum space

According to Bloch's theorem, the wavefunction solution of Schrödinger equation with periodic potential could be written as

$$\psi(x) = e^{ikx} u(x)\,, \tag{B.1}$$

where $u(x)$ is a periodic function which satisfies $u(x) = u(x+a)$, with a being the lattice spacing. Then the PBC demands

$$\psi(0) = \psi(L) \tag{B.2}$$

where $l = La$ is the size of the lattice. Applying the Bloch equations (B.1) and note in our setup the index of lattice sites runs from 1 to L, we have

$$\psi(0) = \psi(L) \quad \Rightarrow \quad e^{ik\cdot 1\cdot a}u(a) = e^{ik\cdot(L+1)\cdot a}u((L+1)a)$$

$$\Rightarrow \quad 1 = e^{ik\cdot L\cdot a} \quad \Rightarrow \quad k = \frac{2\pi}{L\,a}\cdot n, \quad \begin{cases} n \in \mathbb{Z}_{\neq 0} \cap [-\frac{L}{2}, \frac{L}{2}], & L \text{ is even} \\ n \in \mathbb{Z} \cap [-\frac{L-1}{2}, \frac{L-1}{2}], & L \text{ is odd} \end{cases} \tag{B.3}$$

B.2 1D discrete Fourier transformation

we have

$$\sum_{j=1}^{L} e^{ikja} \overset{(B.3)}{=} \sum_{j=1}^{L} e^{i\frac{2\pi}{L}nj} = \sum_{j=1}^{L} \left(e^{i\frac{2\pi}{L}n}\right)^{j} - 1 = \frac{1 - e^{i\frac{2\pi}{L}n(L+1)}}{1 - e^{i\frac{2\pi}{L}n}} - 1$$

$$= \frac{e^{i\frac{2\pi}{L}n}\left(1 - e^{i2\pi n}\right)}{1 - e^{i\frac{2\pi}{L}n}} = \begin{cases} 0\,, & n \neq 0 \\ L\,, & n = 0 \end{cases}\,, \tag{B.4}$$

therefore the 1D discrete Fourier transformation is given as

$$\sum_{j=1}^{L} e^{i\frac{2\pi}{L}nj} = L\,\delta_{n,0}\,. \tag{B.5}$$

Appendix C

Extended Tomonaga-Luttinger Liquid Theory

We briefly repeat the derivation of the anyonic TLL theory based on [46, 51]. It works with the continuum limit of the anyon-Hubbard model, therefore also its bosonic representation (2.30):

$$\lim_{\substack{L\to\infty \\ a\to 0 \\ L\cdot a = l = \text{const.}}} \hat{H}_{\text{AHM}} \quad \Rightarrow \quad \lim_{\substack{L\to\infty \\ a\to 0 \\ L\cdot a = l = \text{const.}}} \hat{H}^{(\text{B})}_{\text{AHM}}\,, \tag{C.1}$$

then the continuum limit is achieved via systematic renormalization. While the lattice size $l = L \cdot a$ remains finite, the lattice spacing a goes to 0 and the number of sites L goes to infinity, thus anyons are allowed to occupy freely along the lattice with the continuous position index $x \in [0, l]$. The bosonic field operator in the continuum is then

$$\hat{\psi}^\dagger_{\text{B}}(x) = \lim_{a\to 0} \frac{\hat{b}^\dagger_j}{\sqrt{a}}\,, \tag{C.2}$$

which gives the correct commutation relation in the continuum:

$$\left[\hat{\psi}_{\text{B}}(x'), \hat{\psi}^\dagger_{\text{B}}(x)\right]_- = \lim_{a\to 0} \frac{\delta_{i,j}}{a} \equiv \delta(x - x')\,. \tag{C.3}$$

The anyonic field operators $\hat{\psi}_{\text{A}}(x)$ are related to the bosonic ones by the continuum version of the Jordan-Wigner transformation

$$\hat{\psi}_{\text{A}}(x) = e^{i\theta \int_0^x dx'\, \hat{\rho}(x')} \hat{\psi}_{\text{B}}(x)\,, \tag{C.4}$$

with $\hat{\rho}_{\text{B}}(x) = \hat{\psi}^\dagger_{\text{B}}(x)\hat{\psi}_{\text{B}}(x)$. The problem of continuum limit is encoded here, as in the continuum limit $\int_0^x dx'\, \hat{\rho}(x') \in \mathbb{R}$ which doesn't has to be integers as in the lattice case, we lost now the periodicity in θ after the Jordan-Wigner transformation. Further one has to expand the field operators in a to derive the respective low-density effective theories

$$\hat{\psi}_{\text{A,B}}(x+a) = \hat{\psi}_{\text{A,B}}(x) + a\partial_x \hat{\psi}_{\text{A,B}}(x) + \frac{a^2}{2}\Delta_x \hat{\psi}_{\text{A,B}}(x) + \mathcal{O}(a^3)\,. \tag{C.5}$$

Insert (C.5) into the normal ordered Hamiltonian $:\hat{H}^{(\text{B})}_{\text{AHM}}:$ and rescale $Ja^2 = \hbar^2/2m_{\text{eff}} = 1$, the Hamiltonian in the continuum is then

$$\begin{aligned} \hat{H}_{\text{cont.}} = \int dx \Bigg[&: \partial_x \hat{\psi}^\dagger_{\text{B}}(x) \partial_x \hat{\psi}_{\text{B}}(x) : + [V_2(\theta) + c] : \hat{\rho}^2_{\text{B}}(x) : \\ &+ V_3(\theta) : \hat{\rho}^3_{\text{B}}(x) : + V_J(\theta) : \hat{\rho}_{(\text{B})}(x) \hat{J}_{(\text{B})}(x) : \Bigg] \end{aligned} \tag{C.6}$$

with the current operator $\hat{J}_{\rm B} = -i[\hat{\psi}_{\rm B}^\dagger(x)\partial\hat{\psi}_{\rm B}(x) - \text{h.c.}]$ and $c = U/2Ja$, and the respective interaction strengths are

$$\tilde{V}_2(\theta) = 1 - e^{i\theta}\,, \tag{C.7}$$

$$V_J(\theta) = \text{Im}[\tilde{V}_2(\theta)] = -\sin\theta\,, \tag{C.8}$$

$$V_2(\theta) = -\frac{\text{Re}[\tilde{V}_2(\theta)]}{d} = \frac{2(1-\cos\theta)}{a}\,, \tag{C.9}$$

$$V_3(\theta) = -\frac{\text{Re}[\tilde{V}_2(\theta)^2]}{2} = -(1 - 2\cos\theta + \cos 2\theta)\,. \tag{C.10}$$

C.1 Harmonic fluid approach

One can further use the harmonic fluid bosonization approach to approximate bosonic operators with fluctuations of a bosonic density field $\hat{\phi}(x)$ and its dual phase field $\hat{\Theta}(x)$ by using a polar decomposition

$$\hat{\rho}_{\rm B}(x) \approx \left[\rho_0 - \frac{1}{\pi}\partial_x\hat{\phi}(x)\right] \sum_{m=-\infty}^{+\infty} e^{2im[\pi\rho_0 x - \hat{\phi}(x)]}\,, \tag{C.11}$$

$$\hat{\psi}_{\rm B}(x) \approx \sqrt{\rho_0 - \frac{1}{\pi}\partial_x\hat{\phi}(x)} \sum_{m=-\infty}^{+\infty} e^{2im[\pi\rho_0 x - \hat{\phi}(x)]} e^{-i\hat{\Theta}(x)}\,, \tag{C.12}$$

and due to their conjugative feature, they obey the commutation relation

$$\left[\hat{\phi}(x), \partial_{x'}\hat{\Theta}(x')\right]_- = i\delta(x - x')\,, \tag{C.13}$$

and the higher-order density fluctuations are neglected, therefore lattice effects are also neglected and only small density fluctuations are considered. Follow the bosonization dictionary [91] one has for kinetic part

$$\partial_x\hat{\psi}_{\rm B}^\dagger(x)\partial_x\hat{\psi}_{\rm B}(x) \approx \rho_0\left(\partial_x\hat{\Theta}(x)\right)^2\,, \tag{C.14}$$

and the interaction parts are

$$:\hat{\rho}_{\rm B}^2(x): \approx -\frac{2}{\pi}\rho_0\partial_x\hat{\phi} + \frac{1}{\pi^2}\left(\partial_x\hat{\phi}\right)^2\,, \tag{C.15}$$

$$:\hat{\rho}_{\rm B}^3(x): \approx -\frac{3}{\pi}\rho_0^2\partial_x\hat{\phi} + \frac{3\rho_0}{\pi^2}\left(\partial_x\hat{\phi}\right)^2\,, \tag{C.16}$$

$$:\hat{\rho}_{\rm B}(x)\hat{J}_{\rm B}(x): \approx -2\rho_0^2\partial_x\hat{\Theta} + \frac{4\rho_0}{\pi}\partial_x\hat{\Theta}\partial_x\hat{\phi}\,. \tag{C.17}$$

We can further neglect the linear terms in $\partial_x\hat{\phi}$ and $\partial_x\hat{\Theta}$ for the reason that they contribute to a total energy shift as conserved quantities (Total particle number N and total current J) after the integration, therefore the low-energy field theory is expressed in terms of a TLL Hamiltonian

$$\hat{H}_{\rm cont.} \approx \frac{u}{2\pi}\int dx\,\left[\frac{1}{K}\left(\partial_x\hat{\phi}\right)^2 + K\left(\partial_x\hat{\Theta}\right)^2 + \delta\partial_x\hat{\phi}\partial_x\hat{\Theta}\right]\,, \tag{C.18}$$

with the Luttinger parameter K

$$K = \sqrt{\frac{\pi^2\rho}{V_2(\theta) + c + 3\rho_0 V_3(\theta)}}\,, \tag{C.19}$$

the Fermi velocity u

$$u = \frac{2\pi\rho_0}{K}\,, \tag{C.20}$$

and the parity-breaking interaction Δ

$$\Delta = \frac{8\rho_0 V_J(\theta)}{u}\,. \tag{C.21}$$

C.2 Mode expansion

Now we can diagonalize the TLL Hamiltonian (C.18) via a mode expansion, which gives eventually the linear dispersion for the sound velocities to compare with the Bogoliubov results in **Sec.** 3.6.2. As already discussed in **App.** B, due to the Jordan-Wigner transformation, the periodic boundary condition in anyonic lattice would correspond to a twisted boundary condition in the bosonic representation,

$$\hat{\psi}_{\mathrm{B}}(l) = \hat{\psi}_{\mathrm{B}}(0)e^{i\theta N}\,, \tag{C.22}$$

and vice versa. This boundary condition corresponds to the topological feature of anyon. Such twisted boundary condition could be achieved in the Luttinger framework by shifting the total current J as

$$\delta\hat{J} + \frac{\theta N}{\pi} = J\,, \tag{C.23}$$

therefore one can apply a bosonic mode decomposition

$$\hat{\phi}(x) = \phi_0 - \frac{\pi N x}{L} - \frac{i}{2}\sum_{q\neq 0}\sqrt{\frac{2\pi K}{l|q|}}\frac{q}{|q|}e^{-iqx}\left[\hat{\beta}_q^{\dagger} + \hat{\beta}_{-q}\right]\,, \tag{C.24}$$

$$\hat{\Theta}(x) = \Theta_0 + \frac{\pi\delta\hat{J}x}{L} + \frac{i}{2}\sum_{q\neq 0}\sqrt{\frac{2\pi}{Kl|q|}}\frac{q}{|q|}e^{-iqx}\left[\hat{\beta}_q^{\dagger} + \hat{\beta}_{-q}\right]\,, \tag{C.25}$$

where $\hat{\beta}^{\dagger}$ and $\hat{\beta}$ are the bosonic creation and annihilation operators for a collective wave with wave vector $q = 2\pi m/l$. The conserved current J and particle number N can be interpreted as action-angle variables dual to ϕ_0, Θ_0, which are used to label the topological excitations of the system and are omitted as before. Inserting (C.24, C.25) into the TLL Hamiltonian (C.18), we have finally the diagonalized form

$$\hat{H}_{\mathrm{Bonkhoff}} \equiv \hat{H}_{\mathrm{cont.}} \approx \sum_{q\neq 0} u\left[1 + \frac{\Delta}{2}\mathrm{sign}(q)\right]|q|\hat{\beta}^{\dagger}\hat{\beta}\,, \tag{C.26}$$

up to which we could further obtain the asymmetric sound velocities to the left and right. Here it's clear that the parity symmetry breaking comes from the interaction Δ.

Declaration of Authorship

Hereby I declear that the presented Master's thesis with the title "Bogoliubov Theory of Anyons in One Dimensional Lattice" is my original work. All the external sources have been correctly cited and recorded in the Bibliography chapter.

Kaiserslautern, October 11, 2024

Bin-Han Tang